# Effect of alloying elements on the microstructure and degradation properties of magnesium biodegradable alloys for biomedical application

I Antoniac[1], A Blajan[1]

*[1]Faculty of Materials Science and Engineering, University Politehnica of Bucharest, Street Splaiul Independentei no.313, 060042, sector 6, Bucharest, Romania*

**INTRODUCTION:** Magnesium alloys appear to be now a suitable biomaterial for biodegradable implants for different biomedical applications. Unlike its industrial applications in which corrosion is an undesirable event, in medical applications it is an advantage. However, it should be considered that the general corrosion rapidly occurs in the case of magnesium alloys. A way to solve this problem is by choosing suitable alloying elements. For example, is known that for application in bone tissue replacement, calcium is appropriate as alloying element for magnesium alloys [1, 2]. Therefore, to obtain an alloy with a decreased rate of corrosion is very important to use a favorable alloying element ration. In this study, we analyze the effect of different alloying elements on the microstructure and corrosion behavior of some magnesium based alloys from different systems like Mg-Ca, Mg-Zn-Zr and Mg-Zn-Zr-Y-Ag.

**METHODS:** The starting materials for the experimental researches were different magnesium alloys, in casting state. The magnesium alloys were subjected to qualitative and quantitative compositional analysis to achieve a correlation between the results and objectives. The experimental samples were characterized in terms of microstructure using an Olympus optical microscope and a Philips scanning electron microscope (SEM, model ESEM XL 30 TMP). The energy dispersive X-ray (EDX) was used to analyze the chemical composition of the two experimental alloys. The evaluation of corrosion resistance was performed both using electrochemical measurements and hydrogen release in simulated body fluid maintaining the temperature at 37 ± 1 °C [3]. The test for determining the amount of hydrogen released in the simulated environment of the magnesium-based alloy was made according the method proposed by Song et al. [4].

**RESULTS & DISCUSSION:** Optical microscopy analyzes of experimental magnesium alloys showed in generally a biphasic structure $\alpha + \beta$ with dendritic looking specific to cast materials. The different results obtained for hydrogen release and the corrosion will be presented and discussed in correlation with the microstructural aspects of the experimental biodegradable magnesium alloys.

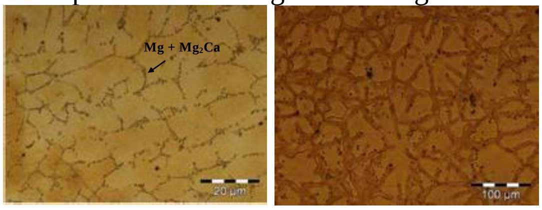

*Fig. 1. Microstructural aspects of some biodegradable magnesium alloys obtained using optical microscopy (200x): left: Mg-Ca; right: Mg-Zn-Zr.*

**CONCLUSIONS:** The aim of this paper was to present a systematic investigation on biodegradable magnesium alloys from different systems, to show the influence of alloying element content on the microstructure and degradation properties. The experimental results definitely demonstrate that the addition of alloying elements induce the microstructural modifications who affect the degradation properties in different way.

**ACKNOWLEDGEMENTS:** The work has been funded by: the UEFISCDI - PN II - Partnerships in priority areas, Contract No. 271/2014.

# Antimicrobial release from mesoporous titania coated implants

S Atefyekta[1], B Ercan[2], J Karlsson[1], EN Taylor[2], S Chung[2], TJ Webster[2], M Andersson[1]

*[1] Dept. Chemical and Biological Engineering, Chalmers University of Technology, Göteborg, Sweden. [2] Dept. Chemical engineering, Northeastern University, Boston, USA*

**INTRODUCTION:** In order to address biomaterial-associated infections caused by formation of adhesive biofilm on the surfaces of prosthetic materials, a practical strategy would be to apply an implant coating having the capability to release antimicrobial substances. This would result in a local antibiotic administration, which is believed to be an efficient treatment with low risks for systemic side effects.

**METHODS:** In this study, the effectiveness of mesoporous titania films as antimicrobial release coating was investigated. Mesoporous titania thin films were formed using evaporation induced self-assembly (EISA) method in combination with spin coating. Synthesis parameters, such as type and amount of template, swelling agent volume ratio, and aging parameters were varied to form mesoporous titania with variable pore sizes. The surfaces were loaded with antimicrobial agents such as Vancomycin, Gentamicin and Daptomycin and applied to grow grow *S.Aeurous* and *Pseudomonas aeruginosa* to evaluate the efficiency towards bacterial colonization. The drug delivery was studied using quartz crystal microbalance with dissipation monitoring (QCM-D) method.

**RESULTS:** Transmission and scanning electron microscopy (TEM and SEM) showed that the materials had a well-defined porous structure with pore sizes ranging between 3 and 7.2 nm, depending on the used template. The antibiotic delivery was studied using QCM-D, showed a successful loading and release of the antibiotics. Results from counting the bacterial colony forming units showed a reduced bacterial adhesion for the drug-loaded films. Furthermore, also the presence of the pores showed to have a desired effect on the bacteria, an effect attributed to the nanoroughness.

**DISCUSSION & CONCLUSIONS**: It was shown that applying a mesoporous thin coating on the substrates, apart from their function as an antibiotic delivery system can reduce the adhesion of bacteria just by creating nano level roughnesses. Mesoporous titania coating with variable pore sizes function better in hindering the bacterial adhesion compared to a non-porous titania coating used as control. Results from QCM-D measurements clearly reveals that a higher amount of antibiotic can be loaded on the surfaces with bigger pore sizes which in turn can lead to a higher release of antibiotic from these surfaces. These observations can be linked well to the bacterial adhesion results which showed clear differences on the adhesion of bacteria strains in the presence of different antibiotics. A decreased attachment was observed when the pore sizes of antibacterial loaded surfaces were increased. These observations confirm that the mesopoorus titania substrates can act as efficient drug release implant coating to combat bacterial adhesion and potential implant related infections. The amount of antibiotic loaded on the coating can be regulated by varying the pore size of the mesoporous titania films.

**ACKNOWLEDGEMENTS:** The Wallenberg Foundation is acknowledged for financial support through their Wallenberg Academy Fellow Program (MA). Northeastern University is also acknowledged for financial support

# Design and development of a 3D printed PLA tissue engineering scaffold functionalized with alginate microbeads

DC Bassett[1], NCR Rodrigues[2], P Sikorski[1] and KW Dalgarno[2]

[1]*Department of Physics, Norwegian University of Science and Technology, Trondheim, Norway.*
[2]*School of Mechanical and Systems Engineering, Newcastle University, UK*

**INTRODUCTION:** Cell based tissue engineering requires scaffolds that are both biofunctional i.e. provide the necessary environment for cell survival and maturation, and possess suitable mechanical properties for their application [1]. Alginate hydrogels perform well as artificial cell matrix biomaterials, providing a biocompatible niche to sustain cell survival [2]. We have improved the prospect of using alginate in bone tissue engineering by enhancing the mechanical stability and response of cells resident to bone to alginate through a process of controlled mineralisation [3]. However, these materials lack sufficient mechanical strength for load bearing applications. Therefore, in this study, we have designed highly porous but mechanically strong polymeric scaffolds made using fused filament deposition 3D printing techniques to house discrete, uniform microscale beads of alginate. This approach was chosen to both organise the spatial distribution of alginate beads and provide physiologically relevant mechanical properties to the hydrogel constructs.

**METHODS:** 3D CAD models were designed using Autodesk Inventor Professional 2015 and exported as STL files. STL files were converted to gcode files to be printed using an Ultimaker 2 3D printer. All scaffolds were printed in poly lactic acid (PLA). To form microbeads of narrow size distributions, an electrostatic bead generator was used as described previously [3]. 15 mm cubic samples were used for mechanical testing in compression. Compressive testing was carried out using a Tinius Olsen H25KS Universal testing machine fitted with a 25 kN load cell. Crosshead speed was 2 mm $min^{-1}$ and samples were tested to failure. Six samples were tested in each group.

**RESULTS:** Highly porous PLA scaffolds based on a 'log-pile' structure were faithfully reproduced from CAD designs. Various design iterations were tested for their ability to house alginate microbeads of diameter 247 +/- 32 µm or 486 +/- 22 µm. A leading design candidate was selected that had struts of rhomohedral cross section, this design was found to hold the larger alginate beads well following plasma treatment to render the scaffolds hydrophilic (Figure 1). Mechanical testing revealed effective yield strengths of 13.4 ± 1.6 MPa in the x/y axis and 16.3 ± 1.2MPa in the z axis and effective moduli of 317.5 ± 35.9 in the x/y axis and 439.5 ± 18.7 MPa in the z axis, therefore the scaffolds had similar mechanical properties to cancellous bone.

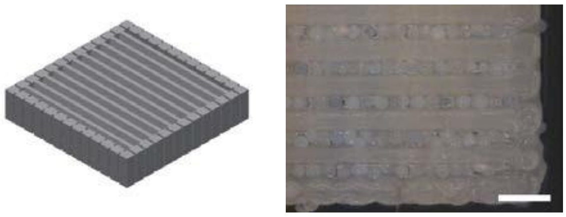

*Fig. 1: Left: CAD design of the PLA scaffold. Right: Light micrograph showing mineralised beads loaded into the PLA scaffold. SB =2mm.*

**DISCUSSION & CONCLUSIONS:** A design was created that successfully housed alginate microbeads, therefore providing a mechanically strong scaffold for a biofunctional hydrogel matrix. This concept therefore offers a new pathway to functionalise polymer scaffolds made by filament fused deposition and separates scaffold manufacture from cell culture providing greater flexibility in scaffold design. The final arrangement of beads within the scaffold was still highly porous, allowing for fluid flow and nutrient exchange around the alginate beads, essential for sustained cell metabolism within the alginate. Work is now continuing by loading these scaffolds with cells encapsulated in alginate microbeads.

**ACKNOWLEDGEMENTS:** The authors gratefully acknowledge funding provided by COST action MP 1301 NEWGEN and from the Research Council of Norway under the FRINATEK program, project no: 214607.

# Raman and SEM characterization of early stage calcium phosphate mineral formation in an alginate matrix

S Bjørnøy, DC Bassett, S Mandaric, P Sikorski

*Department of Physics, Norwegian University of Science and Technology, Trondheim, Norway*

**INTRODUCTION:** Bone tissue is a complex hierarchical composite of collagen and calcium phosphate mineral, constantly being remodelled by cells. This dynamic system is difficult to replicate, however, one emerging strategy is to provide a simpler bioactive material and let implanted or inherent cells create the required complexity. Previously we have developed an alginate-calcium phosphate (CaP) composite which shows good potential in this regard. [1] Here we further characterize this material as it forms and changes with time using advanced SEM techniques, such as density dependent colour (DDC)-SEM [2], to study the morphology of the formed mineral and its distribution within the alginate matrix, XRD, to study the phase of the mineral, and Raman microscopy to study the chemical composition. Improving basic knowledge about the system allows for better design of the composite material. In order to study the alginate gelling process and investigate combined gelling and mineralisation in the alginate-CaP system, we have developed a simple flow-cell experimental setup, where the dynamics of gelling and mineral formation processes can be studied simultaneously *in situ* with optical microscopy, and modeled using a reaction-diffusion approach. Here we describe how this system can be further used to investigate the evolution of CaP phases in biomimetic environments using SEM and Raman spectroscopy.

**METHODS:** Gel samples were made by placing a droplet of alginate containing $PO_4^{3-}$ between a slide and coverslip separated by a polymer membrane. $CaCl_2$ solution was added in the cell to initiate gelling and mineralisation. Gelling and mineral formation were monitored by phase contrast microscopy. *In-situ* Raman spectra were recorded after the introduction of $CaCl_2$ using a Renishaw InVia Reflex Spectrometer with a 785 nm laser. For SEM-characterization the gelled disks were quenched in liquid $N_2$ and freeze- or critical point dried before imaging with a Hitachi S-5500 S(T)EM. A reaction-diffusion model implemented in Matlab was used to model the evolution of ion, alginate and gel concentrations.

**RESULTS:** We have developed a system, which allows us to simultaneously study the gelling, and mineralisation front, and examine the same type of samples with Raman and electron microscopy, thus enabling coupling of well characterized samples with models of the same system. This coupling will aid in understanding the nucleation and growth process of different CaP phases as a function of ion concentrations.

DDC-SEM was used to improve contrast between the organic network and the mineral phase, easing identification of mineral morphology and distribution as shown in Fig 1A. Raman spectroscopy allowed characterization of the formation and transformation of CaP phases during gel formation. Some of the major benefits of this method are that non- and low-crystalline phases may be detected and all phases can be spatially resolved, in contrast to phase-identification with powder XRD. Fig 1B shows example spectra obtained for HAp and DCPD phases.

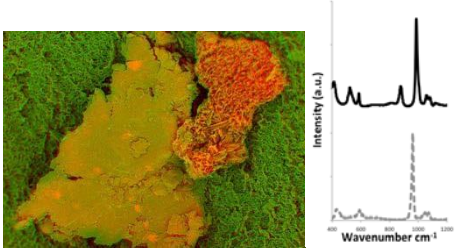

*Fig. 1: Left: DDC-SEM of calcium phosphate in alginate network. Scalebar is 10 µm. Right: Raman spectra of DCPD and HAp.*

**DISCUSSION & CONCLUSIONS:** The *in-situ* Raman spectroscopy and SEM-characterization combined with kinetic models provides new information about the precipitation dynamics of calcium phosphate within an alginate network. Results from this study will contribute to establishing a more general description of simultaneous mineralization and gel formation processes, allowing us to design better composites.

**ACKNOWLEDGEMENTS:** We acknowledge the Research Council of Norway for financial support (FRINATEK project 214607).

# Spectroscopic characterization of natural calcium phosphates by FTIR-DRIFT

A Brangule, KA Gross

*Biomaterials Research Laboratory, Riga Technical University, Paula Valdena 3, Riga LV-1048, Latvia*

**INTRODUCTION:** One of the objectives in calcium phosphate research is to obtain a biomaterial with a degree of crystallinity and structure that resembles bone. These bone-like materials are normally characterized by different spectrometric techniques, more commonly with FTIR. FTIR-DRIFT (Fourier transform infrared spectroscopy – diffuse reflectance infrared reflection) can be used to identify and characterize absorption bands in calcium phosphates with a similar chemistry, but different structure and bonding: human bone, archaeological bone, mammoth tusk and ivory. The bonding footprint from FTIR-DRIFT is important in many industries, including medicine, archaeology, gemmology and customs.

The objectives of this work is to source different apatite based materials from animal and human origin and compare these with synthesized apatite of low crystallinity.

**METHODS:** In this study, we evaluated different poorly crystalline calcium phosphates. The reference was a wet precipitated calcium phosphate and this was compared to human bone, mammoth tusk and ivory. The functional group changes were determined by FTIR–DRIFT (PerkinElmer Spectrum One,) at 450–4000 cm$^{-1}$, at a resolution of 4 cm$^{-1}$, with an average of 8 scans, sampled by diamond sampling sticks. A special preparation method was not required for synthesized powder. Powder for bone analysis was obtained from the inside of bone vertebra but powder for tusk analysis - from the outside of tusk. The FTIR spectra were smoothed with freeware software Specwin32. Baseline correction and curve-fitting analysis was performed using *MagicPlotStudent* software with wavenumbers from literature for $\upsilon_3CO_3$, amide I, amide II and amide III groups. Deconvolution involved both Lorentzian and Gaussian curve fitting.

**RESULTS:** FTIR-DRIFT spectra were analysed in IR region 450 – 1900 cm$^{-1}$. This region, from bones and tusk, displayed overlapped amide I, amide II and amide III peaks in collagen, and inorganic $\upsilon_1,\upsilon_3CO_3$ and $\upsilon_1,\upsilon_3,\upsilon_4PO_4$ bands. Deconvolution of the FTIR spectra show convoluted organic amide bands and inorganic carbonate $\upsilon_3CO_3$ bands. Deconvolution of the organic band showed that amide I, amide II and amide III bands dominated in this region.

Synthesised calcium phosphate spectra were used for identification and deconvolution of $\upsilon_3CO_3$ bands. Deconvolution of the inorganic $\upsilon_3CO_3$ bands showed a type A1 doublet, a type A2 doublet and a type-B doublet in the same region as in bone. This information can be used for identification of carbonate bands in human bones and tusks.

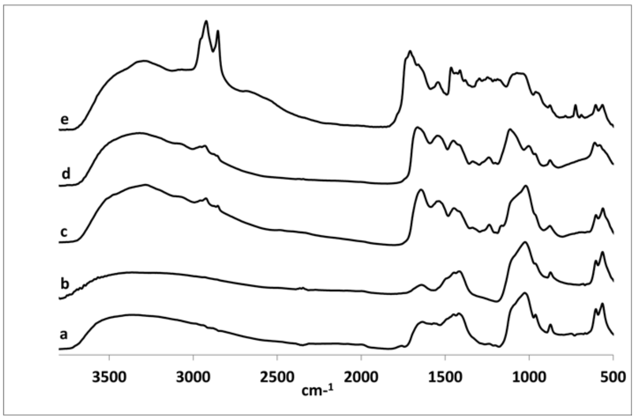

*Fig. 1:FTIR – DRIFT spectra of a) poorly crystalline calcium phosphate, b) archaeological human bone, c) ivory, d) mammoth tusk and e) human bone.*

**DISCUSSION & CONCLUSIONS:** FTIR DRIFT can be used for identification and structure analysis of various calcium phosphate based materials. The method is sufficiently sensitive for detecting inorganic and organic absorption bands. It is non-destructive and is suitable for the analysis of small samples, extending to surface mapping capabilities. This spectroscopic facility is an important part of the toolbox for characterizing, checking and designing calcium phosphates.

# Guiding auditory neurons: ordered growth on micro-structured nanocrystalline diamond surface

Y Cai[1], F Edin[2], P Forsberg[1], M Karlsson[1], H Li[2]

*[1]Department of Engineering Sciences, Ångström Laboratory, Uppsala, University, Box 534, 751 21 Uppsala, Sweden, [2]Department of Surgical Sciences, Otolaryngology and Head & Neck Surgery, Uppsala University Hospital, 751 85 Uppsala, Sweden*

**INTRODUCTION:** Diamond is well known for its chemical inertness, high mechanical strength, wear resistance and extraordinary electrical properties. These unique sets of properties (among others) make diamond interesting to use as a biomaterial. Recently it has also been shown that nanocrystalline diamond (NCD) can be used for sensitive biosensors. Several surface modification methods for NCD has been developed and proteins and DNA has successfully been attached to the NCD surfaces. Diamond is also considered to be a biocompatible material. Previous experiment concerning cell response on NCD surfaces has mainly focused on certain surface chemical modifications, for instance surface termination by using plasma techniques (oxygen, hydrogen, fluorine, ammonia etc). Moreover, these studies have been exploring plain NCD surfaces. In this study we use textured NCD surfaces, consisting of micrometre-sized nail-head-shaped pillars1, for neuron growth. The micro structured NCD surface was fabricated by a sequence of micro/nano-fabrication processes including sputtering, photolithography and plasma etching.

**METHODS:** The textured NCD surface was created by a sequence of standard micro/nano-fabrication procedure including sputtering, photolithography and Bosch process of etching. The NCD wafer was first cleaned for in $H_2SO_4/H_2O_2$ then coated with aluminium by sputtering. A pattern was fabricated on top by utilizing lithography then followed by inductively coupled plasma (ICP) etching. Pillars of silicon with NCD/Al were thus fabricated and finally Al was etched away in a typical aluminium wet etch. The sample was cleaned again to insure a hydrophilic surface. The CVD system was employed for the following oxygen termination. The surfaces was cultured and incubated with neuron cells continuously for 1 week.

**RESULTS:** Outgrowth of axons from neonatal mouse spiral ganglion explants was studied by fluorescence microscopy, confocal laser scanning microscopy and scanning microscopy2. Primary findings reveal axonal growth along the NCD pillar pattern, indicating guided growth of auditory neurons.

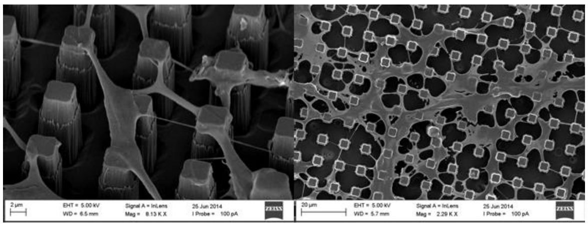

*Fig. 1: Images of neuron attached functionalized NCD diamond surface.*

**DISCUSSION & CONCLUSIONS:** In this study, the axons were studied by scanning microscopy[2] and it showed the potential biocompatibility of such micro-fabricated surface. The obtained morphology revealed a promising neuron guide between each pillar spatial pattern. In the following steps, we will continue use fluorescence microscopy, confocal laser scanning microscopy to detect the neuron growth on such unique surfaces. Furthermore, we will develop more surfaces with pillar scale differentiation. Primary findings reveal axonal growth along the NCD pillar pattern, indicating guided growth of auditory neurons.

**ACKNOWLEDGEMENT:** The author gratefully appreciated support from China Scholarship Council (CSC) for the PhD study.

# Graphene oxide reinforced gelatin-poly(vinyl alcohol) composite scaffolds with promising applications for hard tissue regeneration

L Crica[1], VN Vladimir[1], H Tiainen[2], H Haugen[2], M Ionita[1], H Iovu[1]

*[1]Advanced Polymer Materials Group, University Politehnica of Bucharest, Romania, [2]Department of Biomaterials, Institute for Clinical Dentistry, University of Oslo, Norway*

**INTRODUCTION:** Taking advantage of their remarkable properties such as biocompatibility thermal, mechanical and electrical properties [1], graphene and graphene derivatives based materials receive tremendous attention for numerous applications, among which the field of biomaterials might be one of the most promising. The present study highlights the use of graphene oxide (GO) as reinforcing agent for gelatin (Gel)-poly(vinyl alcohol) (PVA) scaffolds with potential applications for hard tissue regeneration.

**METHODS:** Gel-PVA/GO biocomposites with 0.5, 1, 2 and 3 wt.% GO were prepared by freeze-drying method. The synthesis route started with dispersing through sonication of GO required amount in deionized water. Gel was added in portions under constantly stirring at 60 °C in order to reach 5 wt.% concentration. The next step was adding an equal volume of 5 wt.% PVA solution, followed by sonication for 30 min. The Gel-PVA/GO solutions were poured on Petri dishes and kept at -80 °C overnight. Subsequently, each sample was subjected to a 3-cycle treatment which involved melting at room temperature for 3 hours and refreezing at -80 °C for 21 hours. Samples in their final form were freeze-dried for 100 h.

**RESULTS:** Structural analysis was carried by Fourier Transform Infrared Spectroscopy (FT-IR), and results (figure not shown) indicated the presence of all constituents with no evident bonding interaction. Through cross-sectional scanning electron microscopy (SEM, *Figure 1*) porous morphologies were revealed for all composites, with pore sizes up to few tens μm. Mechanical performances were evaluated through compressive tests. For each sample, a number of 10 specimens with same diameter and height were subjected to 0.5 N compressive forces at a speed of 0.5 mm/sec. Results are illustrated in *Figure 2*. All the curves follow the smooth characteristic pattern of an elastomer compression, indicating a rather more elastic nature of the samples. In comparison with unloaded GO samples, it was observed that, even at such small concentrations, GO improved mechanical resistances of the scaffolds by ~120% at 10% strain. Yet, no significant differences were observed between 0.5 wt.% GO and higher concentrations.

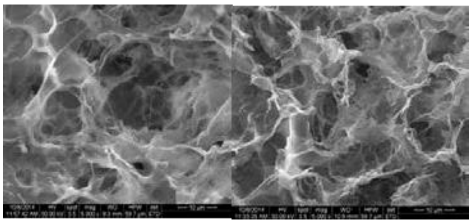

*Fig. 1: Cross-section SEM micrographs of Gel-PVA (left) and Gel-PVA/GO 3 wt.%.*

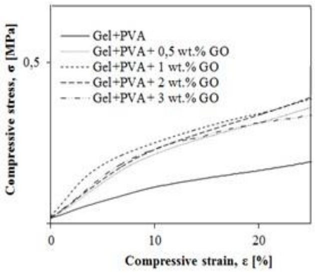

*Fig. 2: Mechanical behavior of Gel-PVA and Gel-PVA/GO biocomposites.*

**DISCUSSION & CONCLUSIONS:** The main goal of mixing the two polymers with GO is the development of porous composite scaffolds with improved mechanical features. Our previous studies suggest also the possibility of optimizing porosity [2] and beneficial effects over cells cultures [3] by adjusting the GO amount. Whereas the current study demonstrated the ability of GO to improve mechanically the final material. Therefore, the currently developed biocomposites are expected to be attractive for hard tissue regeneration applications.

**ACKNOWLEDGEMENTS:** This work was supported by a grant of the Romanian National Authority for Scientific Research, Executive Agency for Higher Education, Research, Development and Innovation; project number PN-II-PCCA-140/2012, EEA Grants project number 12/12.07.2014, and POSDRU/156/1.2/G135764.

# Protein adsorption can be reversibly switched ON and OFF on mixed polymer brushes

M Delcroix[1], C Dupont-Gillain[1]

[1]*Institute of Condensed Matter and Nanosciences, Université catholique de Louvain, Belgium*

**INTRODUCTION:** Protein adsorption, a ubiquitous and mostly irreversible phenomenon, can nowadays be spatially controlled, eg using nanopatterned substrates. The next challenge consists in achieving temporal control over protein adsorption, with foreseen applications in drug delivery and diagnostics, or more generally for responsive devices. The aim of this work is to design smart interfaces showing protein adsorption properties which can be switched ON and OFF at will. The strategy of the research rests on the use of binary polymer brushes of poly(ethylene oxide) (PEO), a protein-repellent polymer, and poly(acrylic acid) (PAA), a polyelectrolyte. PAA conformation varies with pH and ionic strength (I) of the medium, leading to preferential exposure of PEO or PAA depending on conditions.

**METHODS:** Mixed brushes of PEO and PAA were synthesized using a "grafting to" approach on a gold substrate, and were extensively characterized. The fraction of each polymer in the obtained brushes was determined using X-ray photoelectron spectroscopy (XPS). Using PAA homobrushes, PAA conformation and protein adsorption were systematically investigated as a function of pH and I, using quartz crystal microbalance (QCM). The ability of mixed PEO/PAA brushes to switch adsorption ON and OFF was then investigated using XPS and QCM. The proteins selected for the study were albumin, collagen, lysozyme and IgG.

**RESULTS:** A range of brushes with varying PEO/PAA ratio was obtained by simultaneous grafting from solutions with different proportions of these polymers [1]. Conditions of pH and I leading to a PAA conformation suitable for the adsorption or desorption of proteins on mixed PEO/PAA brushes were identified on PAA homobrushes [2], as illustrated in Fig. 1 for albumin. As presented in Fig. 2, adsorption was then successfully switched ON and OFF for different proteins (albumin, lysozyme, collagen) [3]. The triggered behavior was reversible and could be repeated.

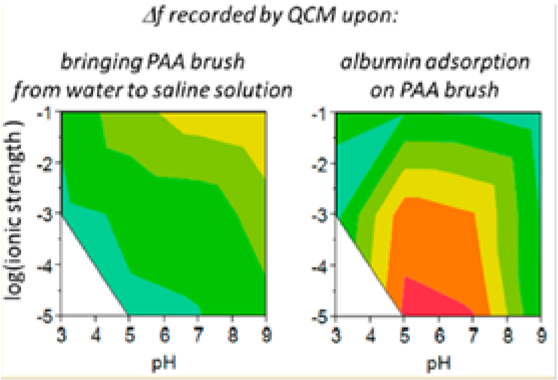

*Fig. 1: Δf values recorded by QCM in given pH and I conditions (red = more negative Δf values).*

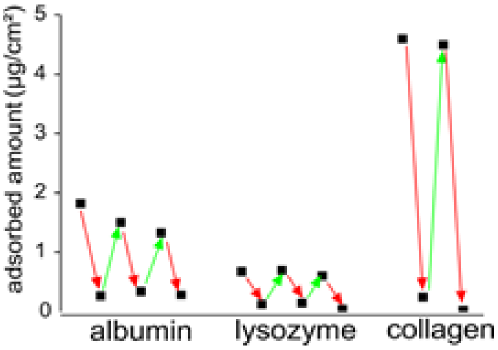

*Fig. 2: Cycles of protein adsorption/desorption performed on mixed PEO/PAA brushes.*

**DISCUSSION & CONCLUSIONS:** The results obtained with proteins showing very different characteristics highlight the robustness and versatility of the approach. The created high performance smart interfaces will find applications in biosensors, drug delivery or nanotransport.

**ACKNOWLEDGEMENTS:** The authors acknowledge F. Du Prez and W. Van Camp (PRG, Ghent University, Belgium) for kindly providing PAA, and S. Demoustier-Champagne for discussion. M. D. thanks the Belgian National Foundation for Scientific Research for her Research Fellow position.

# Flame sintered HAP adopted to bone properties

E Freimanis[1], L Pluduma[2], KA Gross[2], M Kylmälahti[3], Y Dekhtyar[1], H Koivuluoto, P Vuoristo[3]

[1]Institute of Biomedical Engineering and Nanotechnology, Riga Technical University, Latvia, [2]Biomaterials Science and Research Laboratory, Riga Technical University, Latvia, [3]Thermal Spray Facility, Tampere University of Technology, Finland

**INTRODUCTION:** Titanium prostheses coated with hydroxyapatite (HAp) provide a biocompatible surface for interaction with bone tissue. Recent studies demonstrated that the bone surface has an electrical potential that influences attachment of osteoblastic cells to the bone [1,2]. Therefore, the HAp surface could benefit from an electric potential equal to bone. This could be achieved with HAp flame deposition, where HAp particles are molten and accelerated towards the substrate. An electric field is directed onto the coating while injecting water vapor to impart an electric field on the surface of the HAp layer. The research study will report on the electrical potential formed on the surface after such processing.

**METHODS:** During the experiment, three HAp flame deposition modes were used:

1. HAp powder sprayed in air (thermal spraying) (no *E*, no $H_2O$);
2. HAp powder sprayed and after deposition stored in water vapor saturated atmosphere (no *E*, with $H_2O$).
3. HAp powder was sprayed, and the coating subjected to an electric field (*E*) and water vapor ($E=5\cdot10^5$ V/m) (with *E*, with $H_2O$).

The electric potential of the deposited HAp surface was measured by *Kelvin probe microscopy* technique. Measurement error for this device is $\pm5\cdot10^{-6}$ V.

**RESULTS:** The electric potential (the induced charge is directly connected to the potential) of the HAP surface varied with the deposition mode (*Fig.1*).

The HAp samples, coated and kept in a water vapor, had the highest surface electrical potential. It was assumed that HAp lost hydroxide groups ($OH^-$) because of the high temperature of the spraying process. Therefore, the HAp coating lost charge that the hydroxide group was carrying. Exposure of the sample to the atmosphere with high humidity brought $OH^-$ back to the sample surface [3] and increased its electric potential.

The electrical potential of the deposited HAp was similar to the mature bovine bones surface (F*ig. 1.*)[4].

**DISCUSSION & CONCLUSIONS:** The flame deposition is an instrument to engineer electric potential of the HAp coating. It was proven thatan atmosphere saturated with water significantly increases the electric potential of the HAp surface after thermal spraying (electric potential increased from 0,71 V to 1,17 V when kept in water vapor). By this method, the electric potential of the HAp surface can be achieved close the one of the bones (electric potential of bones is 1,04 V) [4]. The electric field that was applied during spraying process didn't affect electric potential.

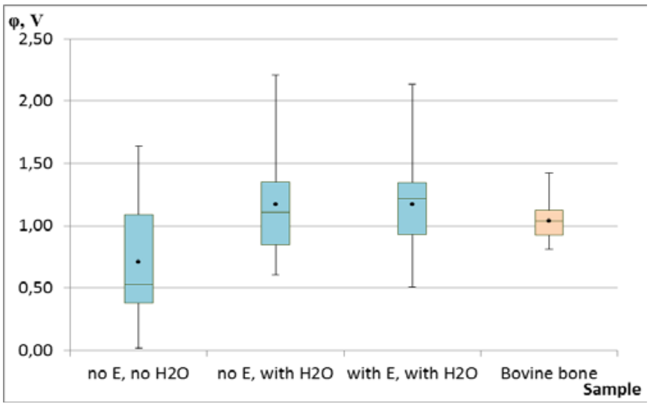

*Fig. 1: The electric potential (φ) values of different HAp coatings and compared to the electric potential of bone. The plot shows 25 and 75 % quartiles, min. and max. values and average value (displayed as a dot).*

# Influence of alkali metal additives on phase transition of translucent $ZrO_2/SiO_2$ glass ceramics prepared by a sol-gel method

L Fu, M Andersson, E Unosson, C Persson, H Engqvist, W Xia

*Division of Applied Materials Science, Department of Engineering Sciences, Uppsala University, Uppsala, Sweden*

**INTRODUCTION:** Translucent $ZrO_2/SiO_2$ glass ceramics prepared by a sol-gel method could be an alternative to the commonly used lithium disilicate for dental applications [l]. Advantages with sol-gel is that it enables mixing at an atomic level and the dried gel can be processed at lower temperature. However, shrinkage of up to 50% may occur during drying and sintering of the gel, which leads to cracks that may propagate throughout the whole sample. This limits the application of sol-gel method while making large bulk glass ceramics. The aim of this study was to lower the glass transition temperature by adding alkali metal, and hence achieve specimens with a lower porosity, as well as a lower amount of cracks.

**METHODS:** A sol-gel was produced using alkoxide precursors including silicon tetraoxysilane (TEOS) and Zirconium (IV) propoxide solution. The precursors were mixed with ethanol (99 %) and HCl (0.4 M) and kept under stirring to ensure homogeneity of the sol. Lithium chloride (LiCl) and sodium chloride (NaCl) were added to the above sol, which was then poured into disc-shaped Teflon moulds at room temperature for gelation. After a controlled aging process, a two-step drying process was carried out: (1) at 100°C for 5h in 100% humidity atmosphere; (2) at 150°C for 15h without humidity. To remove organic compounds and control the crystal size a calcination plateau was used during sintering. The temperature of the calcination plateau was 400°C or 800°C. Samples were held for 5 h at 400°C and for 1 h at 800°C. Two final sintering temperatures, 1000°C or 1100°C, were chosen, and the holding time was 10 h. The phase transition was analysed by thermogravimetric analysis (TGA/SDTA851$^e$, Mettler Toledo) analysis and X-ray diffraction analysis (Siemens Diffractometer D5000)

**RESULTS:** Figure 1 shows the XRD patterns of samples containing different amount of LiCl and NaCl. An increase of Li content resulted in the formation of $ZrSiO_4$ while no changes were found when adding Na at 1000°C. When sintered at 1100°C, $SiO_2$ and monoclinic $ZrO_2$ were formed when adding LiCl and NaCl.

**DISCUSSION & CONCLUSIONS:** According to a previous study [2], only amorphous $SiO_2$ and tetragonal $ZrO_2$ are found in $ZrO_2/SiO_2$ glass ceramics when sintered below 1100°C. Clear peaks of $ZrSiO_4$ were found when LiCl was added, which indicates that lithium could be used for lowering the glass transition temperature, and decrease the reaction temperature of $ZrO_2$ and $SiO_2$. However, sodium did not have the same effect.

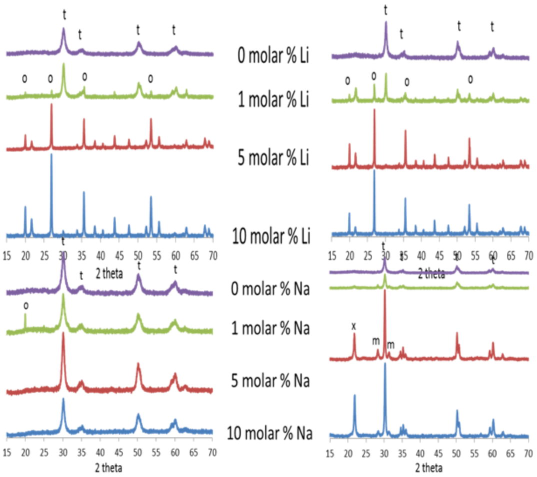

*Fig. 1: XRD patterns of samples with different amounts of LiCl and NaCl (samples sintered at 1000°C are presented to the left and at 1100°C to the right.) m- monoclinic $ZrO_2$, x - $SiO_2$, o - $ZrSiO_4$, t - tetragonal $ZrO_2$*

**ACKNOWLEDGEMENTS:** The authors thank Carl Tryggers Stiftelse for the financial support.

# Micro-CT imaging as a tool to study the fracture behaviour of bone cements

SG Gallinetti[1], C Öhman[1]

[1]*Division of Applied Materials Science, Department of Engineering Sciences, Ångström Laboratory, Uppsala University, Uppsala, Sweden*

**INTRODUCTION:** In the last decays the use of micro-computed tomography (or micro-CT) in bone microstructure analysis has been increasing due to its ability of non-destructive 3D imaging at high resolution. This technique is not just useful to study bone but can also be applied to implants or materials for bone augmentation. Among the latter calcium phosphate cements (CPCs) are highly interesting materials due to their injectability and chemical similarities to the mineral part of bone tissue [1]. However, CPCs are brittle materials and even if they are used in non-load-bearing sites or sites of pure compressive loading it would be important to understand their fracture behaviour. The aim of this preliminary study was to investigate the possibility to use micro-CT imaging to study the fracture behaviour of CPCs during compression tests.

**METHODS:** Brushite cement were prepared by mixing monocalcium phosphate monohydrate (sieved to < 75 µm) and β-Tricalcium Phosphate powders, containing respectively 1 wt% of disodium dihydrogen pyrophosphate, at a molar ratio of 45:55, with 0.5 M citric acid at a liquid to powder ratio of 0.22 ml/g. The mixing was mechanical using a Cap-Vibrator (Ivoclar Vivadent). Samples with a diameter of 6 mm and a height 12 mm were moulded for compressive testing. After setting in PBS for 24 hours, the samples were polished and scanned with a micro-CT (Skyscann 1172, Bruker), using a source voltage of 100 kV, a current of 100 µA, an aluminium and cupper filter and an isotropic pixel size of 9 $\mu m^2$. Wet compressive strength (CS) was measured using an universal testing machine (Shimadzu, AGS-X), with a crosshead speed of 1 mm/min. Thereafter the samples were rescanned in the micro-CT to visualise the fracture in 3D. Reconstruction, 3D visualisation and analysis of the micro-CT images were performed using respectively the softwares NRecon, CTvox and CTAn (Skyscan, Bruker).

**RESULTS:** The porosity determined by the micro-CT was 1.63 % ± 0.33 %. The pore size distribution was determined and ranged from 9 µm to 905 µm. The average CS was found to be 74.4 MPa ± 18.1 MPa. CS decreased with increased porosity. After compressive testing the samples displayed several cracks in the bulk, although just a few went through the whole sample causing its failure (see Fig. 1b).

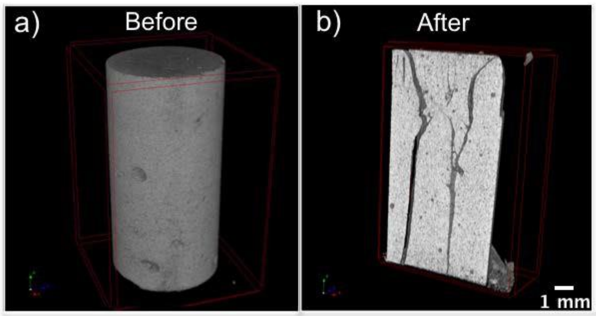

*Fig. 1: Micro CT reconstructions of a) the CPC before testing, and b) a vertical section of the material after compressive testing.*

**DISCUSSION & CONCLUSIONS:** As expected the less porous the CPC samples were, the higher CS was obtained. Micro-CT images before and after CS testing are shown in Fig 1. The CPC after compression tests displayed several cracks, which are clearly visible with this technique (Fig 1b). Micro-CT analysis could be used to closer study the fracture region, in terms of parameters such as porosity and pore size distribution, to better understand the failure mechanisms. This is also the next step for this preliminary study. The resolution could however be a possible limitation since the pixel size will determine the smallest visible pores (max resolution of machine 1 µm). Nevertheless, it is generally larger defects that cause the failure and if necessary other methods [2] could be used to determine the total porosity of the sample.

In conclusion, micro-CT imaging seems to be a promising method to study crack propagation and fracture behaviour in CPCs.

**ACKNOWLEDGEMENTS:** The authors acknowledge Carl Tryggers Stiftelse (CTS 13:533) and Stiftelsen Lars Hiertas Minne (FO2013-0617) for funding.

# Electrochemical attachment of doxycycline to titanium surfaces

S Geißler, H Tiainen, HJ Haugen

*Department of Biomaterials, Institute for Clinical Dentistry, University of Oslo, Norway*

**INTRODUCTION:** Cathodic polarisation has been used to bind doxycycline to implant surfaces aiming at infection control and stimulation of bone formation [1]. It was hypothesised that the molecule binds covalently to a complex layer of hydrogen and oxygen created on the metal surface during the polarisation process. However, the exact binding mechanisms and their effect on short- and long-term availability of doxycycline still remain poorly understood.

**METHODS:** The extent of adsorbed doxycycline on mirror-polished titanium coins that were cathodically polarised for 3 h with a current density of 1 mA/cm$^2$ in 2 M sodium acetate buffer at pH 3 was examined. Doxycycline hyclate was added to the buffer with a concentration of 1 mg/ml. After polarisation, the coins were thoroughly rinsed with deionised water and dried with nitrogen gas. Surface topography was analysed by AFM. Characterisation of the surface chemistry was done by XPS. Furthermore, the presence of doxycycline was evaluated using diffuse reflectance FTIR and fluorescence microscopy. Following this, the coins were immersed in DI water for 10 h and the analyses were repeated.

**RESULTS:** The doxycycline coated coins showed a significant increase in nano-roughness compared to the polished coins. Reduction of the substrate XPS signal and increase of the carbon and nitrogen signal confirmed the presence of an organic layer on the surface. Bands characteristic for doxycycline were seen in the infrared spectra. In addition, the build-up of a fluorescent film was observed. After immersion, the roughness had decreased and the morphology of the surface had changed significantly (Fig. 1). Increased substrate signals as well as decreased carbon and nitrogen signals were detected. The characteristic infrared bands were weakened and fluorescence had disappeared completely.

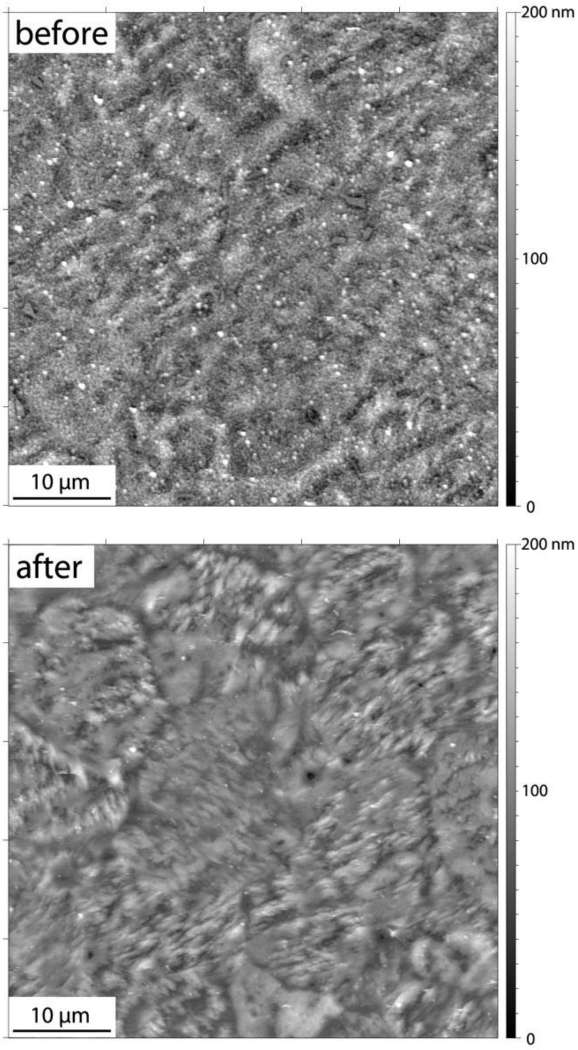

*Fig. 1: AFM images of the doxycycline coated surface before (top) and after immersion (bottom).*

**DISCUSSION & CONCLUSIONS:** An adsorbed layer of doxycycline was found to be present after the polarisation process. This layer could be easily removed by immersion in water and thus only short-term effects can be expected. The remaining lower substrate signal and increased carbon signal indicate that there still is organic material attached to the surface. The nature of this material, the way it is bound to the surface and the potential release of it need to be further explored.

**ACKNOWLEDGEMENTS:** This study was supported by Research Council of Norway grant NFR 230258.

# A 2D1/2 environment with tunable surface mechanical properties for the control of stem cell behavior

L Germain[1,2], M Kuterbekov[2], A des Rieux[1], C Dupont-Gillain[2]

*[1] Advanced Drug Delivery and Biomaterial, Louvain Drug Research Institute, Université catholique de Louvain, Brussel, Belgium [2] Bio & Soft Matter, Institute of Condensed Matter and Nanosciences, Université catholique de Louvain, Louvain-la-Neuve, Belgium*

**INTRODUCTION:** One fundamental aim of tissue engineering is the personalization of grafts. 3D printing is a convenient way to produce scaffolds with a tailored architecture. Beside, stem cells offer promising possibilities in this field because they can be differentiated into the desired cell type. One way to differentiate stem cells is to add bioactive compounds in the culture medium, but this approach may lack efficiency and selectivity, is expensive, and may cause regulatory issues. Physical environment provided by the substrate to which cells adhere are also known to influence cell differentiation. The aim of the project is to coat the surface of a 3D-printed scaffold with a polymer allowing the mechanical properties to be tuned, and to study the influence of different coatings on adipose-derived mesenchymal stem cell (AMSC) behavior. The cells will be exposed to a so-called 2D1/2 environment, ie to a well-controlled microscopic 2D environment (constituted by the millimeter-sized threads of the scaffold) that is part of a 3D macroscopic scaffold.

**METHODS:** 3D structures are built in poly(lactic acid) (PLA) by fused deposition modeling (FDM). These scaffolds are then coated with a poly(dimethylsiloxane) (PDMS) layer as follows: PLA is immersed in a ternary solution of (i) PDMS base and curing agent, (ii) a good solvent of PLA (dioxane), and (iii) a non solvent of PLA which is a good solvent for PDMS (hexane). In this way, the surface of PLA is swollen, and the PDMS chains interpenetrate the PLA chains. Then PDMS is cured. The cross-linking level of PDMS is varied to obtain different surface mechanical properties.

**RESULTS:** Printing conditions were optimized and a µCT scan of a printed scaffold reported a good fidelity compared to the designed model (Fig.1). The presence of the coating was assessed through selective dissolution, and through water contact angle measurements in dynamic conditions, which were significantly different between coated and uncoated samples (Fig.2). Moreover no clogging of the structure was detected after coating.

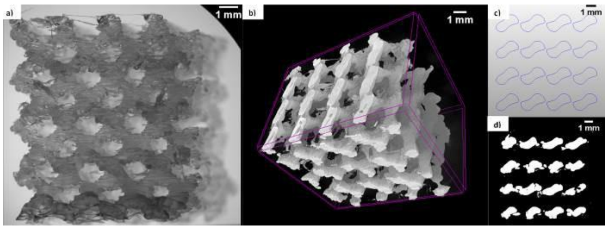

*Fig. 1: Picture (a) and µCT scan (b) of the printed PLA structure. Model (c) and printed (d) shape of one representative layer within the scaffold*

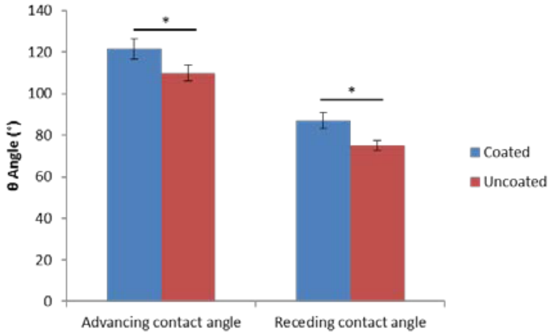

*Fig. 2: Advancing and receding water contact angle of coated and uncoated PLA cylinder (mean±SD, n=3,*p<0.05)*

**DISCUSSION & CONCLUSIONS:** Future work will be centered on the characterization of the coating physical and mechanical properties (thickness, uniformity and elasticity) with µCT, SEM and AFM. Finally, AMSC will be seeded on the obtained scaffolds in order to study their attachment (actin and vinculin coloring), proliferation (picogreen and MTS assay), viability (live and dead test) and differentiation (RT-qPCR). The obtained results will bring new knowledge on the influence of surface mechanical properties on stem cells, in environments suitable for tissue engineering approaches. This should pave the way to innovative strategies for regenerative medicine.

**ACKNOWLEDGEMENTS:** L.G. thanks Carlos A. Fuentes Rojas from the Composite Materials Group (Department of Materials Engineering, KU Leuven) for the µCT scanning.

# Integration of biphasic calcium phosphate bioceramics mixed with autologous mesenchymal cells in osteoporotic rabbit's jaw

A Grishulonoks[1], I Chakstina[2], A Jakovlevs[3], V Zalite[4], I Salma[1], A Skagers[1], V Klimecs[1]

*[1]Department of Oral and Maxillofacial Surgery, Riga Stradins university, [2]Laboratory of biodosimetry and bioanalistical methods, University of Latvia, [3]Department of Pathology, Riga Stradins university, [4]Rudolfs Cimdins Riga Center for development and innovation of Biomaterials, Riga Technical university, Latvia.*

**INTRODUCTION:** Bone tissue engineering using biphasic calcium phosphate bioceramics as scaffold saturated by autologous mesenchymal cells in autologous enviroinement of host living organism as bioreactor is one challenge for substitution of autologous bone grafting [1-2]. The fate of transplanted mesenchymal cells is discused between new bone formation [3-4] and early death with release of some osteotrophic growth factors [5] and mediators for cell recruitments remains unknown.

**METHODS:** Experimental osteoporosis was induced in 8 2,5 years female rabbits by ovarioectomy and 1 mg/kg of methylprednisolone daily for 8 weeks. On 4 animal the holes was created in bouth angles of lower jaw; on the left side filled with a biphasic calcium phosphate bioceramics (HAP/TCP 90/10) granules; on the right side the same granules mixed with autologous fat tissue-derived mesenchymal cells. The two control groups each had 2 rabbits – with the analagous defect of osteoporotic jawbone without bioceramics and without of any defect. After 3 months bone samples for Hem/Eoz staining and mBiotin-streptavidin method for immunohistochemical detection of collagen I were prepared. Semi-quantitative counting method was used for quantification of collagen I positive cells.

**RESULTS:** In healthy bone granules mainly were embeded in new-formed bone, but in osteoporotic bone surrounded by fibrous tissue layer more thick in samples where mesenchymal cells were added. In cases of HAp/TCP bioceramics in osteoporotic rabbit's jaw a lot of collagen I positive structures were counted. Expression of collagen I in cases where granules were mixed with autologous mesenchymal cells noticed numerous positive structures.

*Table 1. Average expression of collagen I in osteoporotic jaw bone defects*

| **Osteoporotic jaw bone defect** | **Expression of collagen I** |
|---|---|
| Defect without filling | +++ |
| Filled with HAP/TCP 90/10 granules | ++++ |
| Filled with HAP/TCP granules and mesenchymal cells | +++ |

**DISCUSSION & CONCLUSIONS:** Integration of HAP/TCP granules in defect of osteoporotic rabbit jaw is through encapsulation by fibrous tissue while in healthy bone osseointegration occurs. The addition of autologous mesenchymal cells resulted in thicker capsule without significant influence on collagen I expression. No signs of inflammation were detected.

# Influence of three-dimensional topographies on osteoblast-like and fibroblast cells

JK Hohmnn[1], G von Freymann[1,2]

*[1] Physics Department and Research Centre OPTIMAS, University of Kaiserslautern, Germany*
*[2]Fraunhofer Institute for Physical Measurement Techniques IPM, Department of Materials Characterization and Testing, Kaiserslautern, Germany*

**INTRODUCTION:** Biological cells are influenced by various signals of their three-dimensional (3D) environment, e.g. through biochemical pathways or physical characteristics of the biointerface, but very little is known about the latter [1]. To achieve a better understanding of cell-template interaction we study the influence of well defined and systematically designed environments on osteoblast-like and fibroblast cells.

**METHODS:** We fabricate microstructures *via* direct laser writing, which enables us to produce three-dimensional features with nearly arbitrary forms [2]. Briefly, the basic idea of the technique is to focus laser light into a photo resist, which is polymerized via two photon absorption within a small focal volume. Non-illuminated areas of the resist are washed away afterwards. The structures are uniformly coated with $TiO_2$ *via* atomic layer deposition, creating a biocompatible and chemical homogeneous surface. To observe proliferation, morphology, differentiation and adhesion of different cell types, SaOs-2 osteosarcoma or NIH 3T3 fibroblast cells are seeded onto the structures. The cells are observed with optical and confocal laser scanning microscopy using different stainings to determine different cell components like nucleus, actin filament, focal adhesion contacts and alkaline phosphatase, an osteoblastic marker (for a detailed description see [3]).

**RESULTS** We report on how geometric parameters influence viability parameters of different cell types. Thereby, we observe that osteoblast-like and fibroblast cells react differently to specific geometric features, which are systematically varied, e.g. cylindrical posts that are arranged on a hexagonal grid (10 µm - 50 µm post distance) and connected with horizontal rods, cylindrical posts that are arranged on a square grid with different post distances, and posts connected with diagonal or trellis-fence rods. We observe that, e.g., osteosarcoma cells show a higher proliferation rate (up to 170 %) on certain structures compared to unstructured surfaces and that they show different morphological features. Osteosarcoma cells on all structures and on unstructured areas possess the osteoblastic marker alkaline phosphatase. Fibroblasts show a different behavior concerning proliferation and morphology. The proliferation rate on structured areas is lower than on unstructured areas, but nevertheless varying in different structures.

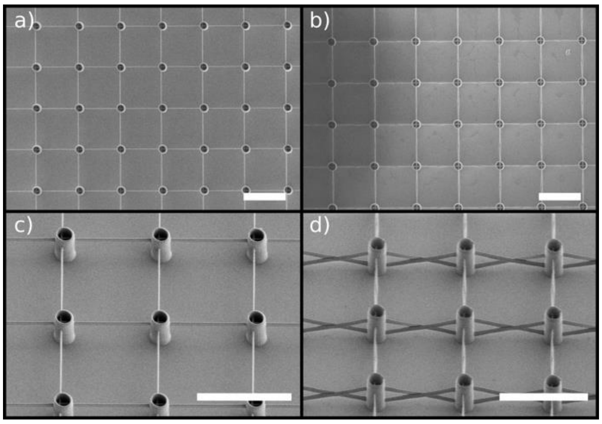

*Fig. 1: Scanning electron micrographs of 3D structures: square grids with 25 µm post distance and horizontal (a - top view, c - tilted view) or trellis-fence rods (b - top view, d - tilted view), scale bar 25 µm, figure modified after [3]*

***DISCUSSION & CONCLUSIONS:*** Our findings show that 3D physical characteristics of structures are able to influence cell proliferation and morphology of both osteosarcoma and fibroblast cells. This might lead to a better understanding of cell-template interaction.

**ACKNOWLEDGEMENTS:** We thank Dr. T. Löber (NSC, TU Kaiserslautern) for FIB preparations, Prof. Dr. C. Ziegler for access to her cell culture laboratory and Prof. Dr. E. Neuhaus (TU Kaiserslautern) for access to his laser scanning microscope.

# Synthesis, characterization and *in vitro* studies of polysulfone/grapheme oxide composite membranes

L Crica, SI Voicu, MA Pandele, M Ionita, H Iovu

*Advanced Polymer Materials GROUP, University Politehnica of Bucharest, Romania*

**INTRODUCTION:** Being characterized by their porous structures and low cost, polymer membranes are extensively studied and rapidly gained popularity in numerous fields of research. Among polymers, one of the most addressed in this respect is polysulfone (PSF), with applications such as wastewater treatments, biosensors or as a biomaterial [1]. This study presents the structural, morphological and physical characterisation, as well as biological performances of graphene oxide loaded polysulfone composite membranes (PSF/GO).

**METHODS:** PSF/GO composite membranes with concentrations of 0.25, 0.5 and 1 wt.% GO were prepared by a phase inversion method [2]. The structural and morphology features were determined through X-ray diffraction, transmission and scanning electron microscopy. Subsequently, water and ethanol flux tests, mechanical behaviour and thermogravimetry were emerged. The biological activity of the substrates was evaluated in terms of cytocompatibility, cell viability and proliferation.

**RESULTS:** All composite membranes were porous and asymmetric (*Figure 1 A*), with an efficient dispersion of GO within the PSF matrix (*Figure 1 B*). It was observed that the addition of GO enhances the thermostability and tensile response of polymer membranes, but it also inhibits water and ethanol flux throughout the membranes. Cytotoxicity evaluation revealed low cytotoxicity potential of the PSF substrate towards mouse mesenchymal stem cells (MSCs), with no additional effect from the 0.25–1 wt.% graphene oxide content. Good cell viability was found in contact with all studied compositions, while the proliferation potential described a tendency to increase in cells cultivated in the presence of GO, as compared to the PSF control (*Figure 1 C)*.

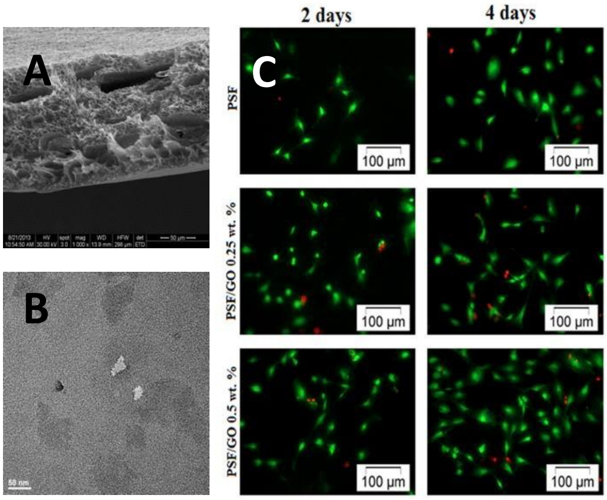

*Fig. 1: SEM image of PSF/GO 1 wt.% asymmetric membrane (A), TEM image of PSF/GO 0.5 wt.% revealing good dispersion of GO sheets and qualitative biological assessments through fluorescence microscopy (C).*

**DISCUSSION & CONCLUSIONS:** GO incorporation within PS matrix influences the structure and morphology, improves thermal, mechanical and in vitro response of the material. The obtained results suggest that the concentration of GO can have a favorable effect on the proliferation potential of mouse MSCs found in contact with PS. Therefore PSF/GO membranes might find their medical applications as tissue regeneration porous supports, *i.e.* for bone or vascular tissue regeneration.

**ACKNOWLEDGEMENTS:** This work was supported by a grant of the Romanian National Authority for Scientific Research, Executive Agency for Higher Education, Research, Development and Innovation; project number PN-II-TE 17/26.04.2013 and by EEA Grants project number 12/12.07.2014

# Correlations between structure and properties of calcium phosphate cements

Z Irbe[1], D Loca[1], D Vempere[1], L Berzina-Cimdina[1]

[1] *Riga Technical University, Institute of General Chemical Engineering, Riga, LV.*

**INTRODUCTION:** Calcium phosphate cement pastes are composed of two or more starting materials and set in reaction between starting materials that precipitate to form a new crystalic solid phase.

The shape and size of the precipitated crystals, as well as the amount of space between crystals (porosity) affects the properties of the set cement.

In this work it is shown how differences in crystal structure affect the compressive strength of the cement.

**METHODS:** α-TCP (synthesised at 1350°C from calcium carbonate and dicalcium phosphate and milled) was the solid component of the cement. To modify cement microstructure it was set by mixing with sodium phosphate setting solutions with various pH values.

The compressive strength was determined using an universal testing machine at constant speed of 1 mm/s until failure. The shape of precipitated crystals was observed using field emission scanning electron microscopy (SEM). The porosity of samples was determined using Archimedes method.

**RESULTS:** If the porosity is kept constant, compressive strength is higher, if the precipitated crystals are large and flat compared with smaller needle like crystals, see Fig. 1 and Fig. 2.

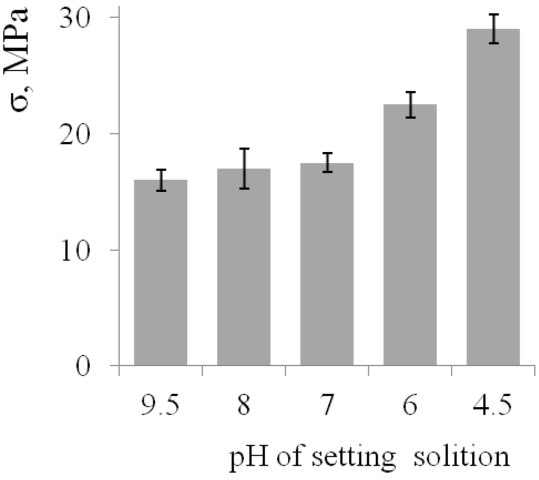

*Fig. 1: Compressive strength of cements (aged 24 h) with different pH of the cement setting liquid.*

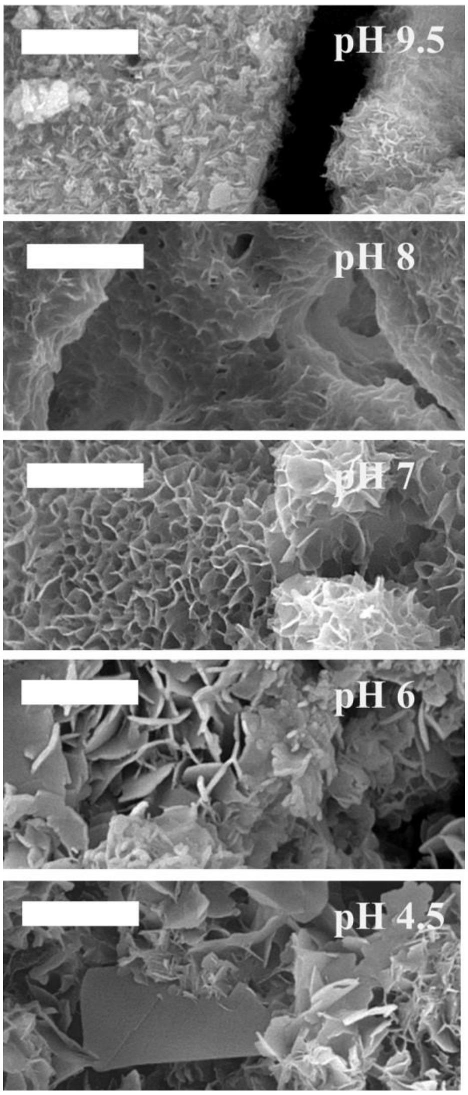

*Fig. 2: SEM images of cement aged (24 h) microstructure, pH of setting solution is given; setting solution contains 0.5 M phosphate ions.*

**DISCUSSION & CONCLUSIONS:** Mechanical properties of calcium phosphate cement can be improved, if larger and flatter crystals are precipitated upon cement setting. The shape of precipitated crystals can be altered by changing the pH of the environment as the cement sets.

**ACKNOWLEDGEMENTS:** This work has been supported by the National Research Programme No. 2014.10-4/VPP-3/21 “MultIfunctional Materials and composItes, photonicS and nanotechnology (IMIS$^2$)” Project No. 4 “Nanomaterials and nanotechnologies for medical applications”.

# Energy efficient water treatment using the blueprint of nature: Combining aquaporins with lipids and mesoporous silica to purify water

S Isaksson[1], F Höök[2], M Andersson[1]

[1] *Dept. of Chemical and Biological Eng., Chalmers University of Technology, Gothenburg, Sweden*
[2] *Dept. of Applied Physics, Chalmers University of Technology, Gothenburg, Sweden*

**INTRODUCTION:** The growing population in areas where fresh water supplies are scarce is resulting in difficulties satisfying the demands for drinking water. Pollution and environmental changes are increasing the demands further. Improvements in water treatment processes are therefore needed, an achievement we suggest to fulfil by developing a device that treats water using a biomimetic approach (figure 1).

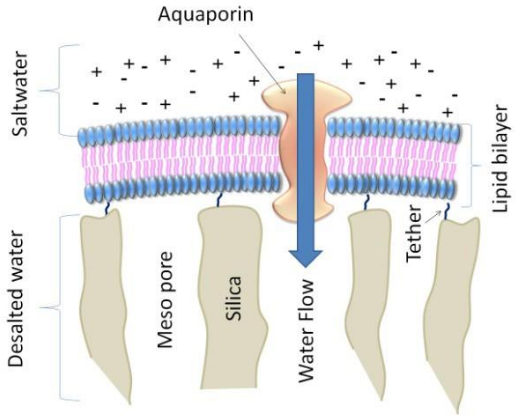

*Fig. 1: Illustration of the proposed water treatment device.*

**METHODS:** Contaminated water is purified using a filter that resembles the membrane of living cells. The cell membrane possesses excellent purification capabilities due to the presence of transmembrane transporter proteins that provide selectivity to an otherwise essentially impermeable lipid bilayer.

The osmotic pressure difference present in the treatment process (figure 1) has to be overcome, a task that is performed by applying an external driving pressure which will force the water molecules to penetrate the membrane through the aquaporins. The lipid bilayer is however not mechanically robust enough to withstand such pressures by itself, which is why we are utilizing a mesostructured support material that provides the design with robustness while supplying the aquaporins with desired aqueous domains on both sides of the bilayer.

The analysis method of choice for studying the surface interactions is QCM-D. Substrate characterisation is carried out using TEM and SAXS whereas the lipid bilayer characteristics are investigated using Fluorescence spectroscopy and cryo-TEM (figure 2).

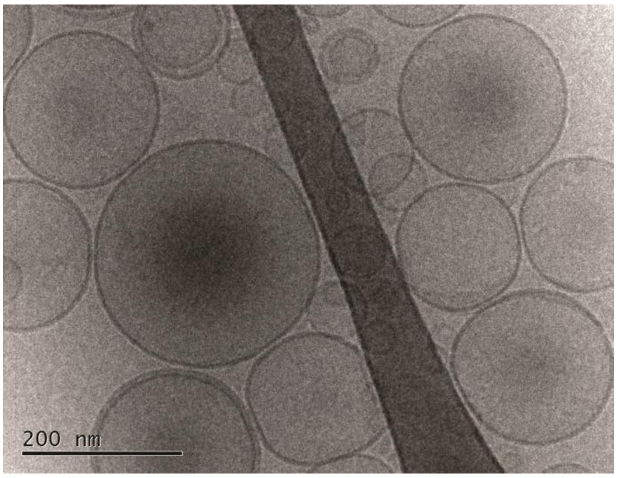

*Fig. 2: Cryo-TEM micrograph of proteoliposomes captured prior to bilayer formation.*

**RESULTS:** We have shown that it is possible to take advantage of the solid supported lipid bilayer design for transmembrane protein incorporation using mesoporous silica as a support for the lipid bilayer. The walls of the pores provide stability to the bilayer while the pore spanning part of the bilayer is surrounded by an aqueous environment suitable for protein incorporation [1].

**DISCUSSION & CONCLUSIONS:** We have proved it possible to deposit a fluid lipid bilayer hosting aquaporins on mesoporous silica using a straightforward approach. The proteins are provided with favourable aqueous environments on both sides of the bilayer by pores that are slightly wider than the aquaporins themselves. The walls in between the pores stabilize the lipid bilayer. All in all, we achieve a robust yet protein friendly design, which bodes well for accomplishing energy efficient water treatment.

**ACKNOWLEDGEMENTS:** The authors acknowledge The Swedish Research council Formas for the financial support of the project.

# Hydroxyapatite-based biocomposite with silver nanoparticles: synthesis and characterization

AA Ivanova[1], RA Surmenev[1, 3*], MA Surmeneva[1], TM Mukhametkaliyev[1], K Loza[2], O Prymak[2], M Epple[2]

*[1]National Research Tomsk Polytechnic University, Tomsk, Russia, [2]Inorganic Chemistry and Center for Nanointegration Duisburg-Essen (CeNIDE), University of Duisburg-Essen, Essen, Germany, [3]Fraunhofer Institute for Interfacial Engineering and Biotechnology IGB, Stuttgart, Germany*

**INTRODUCTION:** Modification of implant surfaces is in the interest of many scientists worldwide [1]. The present study is devoted to development of the antibacterial biocomposite with prolong bactericidal activity and biocompotability. A biocomposite containing hydroxyapatite (HA) and silver nanoparticles (AgNPs) has been fabricated by using wet chemical synthesis and radio frequency (RF) magnetron sputtering.

**METHODS:** Ag-NPs were synthesized by a wet chemical reduction method of silver nitrate using glucose as a reductant and polyvinylpyrrolidone as a stabilizer [2]. AgNPs were deposited onto titanium substrate via dripping/drying technique and were further covered with HA coating by means of RF-magnetron sputtering [3, 4]. The coating was deposited at an RF-power level of 500 W in Ar atmosphere at grounded substrate holder for 180 min. The morphology and composition of the samples were estimated by SEM. To determine the internal structure and phase composition of studied thin films the Grazing-incidence small-angle X-ray scattering was used. Silver release assay was conducted in two different types of artificial fluids: acetate buffer (Ac, pH=5.7) and phosphate buffer (Ph, pH=7.4) using AAS technique by adding to each medium 1 mL of $HNO_3$. *In vitro* behavior of biocomposite in contact with osteoclast-like cells line U-937 was estimated.

**RESULTS:** The negatively charged AgNPs with a spherical shape and a diameter of the metallic core 50±20 nm were coated with dense, nanocrystalline HA film. The diffraction patterns of the formed coatings showed peaks corresponding to HA and metallic silver. The RF magnetron sputter deposition of HA film on the AgNPs layer did not affect the amount of silver on the substrate surface, the nanoparticle size and morphology. SEM of the cross section in backscattering mode showed the layer of silver nanoparticles below the CaP layer (Fig. 1). The release of Ag ions from the developed biocomposite in the phosphate and the acetate buffers within 7 days of immersion were 0.27±0.02 and 0.54±0.02 µg/mL, respectively, which is below the cytotoxic level of Ag ions found in the literature [5]. *In vitro* study showed that Ag-HA biocomposite within first 7 days of incubation did not suppress the differentiation of the cells from the monocyte/macrophage lineage into osteoclasts which had similar behavior to those on HA coating.

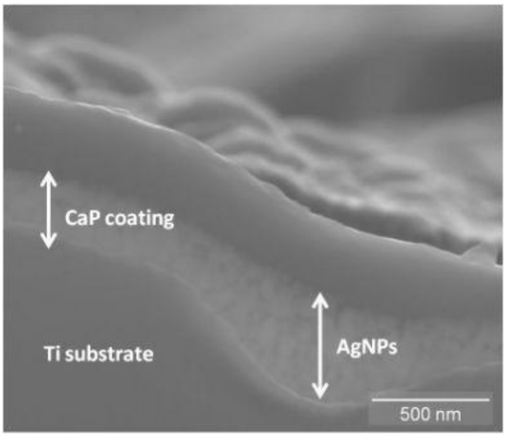

*Fig. 1: The SEM image of the cross-section of AgNPs-HA biocomposite.*

**DISCUSSION & CONCLUSIONS:** We suggest that in order to control the release of silver ions from the biocomposite resorbability of the HA layer should be tuned by changing the coating crystallinity. This strategy may be considered as a further approach to ensure sufficient antibacterial efficacy and low cytotoxicity of the biocomposites.

**ACKNOWLEDGEMENTS:** The authors are thankful to the RFBR (14-08-31027 мол-а, 15-08-08652), the Russian President's Stipend SP-6664.2013.4 and MK-485.2014, NAUKA #11.1359.2014/K.

# Effects on organic degradation in the $TiO_2/H_2O_2$/UV-Vis system

O Janson[1], E Unosson[1], H Engqvist[1], K Welch[2]

*[1]Division of Applied Materials Science, Department of Engineering Sciences, The Ångström Laboratory, Uppsala University, Sweden. [2]Division of Nanotechnology and Functional Materials, Department of Engineering Sciences, The Ångström Laboratory, Uppsala University, Sweden*

**INTRODUCTION:** Restoration of missing teeth using dental implants is a well-established clinical procedure. Today the main problem is the occurrence of peri-implantitis. In order to save implants with peri-implantitis new cleaning protocols need to be developed. One key aspect is to find efficient and safe antibacterial cleaning solutions or gels. One cleaning protocol includes the use peroxide gels combined with titania. This study explores different concentration of components and wavelengths of light activation, within a gel of $TiO_2$ and $H_2O_2$. The gel produces bacterial killing ROS (Reactive Oxygen Species) upon irradiation with UV light, where the ROS is sought to kill bacteria.

This study explores the organic degradation potential in the $TiO_2/H_2O_2$/UV-Vis system by varying $TiO_2$ and $H_2O_2$ photoactivation energy and concentrations within acceptable limits, to detect governing factors and potential synergy effects.

**METHODS:** $TiO_2$ (Degussa P25), $H_2O_2$, Rhodamine B (RhB) and deionized water were mixed in a beaker to a volume of 65 ml, to concentration according to Table 1. An aliquot of 4 ml was introduced in a cubic cuvette for exposure of light of 365 nm, 405 nm and 470 nm and at dark. 1 ml of the supernatant were introduced into a 1,5 ml cuvette to be analyzed in a UV-Vis spectrophotometer (UV-1800, Shimadzu, Kyoto, Japan) to see how much of the dye have degraded.

*Table 1. The compositions of the samples.*

| $H_2O_2$ (wt%) | $TiO_2$ (g/l) | Rhodeamine B (µM) |
|---|---|---|
| 0 | 0 | 15 |
| 6 | 0 | 15 |
| 0 | 0,5 | 15 |
| 6 | 0,5 | 15 |

**RESULTS:** As seen in Fig. 1., an increase in RhB degradation from 2,9 % to 94% is obtained when $TiO_2$ is added and exposed to 365 nm light. At 405 nm the RhB degradation increases from 2,3 % to 75 %. A small increase is found when only $H_2O_2$ is present in the sample. In dark conditions the degradation increases with addition of $H_2O_2$ to the $TiO_2$ sample.

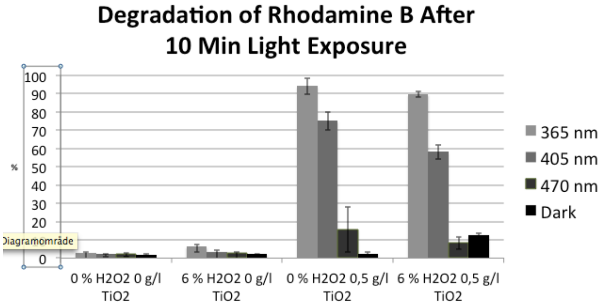

*Fig 1. Degradation of Rhodamine B after 1 minute light exposure at 365, 405, 470 nm and at dark.*

**DISCUSSION & CONCLUSIONS:** The concentration of $TiO_2$ was the parameter that had the most impact on the degradation potential at both 365 and 405 nm. A synergistic effect was also found in dark conditions when adding $H_2O_2$ to $TiO_2$. However, the RhB degradation was still very low. These results indicate that 405 nm light could yield as high as 75 % degradation in 10 min.

**ACKNOWLEDGEMENTS:** Eurostars project NuGel.

# Two-photon growth and modification of a PEG-based hydrogel

C Jungnickel[1], M Tsurkan[2], C Werner[2], M Schlierf[1]

*[1]B CUBE – Center for Molecular Bioengineering, TU Dresden, Germany, [2]IPF – Leibniz-Institut für Polymerforschung Dresden e.V., Germany*

**INTRODUCTION:** Hydrogels are used on an everyday basis in several different fields like contact lenses [1], biomimetic scaffolding [2] and drug delivery [3]. Hydrogels are becoming increasingly popular in biological and medical sciences because of their broad application possibilities for tissue engineering. Hydrogels allow 3D cell culturing and thus better mimic the spatial environment of cells in tissues, compared to 2D tissue culture plates.

**METHODS:** Here, we present a novel approach to build up a hydrogel with nanometer precision in 3D around a living cell *via* two-photon reaction [4]. In comparison to previous approaches, the polymer based hydrogel does not require photo-initiators for its reaction. Instead we use maleimide groups which require no additional activator to bind covalently during the two-photon process. The two-photon process allows a high spatial and temporal control and enables furthermore a precise surface or volume structuring with a broad selection of functionalized biomolecules.

**RESULTS:** In a first set of experiments, we studied surface density and reproducibility of surface patterning using maleimide-modified fluorophores. We wrote a fluorescent pattern with varying laser power and writing speed on the sample surface (Figure 1). The laser power and writing speeds were optimized with the aim of limiting laser pulse energy to minimize photo-damage to biomolecules while at the same time writing mechanically stable structures.

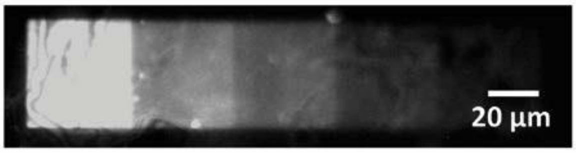

*Fig. 1: Fluorescence image of written fluorescent structures of 40x40 µm$^2$ squares, writing speed 325 µm/s, with decreasing laser power from 8.1 mW to 0.1 mW in 2 mW steps*

As a next step we moved from 2D patterns to 3D structures. We were able to build up 3D PEG-(polyethylene glycol) based hydrogel structures with submicron feature size (Figure 2) without any photo-initiator or additional substrate. The created hydrogel structures exhibit a typical line width of 1 µm and are very regularly structured.

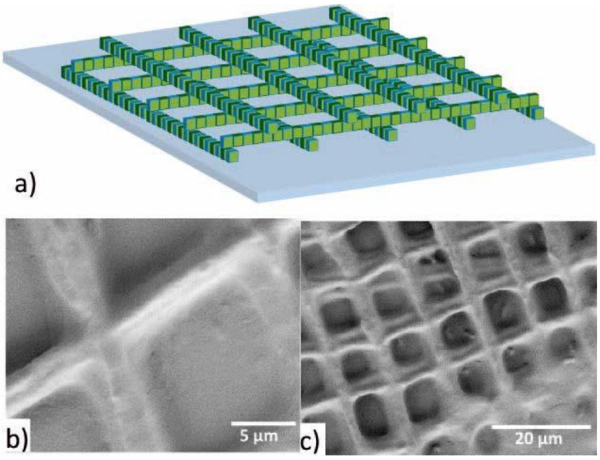

*Fig. 2: 3D Woodpile structures: a) schematic of a written PEG-based hydrogel; b) and c) scanning electron microscope images of dried PEG-maleimide woodpile structures*

**DISCUSSION & CONCLUSIONS:** We introduce a novel approach of submicron defined surface patterning and the creation of a 3D hydrogel without photo-initiators. Therefore it is now possible to trap cells in a hydrogel cage, manipulate and release them afterwards without the toxic effects from a photo-initiator.

**ACKNOWLEDGEMENTS:** The project is funded by BMBF 03Z2EN11.

# Effective substitution of carbonates and silicates for orthophosphates in nanocrystalline hydroxyapatite enriched in $Mn^{2+}$ cations

M Jurkitewicz, K Szurkowska, J Kolmas

*Medical University of Warsaw, Faculty of Pharmacy, Warsaw, Poland*

**INTRODUCTION:** Synthetic hydroxyapatite (HA) is commonly used as bone substitutes, metallic implant coatings or dental materials. An exceptional feature of HA is the ability of partial ionic exchange that determines biological and physicochemical properties [1]. Silicate and carbonate substituted apatites are the subjects of intense studies in materials engineering [2]. These ions are the components of biological apatite (i.e. of bone or enamel). Carbonate is the main "impurity" in biological apatite determining its solubility. Silicon plays a crucial role in bone formation and calcification [3]. Manganese is a trace element which deficiency may lead to a weaker bone growth. In addition, it has a positive impact on osseointegration process due to integrins induction [4]. Thus, it seems reasonable to synthesize and analyse hydroxyapatite materials containing carbonates or silicates and enriched in small amount of manganese.

**METHODS:** Pure, as well as substituted hydroxyapatites were synthesized using wet methods. As a source of silicon, aqueous solution of sodium metasilicate was used. In synthesis of carbonated HA, urea hydrolysis was performed to obtain carbonate ions. In all synthesis, the manganese source was manganese acetate. The obtained powders were dried in air at 100 °C for 5 h. Then they were physicochemically studied using various methods: powder X-ray diffraction (PXRD), infrared spectroscopy (FT-IR), transmission electron microscopy (SEM), solid-state nuclear magnetic resonance (ssNMR) and X-ray fluorescence (WD-XRF).

**RESULTS:** PXRD diffractograms show that the samples are nanocrystalline and contain only one phase. Both silicate and carbonate substitution have an impact on the parameters of the unit cell. Infrared spectra allowed to estimate the carbonate content in $CO_3^{2-}$-containing samples. $^{1}H$ MAS NMR experiments was used to monitor the structural hydroxyl group concentration as well as the presence of adsorbed water. $^{31}P$ NMR study was a helpful tool for structural investigations. $^{13}C$ and $^{29}Si$ Bloch-decay (BD) and cross-polarization (CP) NMR experiments were performed to monitor carbonate and silicate substitution, respectively. WD-XRF was used for elemental analysis of the obtained powders.

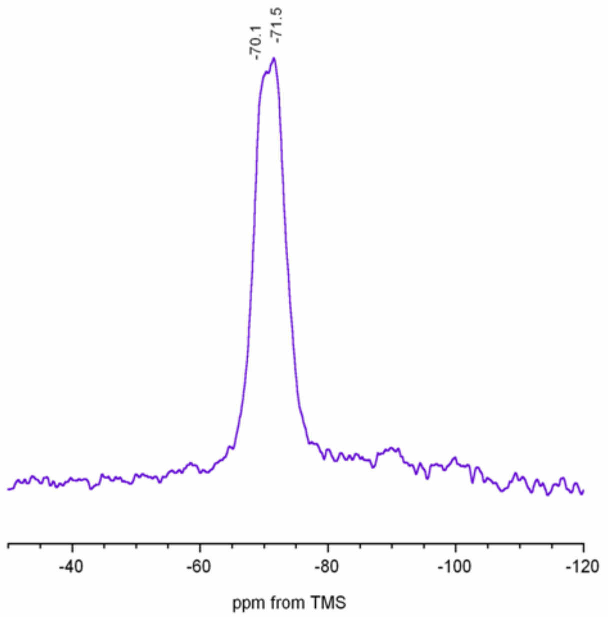

*Fig. 1: $^{29}Si$ CP NMR spectrum of hydroxyapatite containing silicate and $Mn^{2+}$ ions.*

**DISCUSSION & CONCLUSIONS:** We have successfully synthesized hydroxyapatite enriched in manganese and containing carbonate or silicate ions. Our future studies will concern the *in vitro* biocompatibility assays.

**ACKNOWLEDGEMENTS:** J.K. thanks the Foundation for Polish Science for supporting her with the Parent-Bridge Programme that was co-financed by the EU European Regional Development Fund.

# The transient nature of silver chloride charged nanoparticles

D Kalnina[1], KA Gross[1], A Medvids[2], P Onufrijevs[2]

[1]*Biomaterials Research laboratory, Riga Technical University, Riga, Latvia.* [2]*Institute of Technical Physics, Riga Technical University, Riga, Latvia*

**INTRODUCTION:** Incorporation of a second phase into calcium phosphates requires their stability during processing and compatible resorption characteristics to prevent particle release during use in the body. The first consideration needs to be given to obtaining a stable phase for incorporation into a resorbable matrix, especially if the secondary phase is made in aqueous media alongside the synthesis of calcium phosphates.

Incorporation of charged particles requires a more rigid assessment of changes during synthesis. For silver halides made as colloids, the question arises on the stability of the colloids over time. UV spectra provide this opportunity for real-time assessment.

The objective of this study is to evaluate the UV spectra of silver halide colloids over time for determining the stability in solution and then assess the antimicrobial properties.

**METHODS:** Synthesis: Colloids of silver halogens (AgBr, AgI and AgCl) were synthesized by a condensation reaction route from silver nitrate and potassium iodide solutions. ACP suspensions were produced by pouring a calcium nitrate solution into a stirred ammonium hydrogen phosphate solution buffered to pH 10 using ammonium hydroxide so as to provide a Ca/P ratio of 1.7.

Characterization and testing: Absorption spectra of silver halogens colloids in water nanoparticles were obtained using a Shimatzu SolidSpec-3700 spectrometer at room temperature immediately after chemical condensation and with a time increment of 30 minutes.

**RESULTS:** The time dependent AgI and AgBr colloids absorption spectra showed almost stable exciton peaks; these colloids stabilized, as observed from the saturation effect of absorption spectra intensities. However, for AgCl, a strong “red shift” (>0.7eV) of exciton band position was observed in the absorption spectra (Fig.1.) The “red shift” is explained by a Quantum confinement effect. The calculation of the nanoparticle size for particles subjected to a strong quantum confinement effect [3] showed that the initial AgCl size was 3 nm. This small size readily induced changes and that was reflected in changes of the UV spectra.

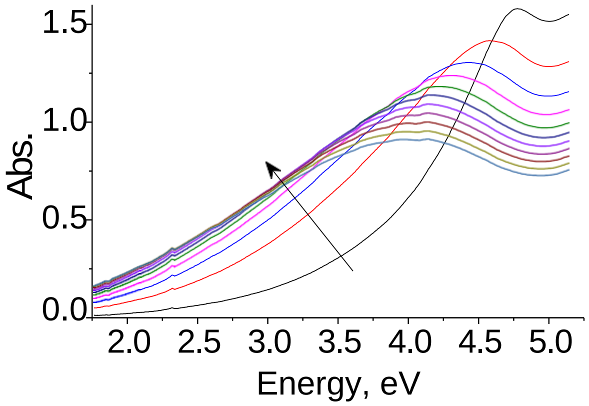

*Fig.1: UV–VIS time dependent absorption spectra of AgCl sol.*

**DISCUSSION & CONCLUSIONS:** The study showed the possibility to use the condensation reaction route method to obtain nanosized AgCl nanoparticles with size comparable to the Bohr radius of the exciton. UV absorption measurements showed a more pronounced change with AgCl than with other silver halides, emphasizing a change in characteristics over time. Processing of silver chlorides required special attention to the time within solution. Further experiments need to be conducted to learn about the change with time.

# HAp/TCP granules for augmentation of narrow alveolar bone before dental implant placement / case report

A Skagers[1], V Klimecs[1], B Nemtsev[2], L Neimane[3], V Zalite[4]

*[1]Department of Oral and Maxillofacial Surgery, Riga Stradins University, Institute of Stomatology, [2]Nemtsev Family clinic, Riga, Latvia, [3]Department of Oral and Maxillofacial Radiology, Riga Stradins University, Institute of Stomatology, [4]Rudolfs Cimdins Riga Center for Development and Innovation of Biomaterials, Riga Technical University, Latvia*

**INTRODUCTION:** After long time absence of teeth alveolar bone resorbs and ridge deformities as knife edge ridge develops [1-2]. The width of the resorbed alveolar crest necessary for dental implant placement can be achieved with *onlay* bone grafts, membrane techniques, bone distraction and bone splitting [3-4]. Granules of synthetic bone substitutes may be challenges for substitution of autologous bone grafting as in our case report.

**METHODS:** On five patients with atrophy of mandibular alveolar bone up to 1 – 2mm on the crest horizontal augmentation with synthetic HAp/TCP granules produced in Rudolfs Cimdins Riga Centre for Development and Innovation of Biomaterials was performed. The treatment plan is completed in presented case. Patient S.A., age 53, female had 2.12mm width of alveolar crest in left posterior mandible. Vertical height from crest to mandibular canal was 15.03mm. On November 29, 2012 using intraoral approach subperiostal tunnel over alveolar bone from buccal side from teeth 33 to 37 was formed and filled with granules HAp/TCP 30/70 0.4<d<1 mm 2.5 ml. On May 29, 2014 three dental implants RS /BEGO 3.75 x 10mm were inserted. On November 11, 2014 implants were exposed and healing screws inserted. Prosthodontic work as metal ceramic bridge was completed in January 2015.

**RESULTS:** 3D CT measurements showed that width of alveolar crest had increased twice. Osseointegration of dental implants was successful.

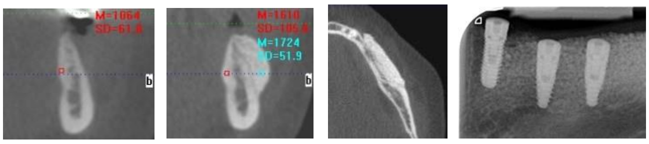

*Fig.1. 3D CT and dental X-ray before and 20/26 months after augmentation and dental implantation*

**CONCLUSION:** In cases of knife edge alveolar bone with enough height the horizontal augmentation by implantation of HAp/TCP granules in subperiostal tunnel results in increase of bone mineral density, formation of stable bone/bioceramics hybrid and successful osseointegration of dental implants.

# The crystallization route determines the range of Ca/P accommodated in apatite

L Komarovska[1], KA Gross[2]

*[1]Faculty of Chemistry, University of Latvia, Latvia, [2]Biomaterials Research Laboratory, Riga Technical University, Latvia*

**INTRODUCTION:** Calcium phosphates are within the class of materials that can be precipitated as nanosized crystals or pass through an amorphous phase that later is crystallized. The latter pathway offers greater flexibility in the composition, and less restrictions that would otherwise be requested in extending a crystalline lattice during crystal formation. While forming an amorphous phase is easier, it is more difficult to preserve the apatite structure during crystallization. This work addresses the inclusion of excess calcium in an amorphous phase to see how much additional calcium is accommodated through crystallization of a monophasic apatite. A series of crystallization routes will be examined to see which production method maintains the apatite phase with increasing Ca/P ratio.

**METHODS:** Amorphous hydroxyapatites with an increasing Ca/P molar ratio (Ca/P ratio of 1.67, 2.0, 2.2, 2.4, 2.6 and 2.8) were synthesized, freeze-dried and then crystallized in three ways: at an elevated temperature and pressure in water or steam, and at an elevated temperature. This was achieved in a hydrothermal bomb and a cylindrical furnace.

For crystallization in hydrothermal conditions, powder was placed into a 18ml hydrothermal vessel (in water or in water vapor) and heated at 150 °C for 2 hours. Calcination at an elevated temperature was performed at 700°C for 2 hours in the furnace to remove absorbed species for characterization.

The crystallization temperature of synthesized powders was determined by differential thermal analysis (DTA) and qualitative phase analysis conducted on X-ray diffraction (XRD) patterns.

**RESULTS:** Crystallization occurred at a lower temperature for higher Ca/P ratio amorphous calcium phosphates, Table 1.

*Table 1. Thermal analysis shows crystallization at a lower temperature for higher Ca/P molar ratios.*

| Ca/P ratio | Crystallization temperature, °C |
|---|---|
| 1.67 | 560 – 597 |
| 2.0 | 530 – 575 |
| 2.2 | 520 – 560 |
| 2.4 | 490 – 555 |

Analysis by X-ray diffraction showed an amorphous phase was retained for Ca/P ratios of 1.67 to 2.60. Greater Ca/P ratios formed a crystalline phase. XRD was also used to identify the crystalline phases after crystallization.

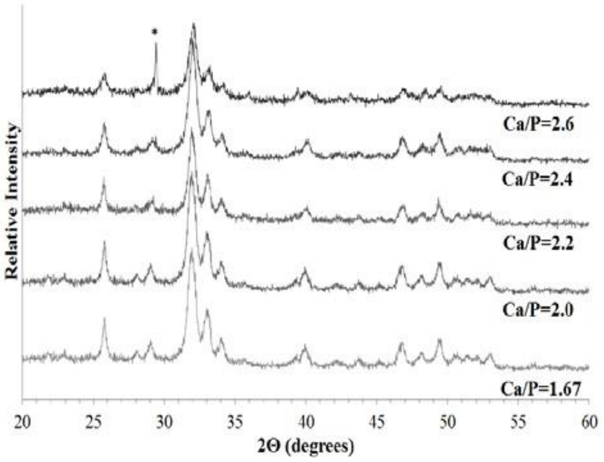

*Fig. 1: Apatite with various Ca/P molar ratios after crystallization in water vapor at 150°C/ 2h.*

Monophasic HAp was gained over a wide range of Ca/P ratios from 1.67 to 2.40 when crystallized in steam, Fig 1. Greater Ca/P ratios of 2.6 and 2.8 showed a minor amount of unidentified peak*. Processing of the amorphous phase in water at elevated temperature and pressure, as well as crystallization in the cylindrical furnace only retained an apatite up to Ca/P of 2.2.

**DISCUSSION & CONCLUSIONS:** The amorphous phase maintained a single phase over a larger Ca/P ratio range than the crystallized apatite. The amorphous phase occurred for Ca/P from 1.67 to 2.6, however crystalline apatite was only kept for compositions up to Ca/P of 2.4. This reflected the greater flexibility of the amorphous phase to accommodate variations in chemistry. The processing method dictated the flexibility in the apatite that could be accommodated. Heating is steam maintained the apatite lattice, while in water or at a higher temperature in air, decomposition occurred more readily.

# Structure of rf-magnetron calcium phosphate coating obtained at different modes of deposition

Yu Sharkeev[1,2], KA Gross[3], K Kulyashova[1], A Sainova[1,4], E Dauksta[3]

*[1]ISPMS SB RAS, Tomsk, Russia, [2]Institute of Physics and Technology TPU, Tomsk, Russia, [3]Institute of Biomaterials and Biomechanics RTU, Riga, Latvia, [4]Faculty of physics and engineering TSU, Tomsk, Russia*

**INTRODUCTION:** Calcium phosphate (CaP) coatings on the base of hydroxyapatite (HA) are widely used in biomedicine. Morphology of implant surface, element and phase composition and structure of coating are often the determining factors in the "success" of the implant. Therefore, the effect of the mode of deposition on structure of the rf-magnetron CaP coating has been studied in the paper.

**METHODS:** Pure titanium VT1-0 was used as substrate material. Formation of the CaP coatings was carried out using a rf-magnetron installation "Yakhont-2M" with a power source frequency of 13.56 MHz. The standard sputtering mode was following. Working gas is argon, chamber working gas pressure is 1 Pa, sputtering period is 3 hours, the RF-discharge power is 250 W. The magnetron CaP target was formed from the HA powder by pressing and annealing in the air at 1273 K. The CaP coatings were examined with X-ray diffractometer (Bruker D8Advance, Bruker, Germany) with Cu Kα radiation. The X-ray generator was operated at 40 kV and 40 mA. The 2Θ angle was varied in range of 5–90° with step of 0.01°. Raman spectra were obtained in Renishaw inVia Raman microscope with laser source operating at 514 nm, power of the laser beam is 50 mW.

**RESULTS:** The XRD analysis of diffraction pattern of titanium substrate with CaP coating showed only reflections from the titanium substrate. Hydrothermal treatment does not lead to crystallization of coating. Reflections from $TiO_2$ (rutile) appeared after isothermal annealing of coating in the air at 700°C. Weak peaks at the 2Θ angle range of 31-34° are also appears. There are the most intensive peaks featuring HA phase – $Ca_5(PO_4)_3OH$ at this 2 Θ range. The research of the coatings with grazing angle X-Ray diffraction confirmed the formation of the $Ca_5(PO_4)_3OH$ phase in coating.

Fig.1 presents Raman spectra of CaP coatings obtained at the following modes of deposition: standard mode, electric bias on the substrate was of -50 V and +50 V, addition of 18%vol. oxygen ($O_2$) in the chamber working gas. Symmetric vibration bands $PO_4^{3-}$ ($\nu_1$) at the range of the Raman shift of 920-980 $cm^{-1}$ are the most intensive bands in apatite specter. Location of the line at the range of 945-950 $cm^{-1}$ confirms presence of disordered phosphate lattice of apatite or formation of amorphous structure of the obtained CaP coating. Addition of 18 vol. % $O_2$ in the chamber working gas resulted in appearance of additional low intensive band (shown by arrow on the fig.). It can be explained by forming of tricalcium phosphate (TCP) or other non-stoichiometric calcium phosphate in coating.

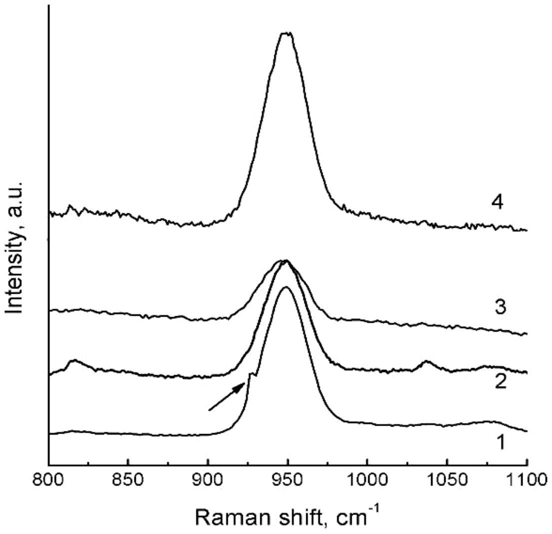

*Fig. 1: Raman spectra of CaP coatings obtained at the following modes of deposition: addition of 18% vol. $O_2$ in the working gas atmosphere (1), standard mode (2), electric bias on the substrate of -50 V (3) and +50 V (4)*

**DISCUSSION & CONCLUSIONS:** Amorphous CaP coatings were obtained at different deposition modes. Crystallized structure was obtained by annealing. Addition of oxygen in the working gas atmosphere resulted in appearance of weak band of TCP or non-stoichiometric CaP on the Raman spectra.

**ACKNOWLEDGEMENTS:** Work was carried out under support of the 7th Framework Program for Research, Technological Development and Demonstration, project № 612691.

# Mesoscopically ordered polymer-apatite nanocomposite inspired from bone nanostructure

A Kumar, W He, AR Bagha, M Andersson

*Department of Chemical and Biological Engineering, Chalmers University of Technology, Gothenburg, Sweden*

**INTRODUCTION:** Biomimetic composites inspired from natural bone composition and structure might pave way to osseointegrative and regenerative orthopaedic implants. Natural bone is a nanocomposite composed of micron-sized subunits with ordered assemblies of collagen fibrils reinforced with poorly crystalline hydroxyapatite (HA). Inspired by the chemistry and nanostructure of cortical bone we have developed a synthetic, mesoscopically ordered, polymer-HA nanocomposite with the HA particles moderately aligned and uniformly embedded in a highly ordered polymer matrix, with potential as bioactive and mechanically stable implant.

**METHODS:** In order to mimic HA mineralization within collagen fibrils, we used molecular self-assembly of lyotropic liquid crystals (LLC) as ordered synthetic mimics of collagen fibrils. In addition the LLCs were covalently crosslinked to form a resilient and flexible polymeric matrix while preserving the ordered structure. Next, bone-like HA was formed in-situ from respective ions within the nanoscopic aqueous domains of the LLCs yielding a composite material with a well-defined nanostructure. The primary LLCs investigated for this purpose were cubic and hexagonal phases formed using synthetic amphiphiles like triblock copolymers. The amphiphiles were chemically modified with diacrylate groups at their head to make them cross linkable in the presence of light or heat.

**RESULTS:** Small angle X-ray scattering data confirmed the presence of meso-ordered (hexagonal and cubic) structure of the nanocomposite suggesting that the ordered assembly was retained following mineralization. Morphologically, transmission electron microscopy (TEM) and X-ray diffraction showed that spherical amorphous calcium phosphates of 30-40 nm in size were formed in the composite immediately after mineralization, which on aging converted to rod shaped, poorly crystalline HA. Moreover TEM images of grounded composites show moderate alignment of the HA nanoparticles due to the possible orientation from the LLC matrix. Analysis of the composite using Raman spectroscopy and energy dispersive X-ray scattering confirmed that the HA was carbonate substituted and calcium deficient, matching the chemistry of bone apatite that might be a result of forming them in confined domains of the LLC[1]. Mechanically, the composite showed compressive strength of 3-4 MPa, which could relate to low HA composition in the polymer (25% by weight) although this value is comparable to cancellous bone, an important result for further developing the implant. In-vitro biodegradation studies of the composite proved it to be dimensionally stable with an average weight loss of 40-42% over a period of 35 days. In addition, we also observed that at high ionic strengths of calcium phosphate precursor, the hexagonal LLC proved to control the phase of the mineral to HA while cubic LLC produced a mixture of calcium phosphates like brushite and monetite in addition to HA. This observation suggests that decreasing the size of the confined domains and dimensional freedom has a strong effect on calcium phosphate morphogenesis.

**DISCUSSION & CONCLUSIONS:** In this work, we have used molecular self-assembly and covalent crosslinking of LLC structures to form a mesoscopically ordered polymer-apatite nanocomposite having similar apatite chemistry to bone and an ordered nanostructure inspired from bone. The composite showed mechanical properties comparable to cancellous bone and has potential applications as orthopedic implants.

**ACKNOWLEDGEMENTS:** We acknowledge Max-Lab (Lund, Sweden) for the allocation of beam time and assistance with SAXS measurements.

# High pressure and biotechnologies

M Prakasam[1], A Largeteau[1], A Plumecocq[2], G Demazeau[2]
[1] *CNRS, University of Bordeaux, ICMCB, 87 Avenue du Dr Albert Schweitzer, 33600 Pessac, France,*
[2] *HPBioTECH, 31 Avenue de la Poterie, 33170 Gradignan, France*

**INTRODUCTION:** Two main objectives can be assigned for high-pressure processes in biotechnologies: (i) the preparation of biomaterials and (ii) the microbial safety of the different products developed in biotechnologies (vectors, health products, etc) while preserving the therapeutic properties.

Concerning the high pressure processes, two different application modes can be described versus the pressure uniformity: (i) High Hydrostatic (or isostatic) Pressure processes (HHP Processes) where the pressure value is the same in all the directions of the space, (ii) Non-Isostatic Pressure Processes (NIP Processes) where the pressure value is different versus the direction.

In both case, the key-point is the weak energy developed by pressure application.

In Biotechnologies, the NIP Processes are mainly used to prepare biomaterials (ceramics, etc.) with the control of the main characteristics of the grains (size, morphology, crystallinity). The development of different techniques in ICMCB has led to the control of the ceramics microstructure.

The HHP processes are mainly developed for improving microbial safety while preserving the intrinsic properties of the treated products (cold pasteurization) or drugs impregnation at the surface in order to functionalize biomaterials (through a control of the microstructure of the first layers). Through a recent accurate analysis of the different parameters involved in HHP Processes, HPBioTECH has evaluated the impact of each of them (or their combination) both on the microbial inactivation or drug impregnation.

**EXPERIMENTAL DEVELOPMENTS:** Two main different techniques are involved for HHP and NIP Processes.

In HHP Processes, pressure is applied versus a liquid- transmitting medium (as water or an eutectic between water and glycol versus the temperature). In the main cases, in order to prevent the microbial recontamination after the HHP treatment, the product is prepackaged. The HHP treatment of both product and packaging imposes some specific properties for the polymers used in the packaging design [mechanical properties, preservation of the barrier properties (in particular versus water vapor and oxygen) and chemical integrity (in particular for the internal layer in contact with the biological product)].

Concerning the NIP Processes, the preparation of ceramics requires the control of different steps. The control of the grain–size has been developed by spray drying or hydrothermal precipitation. The morphology of the grains can be control through a hydrothermal treatment. In parallel such a treatment can improve their crystallinity. To obtain densified ceramics, we develop different techniques of sintering: microwave without or with uniaxial pressure, hydrothermal, hot pressing or spark plasma.

The microstructure of the first layers of the biomaterials is adapted versus the applications and the nature of the biological component used for its functionalization.

**CONCLUSION:** The combination of HHP and NIP Processes is able to lead to functionalized biomaterials with a high microbial safety. Different applications resulting of this combination are in progress.

# Selenium-doped hydroxyapatite: physicochemical properties

A Laskus, E Groszyk, J Kolmas

*Medical University of Warsaw, Faculty of Pharmacy, Warsaw, Poland*

**INTRODUCTION:** Selenium is an important trace element. As a component of various enzymes, it plays a crucial role in several metabolic processes [1]. It is also known, that selenium exhibits anticancerogenic properties and may inhibit the growth of tumor [2]. Synthetic hydroxyapatite with the formula $Ca_{10}(PO_4)_6(OH)_2$, due to high biocompatibility, is widely is in bone and dental surgery as bone substitutes and dental materials [3]. Hydroxyapatite can be modified by the incorporation of additional ions into the structure. Thus, we have decided to synthesize hydroxyapatite enriched in selenium and to investigate its physicochemical properties. In addition, preliminary tests of toxicity were carried out.

**METHODS:** Hydroxyapatite powders enriched in selenium were synthesized using wet methods**.** Selenates, selenites and acidic selenites were used as sources of selenium. Briefly, a solution of ammonium hydrogenphosphate and selected selenium salt was added to calcium nitrate solution. pH and temperature were set to 8-9 and 50 °C, respectively. The precipitates were aged, decanted and filtered. The powders were soaked in water to remove ammonia solution. The obtained powders were dried in air at 100 °C for 5 h. Then various analytical methods were used for the physicochemical studies: powder X-ray diffraction (PXRD), infrared spectroscopy (FT-IR), transmission electron microscopy (SEM), solid-state nuclear magnetic resonance ($^{1}H$, $^{31}P$ and $^{77}Se$ NMR) and X-ray fluorescence (WD-XRF).

**RESULTS:** Powder diffractograms show that the powders exhibit hydroxyapatite structure. The samples don't contain other crystalline phases. TEM analysis demonstrates that selenium incorporation decreases the crystal size. WD-XRF allowed us to perform the elemental analysis and measure the Ca\P+Se molar ratio. FT-IR and NMR methods were used for structural analysis: location of selenium oxyanions, hydroxyl group concentration, presence of acidic phosphates, detection of water and its location, etc.

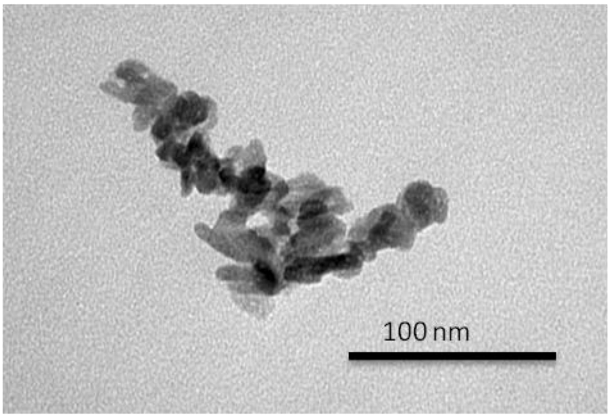

*Fig. 1: SEM image of hydroxyapatite containing selenates.*

**DISCUSSION & CONCLUSIONS:** Selenium-doped hydroxyapatites using different sources of selenium were successfully synthesized and their detailed structural analysis was performed. Preliminary toxicity tests were done on the selected samples. We believe that selenium containing hydroxyapatite may be a promising material for reconstructive surgery.

**ACKNOWLEDGEMENTS:** J.K. thanks the Foundation for Polish Science for supporting her with the Parent-Bridge Programme that was co-financed by the EU European Regional Development Fund.

# Silver doped hydroxyapatite scaffolds coated with sodium alginate and chitosan for controlled drug delivery

A Dubnika[1], D Loca[1], J Locs[1], L Berzina-Cimdina[1]

*[1]Rudolfs Cimdins Riga Biomaterials Innovations and Development Centre, Riga Technical University, Riga, Latvia*

**INTRODUCTION:** Every year the number of surgical procedures where calcium phosphate implant materials are used is increasing. It is possible to include different ions into hydroxyapatite structure to improve its properties. By including silver ions into hydroxyapatite structure, antibacterial activity of the material can be ensured [1]. Wide researches into development of controlled drug delivery systems based on hydroxyapatite were started only within the last decade, therefore it is still an ongoing process to look for the optimal drug delivery conditions to control the drug release. The aim of current research was to prepare silver doped hydroxyapatite porous scaffolds coated with chitosan and alginate for controlled lidocaine delivery and to evaluate the effect of system preparation method on drug release profile.

**METHODS:** Silver doped hydroxyapatite (HAp/Ag) was synthesized by two different wet precipitation methods: A method from CaO, $H_3PO_4$, $AgNO_3$; B method from $Ca(NO_3)_2$, $(NH_4)_2HPO_4$, $NH_4OH$, $AgNO_3$ [1]. Synthesized HAp/Ag composites contain up to 1% silver. HAp/Ag powder was used for the preparation of porous scaffolds with *in situ* foaming method [2]. Polymer and lidocaine hydrochloride solutions in sintered HAp/Ag scaffolds were incorporated using vacuum impregnation and release of lidocaine hydrochloride was determined using ultra high performance liquid chromatography method.

**RESULTS:** FTIR analysis suggested that no chemical reaction between HAp/Ag, lidocaine and alginate/chitosan occurs during the impregnation process.

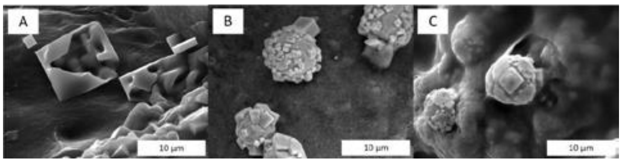

*Fig. 1: SEM microphotographs of A method Hap/Ag with A –alginate/lidocaine/alginate coating; B – lidocaine/alginate/alginate coating; C – HAp/Ag lidocaine/alginate/chitosan coating.*

Moreover SEM microphotographs showed that silver particles act as crystallization centres for lidocaine crystal growth (see Fig.1.).

From the lidocaine release results it was concluded that the presence of silver affects the morphology of lidocaine and polymer coating formation. Therefore the lidocaine was released faster form silver-containing scaffolds coated with alginate/lidocaine/alginate and lidocaine/chitosan/alginate compared to the pure HAp scaffolds. For HAp/Ag scaffolds with these coatings all introduced lidocaine was released in the first 10 to 24 h. Controlled lidocaine release can be obtained if the HAp/Ag porous scaffolds are impregnated with lidocaine and 2 times coated with alginate (see fig.2.).

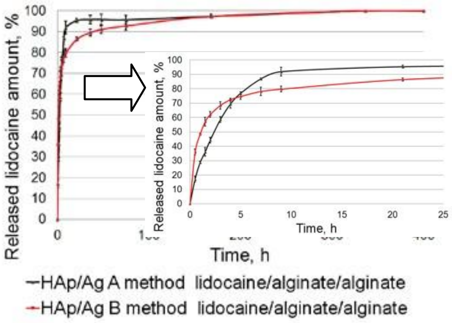

*Fig. 2: Lidocaine release kinetics from HAp/Ag lidocaine/alginate/alginate composite materials*

**DISCUSSION & CONCLUSIONS:** Controlled drug release on the basis of Hap/Ag material was observed from 25 to 360 h (two weeks).

**ACKNOWLEDGEMENTS:** This work has been partly supported by the National Research Programme "MultIfunctional Materials and composItes, photonicS and nanotechnology (IMIS$^2$)" Project No. 4 "Nanomaterials and nanotechnologies for medical applications".

# Silk microfiber reinforced calcium phosphate bone cements for local drug delivery

D Loca[1], J Locs[1], S Mandal[2], A Smirnova[1], M Sokolova[1], Z Irbe[1], L Berzina-Cimdina[1]

*[1]Rudolfs Cimdins Riga Biomaterials Innovations and Development Centre of Riga Technical University, Riga, Latvia. [2]Materials Research Centre, Indian Institute of Science, Bangalore - 560012*

**INTRODUCTION:** Among calcium phosphate biomaterials, calcium phosphate bone cements (CPC) have attracted increased attention because of their ability of self-setting *in vivo* and injectability. Such property combination opens up new opportunities for minimally invasive surgical procedures [1]. However, any surgical procedure carries the risk for inflammation and bone infection, which could be prevented combining CPC with anti-inflammatory drugs microencapsulated in biodegradable polymer matrix. Another limitation of CPCs is their low mechanical strength. Moreover, drug capsules may act as defects in CPC matrix lowering the strength of the cements [2]. To improve the mechanical properties of α-tricalcium phosphate (α-TCP) based CPC for drug delivery applications, cements were reinforced with silk microfibers. The effect of drug loaded microcapsules and reinforcing fibres on CPC mechanical properties and drug release kinetics was investigated.

**METHODS:** CPC solid phase was α-tricalcium phosphate powder (α-TCP). Cement liquid phase was a mixture of 0.5 M $Na_2HPO_4$ and 0.5 M $NaH_2PO_4$ solutions (volume ratio 20:1). The CPC samples with solid to liquid phase ratio of 1.89 g/ml, 1.75 g/ml and 1.23 g/ml were used in this study. Nanosized hydroxyapatite was synthesized using wet precipitation reaction between calcium hydroxide and orthophosphoric acid [3]. Vancomycin hydrochloride loaded poly(lactic acid) (PLA) microcapsules were prepared using slightly modified double emulsification technique.

**RESULTS:** During the research it was found that variations of solid to liquid phase ratio strongly influenced the initial burst release of vancomycin in the first 24 h. Modification of CPC with PLA/vancomycin microcapsules loaded and coated with nanosized hydroxyapatite resulted in 85.3±3.1% of drug release within 43 days, while only 30.4±1.3% of drug was released from CPC modified with PLA/vancomycin microcapsules.

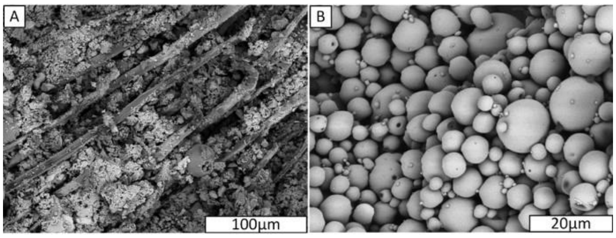

*Fig. 1: A: PLA/vancomycin and silk microfibers containing CPC; B: PLA/vancomycin microcapsules*

Moreover, addition of silk microfibers to CPCs, increased the cement mechanical properties for more than 20% and modified the drug release profiles. Additionally the scaffold architecture in terms of pore size distribution as well as fiber orientation of the newly synthesized scaffold were quantified using micro-computed tomography results.

**DISCUSSION & CONCLUSIONS:** More often in clinical praxis the systemic antibiotic treatment are combined with the local drug delivery to reach the most optimal effect. In the current research the possibility to obtain different vancomycin release profiles with modified initial burst release depending on the CPC composition was shown.

**ACKNOWLEDGEMENTS:** This work has been partly supported by the National Research Programme “MultIfunctional Materials and composItes, photonicS and nanotechnology (IMIS$^2$)” Project No. 4 “Nanomaterials and nanotechnologies for medical applications”.

# Biomolecular coating of nickel-titanium memory shape metals

SM Longela[1], HJ Haugen[1], S. P. Lyngstadaas[1], J Reseland [1], H Tiainen[1]

[1]*Department of Biomaterials, Faculty of Dentistry, University of Oslo, Norway*

**INTRODUCTION:** A simple yet effective surface coating procedure for implants is highly demanded. Here we are presenting a method which combines chemical surface modification with a bioactive coating of synthetic peptides on shape memory nickel-titanium stents to improve re-endothelialization ability and simultaneous reduce rate of stenosis and restenosis or no inflammatory potential.

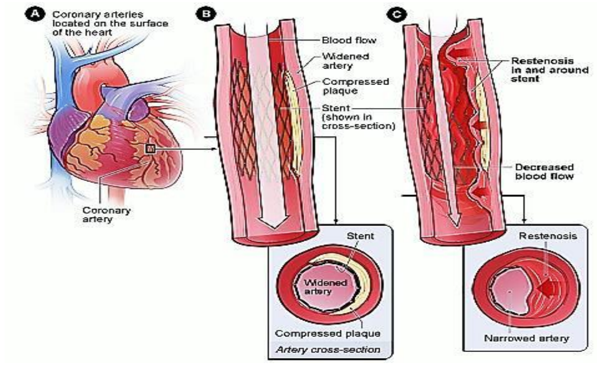

*Fig. 1: Implantation of an arterial stent*[1]

**METHODS:**

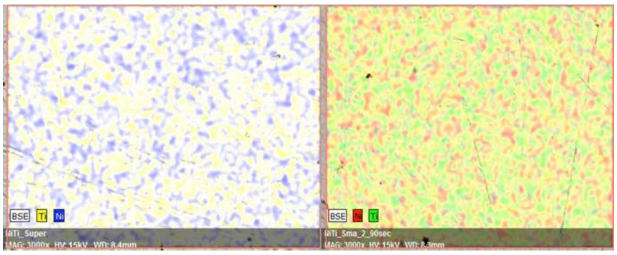

*Fig. 2: NiTi surface microscopy*

**Methods for Immobilizing Biomolecules on implant surface:**

+ Dipping into Peptide+buffer solution
+ Covalent Anchoring by Silane Agents
+ Covalent Binding of Alkanethils
+ Tresyl Chloride Activation
+ Spacer Assistant Adsorption
+ Oligonucleotide Mediated Adsorption

**The specific aims:**

- ☐ Computational simulations of peptide-Surface interaction
- ☐ Identify the pH- region where the binding is optimal
- ☐ Finding the optimal current density and time point for adding biomolecules
- ☐ Find concentration of biomolecule on the surfaces with given processing parameters
- ☐ Investigate release kinetics of the biomolecules
- ☐ In vitro experiment in order to verify which concentration could have highest clinical effect

**RESULTS:** Computational molecular dynamics simulations have helped accurately simulate the behaviour of biomolecules interactions to each other and to the metal surface.

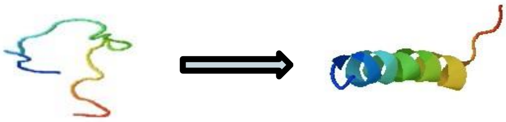

*Fig. 3: Peptide (P2) folding simulation*

In situ experiments have shown satisfactory results hypothesized by computational simulations.

**DISCUSSIONS:** This study revealed that, between chemisorption and physisorption of peptides on Nickel-titanium surfaces, physical covalent binding showed interestingly tremendous effect on calcium mineral deposition on surfaces.

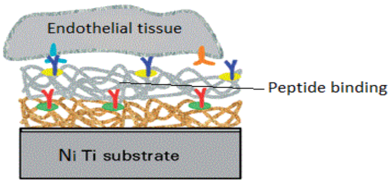

*Fig. 4: Coating mechanism*[2]

**CONCLUSION:** This study focus on improving the concept of peptide coating on Nickel-titanium stents to promote effective arterial repair.

This experimental study develops an easy and practical coating for Nickel-titanium shape memory and superelastic implants with specific synthetic peptides by using an advanced anchor system to promote re-endothelialization of artery wall tissue.

# Novel selenium- and tellurium-based antioxidants as modulators of inflammatory response

X Lu[1], G Mestres[1], P Effati[1],VP Singh[2], J Poon[2], L Engman[2], MK Ott[1]

*[1]Materials in Medicine, Div. of Applied Materials Science, Dpt. Engineering Sciences, Uppsala University, Sweden, [2]Department of Chemistry, BMC, Uppsala University, Sweden*

**INTRODUCTION:** Excessive production of reactive oxygen species (ROS) during inflammation can cause tissue damage and delay tissue repair. Antioxidants may modulate ROS production during inflammation and limit injury. Selenium (Se) and tellurium (Te) possesses potent antioxidant activities and may serve as the basis for creating new antioxidants. In this study, several novel Se and Te containing compounds were evaluated for their ability to scavenge free radicals from macrophages and whether they would affect the function of ostebolastic cells (MC3T3).

**METHODS:** ROS release was measured with luminol amplified chemiluminescence, using a monocytic cell line, THP-1, and primary monocytes obtained from human buffy coat. Briefly, cells were suspended in a white 96 well plate ($2*10^5$ cells per well) in protein free luminol solution (500 µM) that was prepared from a stock of 50 mM luminol (3-aminophthalhydrazide) diluted in 0.2 mM NaOH along with varying concentrations of Se/Te compounds and Trolox (a water soluble derivative of vitamin E). Cells were induced to release ROS using phorbol-12-myristate-13-acetate (PMA; 500 nM). Luminescent signal was recorded every 2 minutes using a microplate reader at 37°C for 120 minutes.

Cell proliferation and differentiation was assessed using alamar blue and alkaline phosphosphatase (ALP) assay. MC3T3 cells seeded in 96 well plates (3000 cells/well) were fed every other day with alpha-MEM with ascorbic acid (50ng/ml) and supplemented with the different compounds. On days 3, 7, 10 and 14, cells were incubated with AlamarBlue and fluorescence was measured using a plate reader. The cells were then lysed and after three freeze-thaw cycles, total protein content and ALP was quantified using a microBCA (measured at 562 nm) and ALP yellow liquid substrate system (measured at 405 nm) respectively.

**RESULTS:** Two compounds, VPS-1 (containing Se) and JF-2 (containing Te) were found to significantly reduce the amount of ROS generated from PMA stimulated THP-1 cells and primary human monocytes.

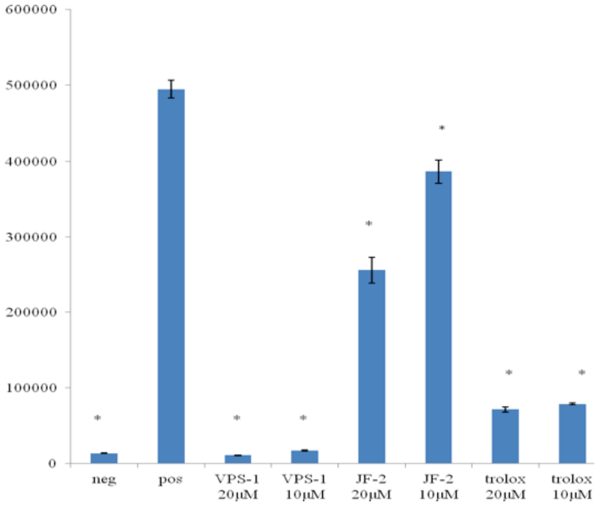

*Fig. 1: Luminol signalling showing generation of ROS from monocytes after exposure to varying concentrations of VPS-1, JF-2, and Trolox. * indicates $p < 0.05$ vs positive control*

VPS-1, JF-2 and Trolox did not negatively affect the viability or ALP activity of MC3T3 over the 14 day experimental period.

**DISCUSSION & CONCLUSIONS:** VPS-1 and JF-2 were able to reduce the generation of ROS from PMA activated macrophages. This reduction may be due to the ability of organic Se and Te compounds to mimic the function of glutathione peroxidase (Gpx)[1]. Gpx enzymes rely on the catalytic activity of Se to convert hydrogen peroxide to water. Antioxidants such as Trolox may directly scavenge intracellular hydrogen peroxide[2]. These compounds may represent a class of antioxidants, which could potentially be incorporated into biomaterials to decrease the degree of inflammation after implantation, or used to treat disorders such as chronic inflammatory diseases.

**ACKNOWLEDGEMENTS:** Vinnova, VINNMER (2013-01260), Carl Trygger (CTS 13:346), Lars Hiertas Minne (FO2013- 0337) and Ollie & Elof Ericssons Stifelse för Vetenskaplig Forskning.

# High-aspect ratio nanostructures for cellular applications

N Buch-Månson[1], S Bonde[1], KR Rostgaard[1], J Bolinsson[2], J Nygård[2], KL Martinez[1]

*[1]Nano-Science Center and Department of Chemistry, University of Copenhagen, Denmark, [2]Nano-Science Center and Center for Quantum Devices, Niels Bohr Institute, University of Copenhagen, Denmark*

**INTRODUCTION:** The endeavour of exploiting arrays of vertical one-dimensional nanostructures for cellular applications is experiencing a pronounced surge of activity [1]. The interest is rooted in the intrinsic properties of high-aspect-ratio nanostructures.

With a height comparable to a mammalian cell, and a diameter 100-1000 times smaller, arrays of nanostructures can be interfaced in various ways with cells and are thereby suitable for various applications spanning from transfection of cells to monitoring of intracellular signals. Each of these applications requires a particular interface of nanostructures with living cells, which can be achieved by tuning the nanotopography of the surface (diameter, length and density).

**METHODS:** We further exploit the theoretical model of cell settling presented in Bonde *et al.* [2] to propose a generic prediction. The model is validated using InAs nanowires produced by electron beam lithography and molecular beam epitaxy as described in [2, 3].

**RESULTS:** In this communication, we will present a theoretical model of cell settling of arrays of nanostructures allowing the rational design of a suitable nanotopography for the application foreseen [4]. After validating the model experimentally, we will present a study of the cell behaviour on arrays of nanostructures and evaluate the effect of the nanotopography on their adhesion, migration and proliferation [2, 3]. The study was performed using ordered arrays of vertical InAs nanowires and the throughput of the systematic cellular studies was facilitated by the design of multidensity nanowire arrays exhibiting 6 different types of nanotopography on a singe chip. We demonstrated that arrays of InAs nanowires provide a cell-promoting surface, which affects both cell division and focal adhesion up-regulation. Furthermore, a systematic variation in NW spacing affects both the detailed cell morphology and adhesion properties.

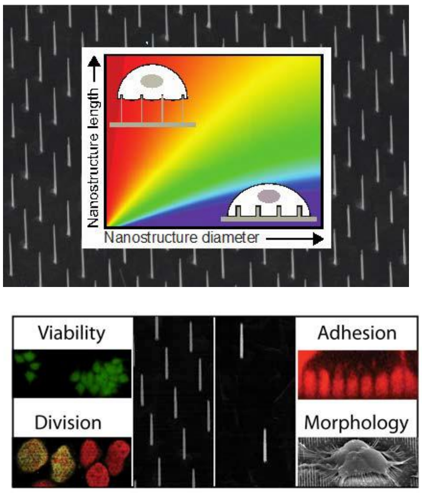

*Fig. 1: illustrating the influence of nanostructure topography on cell settling (Top), and cell behavior on various nanotopgraphies (Bottom).*

**DISCUSSION & CONCLUSIONS:** The results obtained in these combined theoretical and experimental studies allow for rational design of nanostructure arrays for a broad range of future biological applications.

**ACKNOWLEDGEMENTS:** For financial support, we thank the Danish Agency for Science Technology and Innovation (The Danish Council for Strategic Research - CLIPS and ANaCell projects, and The Danish Natural Science Research Council − FTP 11-116984) and UNIK Synthetic Biology (funded by the Danish Ministry for Science, Technology and Innovation)..

# Layer-by-layer assembly of collagen and fibronectin for tissue engineering applications

S Mauquoy[1], C Dupont-Gillain[1]

[1] *Institute of Condensed Matter and Nanosciences, Université catholique de Louvain, Belgium.*

**INTRODUCTION:** In vivo, cells are embedded in a complex extracellular matrix (ECM). Collagen (Col), a structural protein, and fibronectin (Fn), which are involved in signalling from cells to the ECM and conversely, are two major components of the ECM. Tailoring biointerfaces based on these two essential ECM biomolecules will improve the control of cell-material interactions.

Layer-by-layer (LbL) assembly, based on the alternate surface dipping in a polycation and a polyanion solution, is an established approach to design structures with a vertical heterogeneity. Assembling proteins by LbL is however challenging in reason of the polyampholyte character of proteins and of their particular structure. The mechanism of assembly may moreover rely on specific interactions. Here, we aim at combining Fn and Col in LbL assemblies, to create constructs with vertical heterogeneity, with a view to influence adipose-derived mesenchymal stem cells (AMSC) behavior.

**METHODS:** LbL assembly with Fn and native Col (n-Col) or denatured Col (d-Col) was performed on a polystyrene (PS) substrate in PBS (pH 7.4), HEPES buffer (pH 7.4) and acetate buffer (pH 5.4). In some cases, poly(ethyleneimine) (PEI) adsorption was performed prior to the LbL assembly. LbL assemblies are also compared to simultaneous adsorption of Fn and Col (Fn+Col).

Quartz crystal microbalance with dissipation monitoring (QCM-D) is used to obtain information related to the wet deposited mass, ellipsometry to measure the dry thickness of the films, contact angle measurements to characterize their wettability and AFM to examine their morphology.

AMSC are cultured in supplemented DMEM. Adhesion and proliferation experiments are performed with cells at passage 4.

**RESULTS:** Fig. 1 shows that LbL assembly is generally better with d-Col compared to n-Col, and that thicker films are obtained when using PEI as an anchoring layer. The buffer used also influences the assembly, with HEPES buffer giving the best results. The assembly levels up after the adsorption of the first bilayer. Fig. 2 presents the first results of cell behavior on the created films. The created films strongly enhance adhesion. Adhesion after 20h is not influenced by film type. Proliferation is reduced on films with PEI.

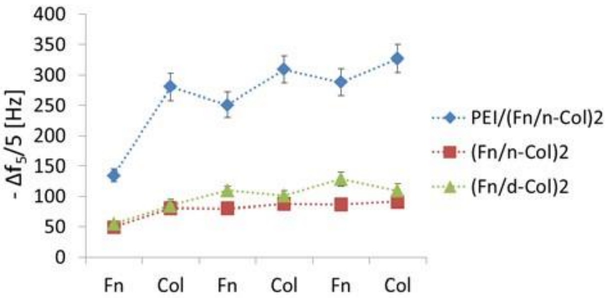

*Fig. 1: Frequency shift measured with QCM-D for assemblies prepared in HEPES buffer.*

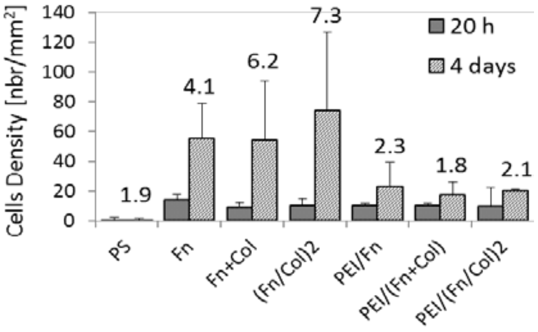

*Fig. 2: Cell density after 20 h and 4 days. The ration of cell density after 4 days and 20h, related to proliferation, is given above graph bars.*

**DISCUSSION & CONCLUSIONS:** The combination of results from all techniques indicates successful build-up of multilayers, with a growth which is however not sustainable. First cell adhesion and proliferation experiment shows a negative impact of PEI on cell proliferation, probably because of a cytotoxic effect. By assembling Col and Fn in a variety of conditions, we now better understand their mode of assembly. More tests are now performed to tune cell behavior and especially cell differentiation using such films.

**ACKNOWLEDGEMENTS:** S. M. thanks the Belgian National Foundation for Scientific Research (FNRS) for her Research Fellow position and for the financial support.

# Impoverishment of media by bioactive hydroxyapatite hinders cell proliferation

G Mestres[1], M Espanol[2], C Persson[1], MP Ginebra[2], M Karlsson Ott[1]

*[1]Materials in Medicine, Div. of Applied Materials Science, Dpt. Engineering Sciences, Uppsala University, Sweden. [2]Biomaterials, Biomechanics and Tissue Engineering, Dpt. Materials Science and Metallurgy, Technical University of Catalonia, Spain.*

**INTRODUCTION:** Hydroxyapatite (HA) resulting from the setting reaction of calcium phosphate cements can provide a template for bone regeneration. HA is a bioactive material known to strongly interact with ions[1] and proteins[2] in the surrounding media, and this interaction is partly related to the microstructure of the material. The aim of this work was to determine the effect of media impoverishment on cell growth, using HA with two different types of microstructure.

**METHODS:** Coarse (C) and fine (F) α-TCP powder were prepared using energetic milling[2]. The C and F α-TCP powders were mixed with distilled water at a ratio of 0.65 ml/g to prepare hydroxyapatite (HA) constituted of plate-like (C-HA; 19.85 $m^2/g$) or needle-like crystals (F-HA; 41.72 $m^2/g$). Discs were moulded (∅ = 15 mm, h = 2 mm), and stored in 0.9 wt.% NaCl solution for 10 days.

$6.5 \cdot 10^3$ Raw 264.7 cells were seeded in 96-well plates. After cell adhesion (4h), the media (200 µl) was replaced by extracts; afterwards the extract was daily refreshed. HA extracts were prepared by soaking HA discs in 1 ml of fresh media, which contained either 10% foetal bovine serum (FBS) and 1% penicillin/ streptomycin (complete media, cM) or 1% penicillin/streptomycin (media, M). The extracts were collected every 24 h and either added to the cells as obtained or supplemented with 10% FBS and/or 1 mM calcium chloride anhydrous. As control, fresh complete media was used. The cell number was quantified after 7 days by measuring lactate dehydrogenase (LDH) released from lysed cells.

The concentration of Ca ([Ca]) and P ([P]) of the extracts prepared in complete media was monitored by ICP-AES, and total protein content was quantified with a microBCA kit.

**RESULTS:** Both C-HA and F-HA took up a significant amount of Ca and proteins from media, in addition to releasing P ions. This behaviour was more pronounced for F-HA (Table 1).

The cell number in the fresh complete media was significantly higher than in all cement extracts, with the F-HA extract causing a more pronounced decrease as compared to C-HA (Fig. 1). A clear trend was observed for both extract types: addition of FBS and Ca together enhanced cell proliferation more than addition of FBS alone, which still enhanced the proliferation more than addition of Ca alone. The extract used as obtained (without extra supplements) caused the lowest cell growth.

*Table 1. [Ca] and [P] from extracts after immersion of HAs in complete media for 7 days.*

| | [Ca] (mM) | [P] (mM) |
|---|---|---|
| Fresh media | 1.23± 0.02 | 1.11± 0.02 |
| C-HA extract | 0.53 ± 0.03 | 1.83 ± 0.05 |
| F-HA extract | 0.30 ± 0 01 | 2.03 ± 0.13 |

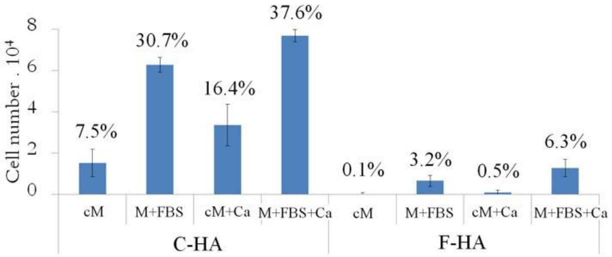

*Fig. 1: Cell number after 7 days in contact with extract (numbers indicate percentage of control).*

**DISCUSSION & CONCLUSIONS:** The higher specific surface area of F-HA caused a greater interaction with Ca, P and proteins than C-HA. The impoverished of Ca and proteins in the media hindered cell growth. Supplementing extracts with physiological amounts of Ca and FBS enhanced cell proliferation, however, this supplementation did not reach the same proliferation level as in fresh media. It can be assumed that other inorganic or organic species also affect the cell proliferation.

**ACKNOWLEDGEMENTS:** Co-funded by Marie Curie Actions via VINNOVA (2013-01260), STINT (IG2011-2047), Lars Hiertas Minne Stiftelsen, and Ollie & Elof Ericssons Stiftelsen.

# *In vitro* bioactivity studies of thermally treated titanium dioxide ceramics

I Narkevica[1], L Bugovecka[1], J Ozolins[1]

[1]*Institute of General Chemical Engineering, Riga Technical University, Latvia.*

**INTRODUCTION:** The ability to induce formation of bonelike apatite on artificial bone implants in the human body is vital to the successful bonding between the implants and bone tissue [1]. Immersion in simulated body fluid (SBF) is often used *in vitro* method for the first indication of potential bioactivity of biomaterials [1,2]. Previous studies have shown that apatite-forming ability of titania is associated not only with its chemical composition and crystallinity, but also with its textural properties [2,3]. The aim of present work was to evaluate the impact of different factors (*e.g.* microstructure, phase composition) on *in vitro* bioactivity of sintered titania ceramics.

**METHODS:** Titania ceramics with various anatase-rutile phase ratios, grain size and specific surface area were prepared by thermally treating pressed compacts at different temperature regimes: conventional and two-step sintering in the temperature range from 600 to 900 °C. The sintered samples were immersed in SBF at 37 °C for 3 weeks to evaluate their apatite-forming ability. The phase composition of the sintered $TiO_2$ and after immersion in SBF was evaluated using X-ray diffractometer. The surface morphologies of specimens before and after immersion in SBF were characterized by field emission scanning electron microscopy incorporating X-ray energy dispersive spectrometry. Sorptometer KELVIN 1042 was used for determination of BET specific surface area. Fourier transform infrared spectroscopy was used to analyse functional groups on the surface of samples after immersion in SBF.

**RESULTS:** The phase composition and microstructure of $TiO_2$ strongly depends upon sintering conditions. The rutile phase content can be varied from 8 to 35%, grain size from 37 ± 4 to 103 ± 12 nm and specific surface area from 18 to 60 $m^2/g$ over the temperature range from 600 to 900°C. No newly formed products after immersion in SBF were observed on the surface of titana ceramics with grain size above 61±6 nm and rutile phase ratio above 14%. In case if grain size was below 50 nm the surface was covered with new particles already after 5 days. SEM micrograph shows that newly formed particles have a plate-like morphology (Fig. 1). New broad diffraction peak was detected in XRD pattern that can be attributed to low crystalline or nanocrystalline hydroxyapatite (Fig. 1). The SEM/EDX, XRD and FTIR spectroscopy results confirmed that the new layer formed on titania surface is low crystallinity carbonate-containing hydroxyapatite or bonelike apatite and formation of new layer can be attributed to *in vitro* bioactivity of material.

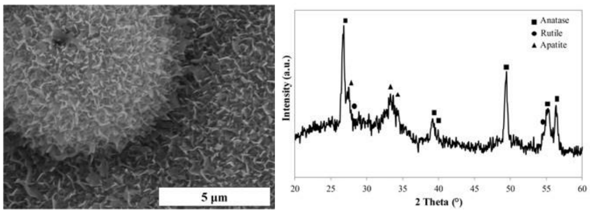

*Fig. 1: SEM micrograph and XRD spectrum of the $TiO_2$ ceramic surface with apatite layer.*

**DISCUSSION & CONCLUSIONS:** Results demonstrate that bonelike apatite formation on titania ceramics is affected by multiple factors including grain size, specific surface area and phase composition. Results indicate that the essential factor for apatite formation is grain size. Smaller grains has a higher molar free energy and due to that they more likely adsorb molecules or ions from surrounding environment onto the surface in order to reduce total free energy and become more stable. Higher specific surface area accelerates apatite formation due to increased amount of Ti-OH groups on the surface. The phase composition has minor influence on apatite-forming ability of titania ceramics comparing to grain size and specific surface area.

**ACKNOWLEDGEMENTS:** This work was supported by the National Research Programme “Multifunctional Materials and composites, photonics and nanotechnology (IMIS2)” Project No. 4 “Nanomaterials and nanotechnologies for medical applications”.

# Synthesis, sintering and characteristics of hydroxyapatite nanopowders

E Palcevskis[1], A Dindune[2], DJ Veljovic[3]

*[1]Plasma & Ceramic Technologies Ltd, Latvia, [2]Institute of Inorganic Chemistry, Riga Technical University, Latvia, [3] Faculty of Technology and Metallurgy, University of Belgrade, Serbia*

**INTRODUCTION:** Calcium phosphates, including hydroxyapatite (HAP) have been paid attention of intensive research as bone filler, bone graft substitutes do to its biocompatibility and osteo-conduction. The main results of investigations of HAP materials performed in frames of EUREKA project E!3033 BIONANOCOMPOSIT (in period of 2003-2012) are shortly summarised in this report.

**METHODS:** The chemical interaction between calcium hydroxide and phosphoric acid was chosen for synthesis of the HAP nanopowder. Various methods for manufacturing dense HAP materials from obtained powders were used and compared (Table 1). Biocompatibility was compared by enumeration of the number of osteoblast-like cells to the materials.

**RESULTS:** The TEM image (Fig. 1) of the synthesized HAP nanopowder shows the agglomerate which consist of nanosized rod-shaped particles in size of 50–100 nm. The powder obtained by spray-drying consisted from quasi spherical granules with average diameter of 20-40 μm.

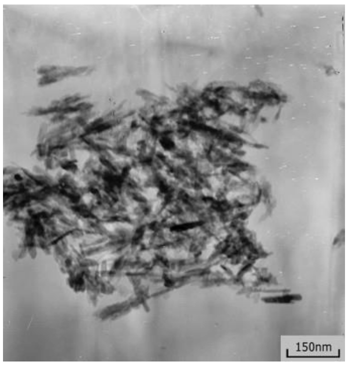

*Fig. 1: The TEM micrograph of initial HAP particles*

The specific surface area of such powder was in the range of 60-70 $m^2/g$. The XRD pattern of the powder showed low crystallinity. The only peaks recognized were those corresponding to the calcium hydroxyapatite phase (JCPDS pattern 9–432 for HAP).

All used methods allows to manufacture the dense HAP materials but more promising method seems to be the MW sintering because only this method allows to obtain dense HAP material at relatively low temperature and in short time – at 900 $^{o}$C in 15 minutes (Table 1). This provides the saving of nanosize microstructure of the material and therefore the high values of fracture toughness up to 1.5 MPa·$m^{1/2}$, microhardness up to 5 GPa and improved biocompatibility [1].

*Table 1. Sintering conditions for production HAP materials with relative density > 95 % and the average grain size of the obtained material.*

| Sintering method and conditions | Sintering temperature, $^{o}$C / time | Average grain size, μm |
|---|---|---|
| Axially pressed (100 MPa) samples in air in common furnace | 1200/ 2 h | 3-10 |
| Axially pressed in microwave (MW) furnace in air | 900/ 15 min<br>1200/ 15 min | 0,1<br>1,6 |
| Could isostatically pressed (CIP) at 400 MPa in common furnace | 1200/ 2 h | 3 |
| Hot pressing at 20 MPa in Argon of CIP samples | 1000/ 2 h | 0.4 |
| CIP samples in MW furnace | 900/ 15 min<br>1200/ 15 min | 0,1<br>3,5 |
| Spark plasma sintering at 40 MPa | 1000/ 10 min | 1-7 |

# A new β-tricalcium phosphate / thermoresponsive hyaluronan hydrogel composite as injectable bone graft substitute delivering drugs

D Petta[1], G Fussell[2], L Hughes[2], DD Buechter[2], CM Sprecher[1], M Alini[1], D Eglin[1], M D'Este[1]

*[1]AO Research Institute Davos, Clavadelerstrasse 8, 7270 Davos, CH. [2]DePuy Synthes Biomaterials, 1230 Wilson Drive, West Chester, PA 19380, USA*

**INTRODUCTION:** Advanced synthetic biomaterials able to reduce or replace the need for autologous bone transplantation are a major clinical need in orthopedics, dentistry and trauma. In this study, we prepared a new composite of β-tricalcium phosphate (TCP) and a thermoresponsive hyaluronan hydrogel (THH). The composite was characterized via dissolution test, scanning electron microscopy (SEM), injectability, release of a bone morphogenetic protein 2 (BMP2) and dexamethasone (DEX).

**METHODS:** THH was prepared from hyaluronan of 1.5MDa molecular weight as per reference [1]. The composite was prepared by mixing a 20% w/v solution of THH with TCP (supplied by Synthes USA Products LLC, particle size 0.125-0.25mm) to a concentration of 40%. SEM images were taken at 5kV after freeze drying, fracturing and coating with 10nm of carbon. Dissolution test consisted in evaluating the shape maintenance 1 month after extruding the composite from an insulin syringe into a phosphate buffer saline (PBS) solution at 37°C. A control test with pure hyaluronan composites was performed. Injection force was measured with an Instron 4302 electromechanical testing machine. For the release study, 100 mg beads of composite containing 5 µg BMP2 (Inductos, Medtronic) were dip into 1 ml of PBS containing 0.1% of bovine serum albumin. At 1h, 3h, 8h, 1d, 2d, 3d, 5d, 8d and 13d, 100 µl of release buffer were withdrawn for ELISA analysis (Duo Set from R&D Systems) and replaced with fresh buffer. DEX release was determined in the same manner using 100 µg of drug per bead and high performance liquid chromatography detection. As control, release from pure TCP and THH was measured.

**RESULTS:** SEM images revealed an even distribution of TCP particles within the matrix and hydrogel penetration up to the micro-porosity level (Fig. 1). Dissolution test was successful, while the composite prepared from pristine hyaluronan did not pass. Injection force showed a transient peak of 12 N and plateaux of 3 N. BMP2 and DEX release are shown in fig 2.

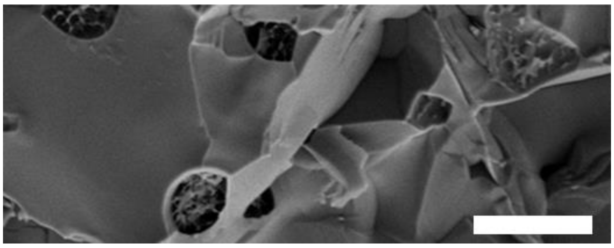

*Fig. 1: SEM image of the composite. THH is visible on the surface and within the microporosity of TCP. Scale bar =5µm.*

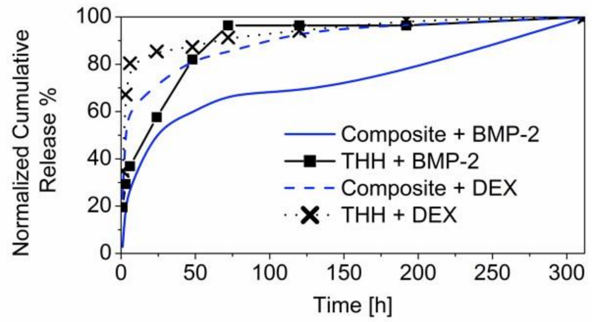

*Fig. 2: Normalized cumulative release of BMP2 and from the composite and THH.*

**DISCUSSION & CONCLUSIONS:** The TCP/THH combination gives an easily injectable paste with good shape retention at 37°C in PBS, suggesting absence of washing-out from body fluids. TCP/THH slows down the release of BMP2 and DEX with synergistic effect compared to the single components, indicating the possibility of loading this composite with hydrophilic, hydrophobic and biological drugs. This versatile off-the-shelf synthetic graft could be supplemented by the surgeon with angiogenic, osteoinductive, anti-inflammatory, analgesic, antibiotic, anticancer molecules depending on the clinical necessity.

**ACKNOWLEDGEMENTS:** M Glarner, D Wahl, D Sutter for excellent technical assistance. DePuy Synthes biomaterials for financial support.

# The effect of antimicrobial peptides released from mesoporous titania on biofilm formation of *Staphylococcus epidermidis*

M Pihl[1], E Andersson[1], M Andersson[1]

[1]*Applied Chemistry, Chalmers University of Technology, Göteborg, Sweden*

**INTRODUCTION:** Today there is an emerging antibiotic resistance in society and the need of finding alternative ways of fighting bacteria is pressing. Infections are often caused by microbial biofilms, i.e. bacteria living on surfaces, encapsulated in an extracellular matrix. They are difficult to eradicate, as they can be up to 1000 times more antibiotic resistant than their corresponding planktonic counterparts [1]. A potential group of substances to control biofilms are antimicrobial peptides, AMPs. They strike widely against bacteria and the first interaction between AMP and microbe is thought to occur via electrostatic interactions. In this study we investigated the antibacterial effect *in vitro* of a PRELP-derived antimicrobial peptide, RRPRPRPRPWWWW-NH2 (RRP9W4N) [2] on biofilm formation of *Staphylococcus epidermidis.*

**METHODS:** Mesoporous thin film titania were formed using the EISA method [3] and characterised with electron microscopy. The loading and relsease of AMP into the mesopores was studied in QCM-D and the effect of the peptide on biofilm formation was studied for two strains of *S. epidermidis*. Biofilm formation was studied with a safranin biofilm assay and LIVE/DEAD *Bac*Light staining and confocal microscopy. Nonporous titania and the antibiotic Cloxacillin were used as controls.

**RESULTS:** In the SEM, mesopores were seen to extend to the surface and in TEM a mesoporous network was seen throughout the sample, indicating the possibility to charge pores with antimicrobial substances.

When RRP9W4N was added to the mesoporous titania an immediate, substantial loading of RRP9W4N into the mesopores took place (500 ng/cm$^2$ within the first 30 minutes) and maximum charging, 650 ng/cm$^2$, was reached already after 2.5 hours. When rinsing began, there was a slow release of peptide from the surface, continuing for the day of the experiment.

In the safranin assay there was statistically significantly less ($p<0.05$) biofilm formation of *S. epidermidis* on the mesoporous surfaces charged with antimicrobials compared to the control mesoporous surface. Statistical significance ($p<0.05$) in biofilm growth was also seen in LIVE/DEAD *Bac*Light staining compared to controls. There was no difference to peptide-charged surfaces and antibiotic soaked surfaces. The amount of biofilm on the antimicrobial soaked surfaces constituted 6-9% of the control biofilm. Most bacteria on the surfaces were alive, ranging from 86-99%.

**DISCUSSION & CONCLUSIONS:** Mesoporous titania offers a possibility to charge antimicrobial peptides into surfaces and acts as a reservoir, slowly releasing peptides into the environment. This ensures a sustained, high local concentration and the antimicrobial peptide RRP9W4N prevents biofilm formation of *S. epidermidis* to a large extent, being equally efficient as Cloxacillin. This is interesting for future applications of antimicrobial implants.

**ACKNOWLEDGEMENTS:** We acknowledge the Centre for Cellular Imaging at the Sahlgrenska Academy, University of Gothenburg for the use of imaging equipment and for the support from the staff. *S. epidermidis* strain Mia was a kind gift of Professor Gunnel Svensäter, Malmö University.

# Comparison of sol-gel derived thin films of calcium hydroxyapatite: dip-coating and spin-coating procedures

A Prichodko, V Jonauske, A Beganskiene, A Kareiva

*Department of Inorganic Chemistry, Vilnius University, Lithuania*

**INTRODUCTION:** Calcium hydroxyapatite (HA) – $Ca_{10}(PO_4)_6(OH)_2$ – was the first calcium phosphate studied for surgical procedures, mainly due to its good compatibility with the inorganic components of bones and teeth. Moreover, HA is a bioactive material that does not cause side effects in the human body. HA is a low toughness brittle material, what limits its use when high mechanical stresses are required. For this reason, HA is widely employed as coating on metallic prosthesis and implants, usually over titanium and its alloys or stainless steels [1]. This system combines the mechanical advantages of the underlying (metallic) substrate and biological affinity of the HA surface to natural tissue. It is critical however that this system does not substantially deteriorate during its lifetime, e.g. through loss of interfacial integrity. The 316L stainless steel has long been used for prosthesis devices such plate, screw, etc., in orthopedic surgery [2].

During recent years, a number of different techniques, such as precipitation, sol-gel, hydrothermal, multiple emulsion, biomimetic deposition, electrodeposition, have been applied for the synthesis of HA. The sol-gel method is preferred due to its low synthesis temperature, high product purity, homogenous molecular mixing and the ability to generate nano-sized particles compared to other alternatives. The synthesis of HA by sol-gel method requires a correct molar ratio of 1.67:1 between Ca and P in the final product. Moreover there are a lot of different calcium and phosphorus precursors used for HA synthesis, as reported sol-gel processes in the literature. Besides, bioactivity of Ca–P based materials is dependent on many factors such as the synthesis procedure, precursor reagents, impurity contents, crystal size and morphology, concentration and mixture order of reagents, pH and temperature. Selection of the route of synthesis depends on the application [3].

**METHODS:** In this work HA thin films on 316L stainless steel substrate were prepared using an aqueous sol-gel chemistry route, as precursors using calcium acetate monohydrate and phosphoric acid in a Ca/P ratio of 1.67 (corresponding to the calcium hydroxyapatite). As complexing agents EDTA deprotonated with triethanolamine and aqueous solution of 3% polyvinyl alcohol were used. Dip-coating and spin-coating techniques were employed to produce sol-gel derived HA coatings. Stainless steel rectangles were dip-coated in the sol solution, with immersing (85 mm/min) and a withdrawal rates (40 mm/min). For spin coating, approximately 0.5 ml of coating solution was placed on top of the substrate using syringe and then spin coated at 2000 RPM for 60 s in air. Both rectangle and circle substrates were annealed up to 30 times following the same procedures accordingly. The samples of HA precursor gels on the substrates were heated in an oven at 850 °C for 5 h with heating rate of 1 °C/min.

**RESULTS:** For the characterization of surface properties, the phase and morphology of the coating layer were analyzed using X-ray diffraction (XRD) analysis, scanning electron microscopy (SEM), atomic force measurement (AFM), Fourier transform infrared spectroscopy (FTIR), and the contact angle measurements were recorded. The results of analyses of calcium hydroxyapatite thin films on stainless steel substrate are evaluated and discussed. Suitability of two different coating techniques were compared.

**DISCUSSION & CONCLUSIONS:** An aqueous sol-gel chemistry route was developed for the synthesis of calcium hydroxyapatite thin films on stainless steel substrate. The obtained results have showed that both dip-coating and spin-coating techniques are suitable for the preparation of HA thin films on stainless steel substrate.

**ACKNOWLEDGEMENTS:** Postdoctoral fellowship to Dr. Aleksandra Prichodko is being funded by European Union Structural Funds project “Postdoctoral Fellowship Implementation in Lithuania” (No. 004/102). This research was also partially funded by COST Action MP1202.

# Rebamipide delivery via cement reduces ROS production in macrophages

M Pujari-Palmer, S Pujari-Palmer, H Engqvist, M Karlsson Ott

*Materials in medicine, Uppsala University Box 256, Uppsala, Sweden 75105*

**INTRODUCTION:** Surgical implantation of a biomaterial triggers inflammation. If inflammation persists, or if the biomaterial continues to activate inflammatory cells, excessive reactive oxygen species (ROS) and inflammatory cytokines will be produced. While ROS can stimulate regeneration, it also impedes regeneration by initiating osteoblast apoptosis, osteoclast differentiation and bone catabolism, and is correlated with the development of fibrotic tissue.[2] In the present study we investigated whether brushite cement was a suitable drug delivery vehicle for delivery of an anti-inflammatory agent, Rebamipide. Brushite is metastable calcium phosphate cement commonly used as a scaffold to to facilitate new bone growth, in vitro.

**METHODS:** Cylindrical composites, 6x12mm, were fabricated by mixing b-tricalcium phosphate and monocalcium phosphate monohydrate in mass ratios of 0.55 to 0.45. Cements were mixed with 0%, 0.5% or 1% (by mass) Rebamipide powder; with a liquid to powder ratio of 0.22 mL/g at 37°.i Wet samples were compressed to failure after 1 day in PBS, at 1mm/min. Drug release was measured with a UV spectrophotometer at 270nm. Raw264.7 macrophages were exposed to 10-fold dilution of cement leach to test viability (alamar blue), or diluted 4 fold to detect ROS production (chemiluminescence assay). A Dunnets t-test was used for statistical analysis.

**RESULTS:** Rebamipide reduced the mechanical strength (25.1 ± 1.6 MPa) of the brushite cements by 30%. The drug release rate was identical for all drug concentrations. Within 4 days 50% of loaded drug was released, without a burst release. Rebamipide reduced the ROS produced by macrophages up to 49% ± 1% (Figure 1). At the highest dose of Rebamipide, 1mM, viability of macrophages was 81% ± 7.8%.

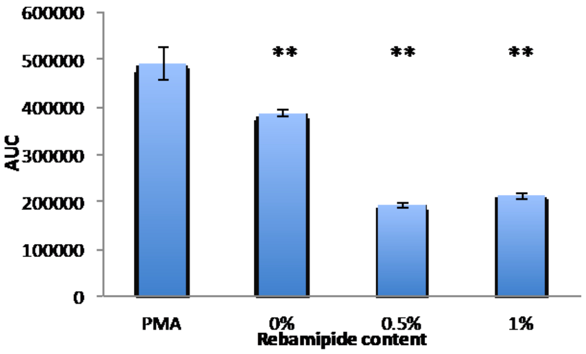

*Fig. 1: Reduction in macrophage ROS drug with drug loaded cement.*

**DISCUSSION & CONCLUSIONS:** Rebamipide is a suitable anti-inflammatory candidate for delivery by cement. The mechanical properties of brushite were moderately impaired by Rebamipide at higher doses. The drug release rate is both predictable and linear, with 50% of the loaded drug released within four days, and sustained release of 1-3% daily. Rebamipide can be delivered from cement in a dose that reduced ROS production in macrophages with minimal reduction in viability.

**ACKNOWLEDGEMENTS:** The authors acknowledge support from the FP7 NMP project Biodesign and the Swedish Research Council (2011-3399).

# Influence of hydroxyapatite nanoparticle morphology on inflammatory response

S Pujari-Palmer[1], S Chen[1], W Xia[1], S Rubino[1], H Weng[2], L Tang[2], M Karlsson Ott[1]

[1]*Applied Material Science, Uppsala University, Uppsala, Sweden,* [2]*Department of Biomedical Engineering, University of Texas at Arlington, Texas, U.S.A.*

**INTRODUCTION:** Wear debris generated from implants has the potential to cause inflammation that eventually results in periprosthetic bone loss. The accumulation of wear particles activate phagocytic cells to release reactive oxygen species (ROS) and initiate a cascade of events that lead to increased bone resorption and aseptic loosening[1]. The chemical composition, zeta potential and particle size are often the focus of wear debris studies. Few studies, however, have investigated how particle morphology affects inflammation. In the present study, hydroxyapatite (HA) nanoparticles with differing morphologies (long rods, short rods, sheets, fibres) were fabricated and the production of ROS from primary human monocytes (MNCs) and neutrophils (PMNCs) was evaluated. Macrophage and neutrophil activation was also studied in an in vivo mouse model.

**METHODS:** Cell Isolation: Human monocytes (MNCs) and polymorphonuclear cells (PMNC) were isolated from the buffy coats of anonymous blood donors. MNCs were isolated using a Ficoll-Paque plus density centrifugation according to the manufacturer's instructions (400g for 20 minutes). The mononuclear cell layer was collected, washed with phosphate buffered saline (PBS), and centrifuged at 100g for 15 minutes, three times. PMNC isolation underwent 2 separation procedures. The blood pellet was resuspended in 3% Dextran/0.9% saline solution for 25 minutes. The upper plasma layer was centrifuged at 250g for 10 minutes. Contaminating erythrocytes were removed by adding 0.2% saline solution to the pellet for 20 seconds. An equal volume of 1.6% saline solution was then added and the cell suspension was centrifuged.

Luminol amplified chemiluminescence: The amount of reactive oxygen species (ROS) released by PMNC and MNC was quantitated by luminol-amplified chemiluminescence. MNCs were seeded with 100ug/ml of nanoparticle solution (200,000 cells/well) at 37°C. PMNCs were seeded with 100ug/ml of nanoparticle solution (162,500 cells/well). Measurements were taken every 2 minutes, for up to 2 hours, using a plate reader (Tecan) in the luminescence mode. MNCs were activated using 0.5µM phorbol myristate acetate (PMA) while PMNCs were activated by 0.25µM PMA. Total ROS was quantified by integrating the area under the chemiluminescence kinetic curve (AUC) using Origin Software. All measurements were performed in medium containing a 4:1 ratio of PBS to RPMI-1640, 100 µM of glucose, 50 mM luminol, 0.1M NaOH, and 2µg/ml horse radish peroxidase (HRP).

**RESULTS:**

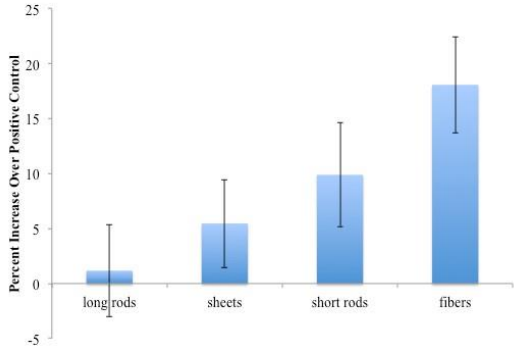

*Figure 1: ROS produced by monocytes/macrophages*

MNCs produced significantly greater ROS when exposed to the fibres as compared to long rods and sheets. PMNCs, though not significant, showed the same trend. Preliminary in vivo results also exhibited higher macrophage and neutrophil activation when treated with fibres as compared to sheets.

**DISCUSSION & CONCLUSIONS:** Both in vitro and in vivo results exhibited greater ROS production with fibers as compared to the other morphologies. Previous studies have reported that the particle shape determines the rate of internalization and translocation in phagocytic cells[2,3]. Fiber shaped particles may more easily associate with, translocate across, and disrupt the cell membrane.

**ACKNOWLEDGEMENTS:**VINNOVA (VINNMER project 2010-01907).

# Animal model for monitoring biomaterial associated inflammation and infection

B Rais[1], M Köster[1], S Lienenklaus[1], S Weiß[1], H Hauser, PP Müller[1]

[1]*Helmholtz-Centre for Infection Research, Inhoffenstrasse 7, 38124, Braunschweig, Germany*

**INTRODUCTION:** An Implant loses its functionality upon microbial infections that are resistant to conventional antibiotic. There is a need of novel biomaterials and reliable test systems to evaluate their biocompatibility. Histology was one of the conventional methods that were used to detect implant-associated inflammation thereby, sacrificing the animal for a single time point study. To this end, an animal model has been established to test the interactions of implants with the tissues. Non-invasive in vivo imaging was employed to determine the extent and kinetics of inflammation.

**METHODS:** We have a two-component system that can detect inflammation and infection simultaneously. Inflammatory cells were isolated from the bone marrow of mice with substantial constitutive expression of luciferase under the transcriptional control of Mx-2 gene promoter (1). Mx-2 promoter responds to type 1 and type 3 interferons during infection in the host (2-4). These immune cells were adoptively transferred to the implanted mouse model. Implants with and without heat killed (HK) bacteria were used to represent inflammatory or infected and biocompatible implants respectively. Different cell types like neutrophils, monocytes or total bone marrow cells were used to study the cell dynamics in presence and absence of inflammation. The biocompatibility of several implant materials was tested such as polymer poly lactic – co – glycolic acid (PLGA), titanium and magnesium.

**RESULTS:** All the cell types isolated from bone marrow of Mx-2 luciferase mice showed a similar kinetics. Luminescence from implants soaked in heat-killed bacteria was 2.5 – 4 fold higher as compared to the biocompatible material. In case of delayed inflammation, adoptively transferred neutrophils were unable to appear at the site of the inflammation that suggests the specific accumulation of neutrophils in presence of inflammation only. PLGA coated titanium plates and PLGA microspheres were found to be the immune stimulatory material amongst other biomaterials.

**DISCUSSION & CONCLUSIONS:**

In conclusion, imaging of immune cells seems to be the promising strategy to monitor inflammation. Implantation procedure is always accompanied with injury that attracted the adoptively transferred immune cells and higher or lower bioluminescence from these cells was dependent upon the inflammatory potential of the implant surface. The model established has the ability to sense inflammation and infection in the same animal. Inflammatory reaction to implant surfaces can be clearly assessed using this strategy.

# Antibacterial sol-gel coating of ceramic $TiO_2$ scaffolds for bone regeneration

S Recklies[1, 2], D Wiedmer[1], C Bossard[1, 3], H Tiainen[1]

*[1]Department of Biomaterials, University of Oslo, Norway. [2]Department of Materials Science and Engineering, University of Erlangen-Nuremberg, Germany, [3]ENSIACET, National Polytechnic Institute of Toulouse, France*

**INTRODUCTION:** Highly porous $TiO_2$ scaffolds may be used to augment and promote bone regeneration for large bone defects caused by periodontitis or peri-implatitis. However, accumulation of pathogenic bacteria and biofilm deposition can endanger the success of bone remodelling. A crystalline sol-gel coating may add bactericidal properties to the substitute material based on the photocatalytic generation of oxidising radicals on the catalyst surface.

**METHODS:** The fabrication process of highly porous $TiO_2$ scaffolds is described elsewhere.[1] The sol-gel coating process steps are illustrated in Figure1.

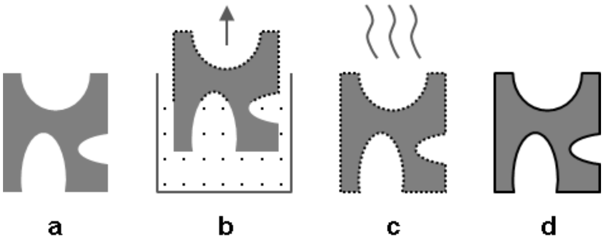

*Fig.1: (a) $TiO_2$ scaffolds were fabricated by polymer sponge method and dipped (b) into a TTIP-HCl-$H_2O$-iPrOH system. After a two-step heating treatment (c) a crystalline, thin coating (d) remains on the substrate.*

The scaffolds were withdrawn from the solution at a low vertical speed ($v_{pull}$ = 6 cm.min$^{-1}$). A two-step heating treatment was applied to evaporate the solvent ($T_{evap}$ = 120°C) and to crystallise the nanoparticle coating ($T_c$ = 450°C). A holding time of 1 h at $T_c$ was chosen to ensure complete crystallisation. The homogeneity of the coatings was examined by scanning electron microscopy (SEM). UV-vis spectroscopy was used to measure the degradation of the organic dye methylene blue (MB) under UV-irradiation due to the photocatalytic capacity of coated and uncoated $TiO_2$ scaffolds.

**RESULTS:** $TiO_2$ scaffolds were covered by a thin, homogenous film after sol-gel coating and heat treatment (Figure 2). Only minor flakes or ruptures of the coating were detected for $v_{pull}$ = 6 cm.min$^{-1}$. Higher withdrawal speeds resulted in the agglomeration of microparticles on the 3D structure, incomplete coating of the struts and partly blocked pore windows.

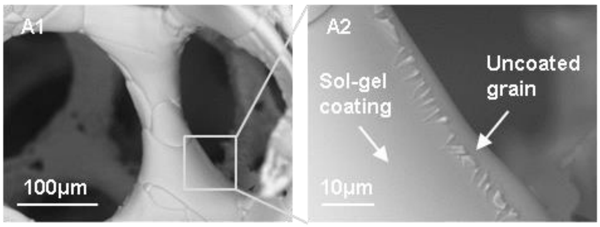

*Fig.2: Highly porous and interconnective scaffold (A1) and detailed view (A2) of the applied sol-gel coating.*

The dip-coated, amorphous $TiO_2$ film overlaying the macroporous rutile substrate was crystallised to nanostructured anatase during the heat treatment at $T_c$ = 450°C and thereby changing the crystal structure of the scaffold surface. The anatase coated scaffolds were found to result in significantly stronger MB degradation in comparison to the uncoated rutile scaffolds indicating enhanced generation of radical oxygen species (ROS) on the anatase surface.

**DISCUSSION & CONCLUSIONS:** The rutile crystal phase of the scaffold substrate forms during the high sintering temperature (1500°C) used to obtain appropriate mechanical strength. However, anatase is known to show superior photocatalytic activity compared to rutile when irradiated with UV-light.[2] One explanation for this may be the increased generation of ROS, mostly $OH^{\bullet}$ and $O_2^{\bullet-}$, on the catalyst surface. The observed increase in MB degradation on the anatase surface seems to agree with this hypothesis. *In vitro* cell and bacteria studies will be conducted to assess cell viability and bactericidal effect of the nano-structured anatase scaffold surfaces.

**ACKNOWLEDGEMENTS:** This study was supported by Research Council of Norway (grant no. 228415) and EUREKA Eurostars E!8320 NuGel.

# Low-modulus acrylic bone cements obtained through modification with unsaturated fatty acids and triglyceride oils

C Persson[1], E Dugast[1], C Robo[1], A López[1], H Engqvist[1]

[1] *Division of Applied Materials Science, Department of Engineering Sciences, The Ångström Laboratory, Uppsala University, Uppsala, Sweden*

**INTRODUCTION:** The excessive stiffness of acrylic bone cements in comparison to the surrounding trabecular bone has been hypothesized to contribute to biomechanically related complications, mainly noted after vertebroplasty [1]. Fatty acids and their derivatives have been suggested as potential property modifiers in these types of cements, but there is no systematic study available evaluating the effect of the same. In this study, six different fatty acids and triglyceride oils were evaluated as possible additives, with the aim of obtaining low-modulus, but sufficiently strong, acrylic based bone cements.

**METHODS:** A commercially available cement intended for vertebroplasty, Osteopal®V (Heraeus Medical GmbH, Hanau, Germany), was used as the base cement. Linoleic acid (LA), ricinoleic acid (RA), methyl linoleate (ML), tung oil (TO), linseed oil (LO) and castor oil (CO) (Sigma-Aldrich, St. Louis, MO, USA) were evaluated as potential additives. Specimens of $\varnothing$=6 mm and h=12 mm were tested under uniaxial compression using an AGS-X materials testing machine (Shimadzu, Kyoto, Japan) after 24 h setting in air at room temperature [2]. A displacement rate of 6mm/min was used. The maximum polymerization temperature ($T_m$) and the setting time (ST) were determined for unmodified cements and cements containing LA, RA and CO according to the ISO5833 standard [2].

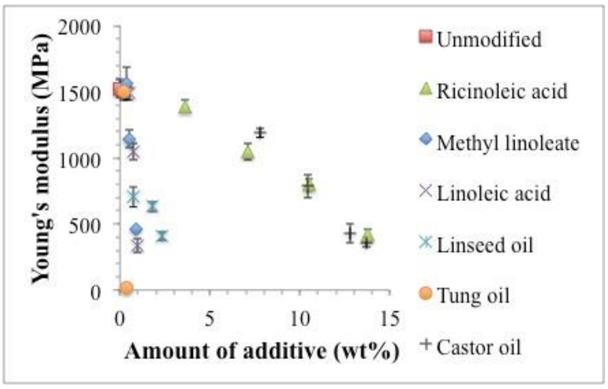

*Fig. 1: Young's modulus of unmodified and modified acrylic cements.*

**RESULTS:** Additives having LA or its derivatives as the main component gave a much stronger effect on the mechanical properties than those containing RA (Figs. 1 and 2). RA and CO gave significantly shorter STs than the control (8.7 ± 1.8 and 10.8 ± 0.8 compared to 14.7 ± 1.7 min). LA gave a ST of 12.4 ± 1.9 min. All low-modulus cements gave significantly lower $T_m$ than the control (29-30°C on average compared to 41°C).

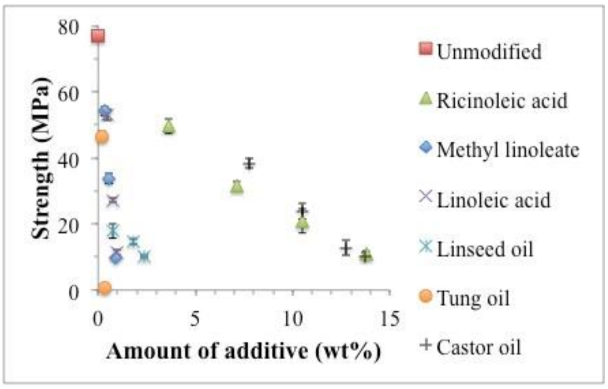

*Fig. 2: Compressive strength of unmodified and modified acrylic cements.*

**DISCUSSION & CONCLUSIONS:** Low-modulus acrylic based bone cements were successfully synthesized, and a large range of Young's moduli could be obtained (Fig. 1). Fatty acids with a high level of unsaturation were more effective than others in lowering the modulus, with LA being particularly promising, as it also gave no significant change to the cement's ST, but a decrease in the polymerization temperature, which could be beneficial from a biological perspective [3].

**ACKNOWLEDGEMENTS:** The authors are grateful for funding from the EU (SPINEGO project FP7-PEOPLE-2010-268134) and VINNOVA (VINNMER project 2010-02073).

# Morphometric analysis and immunohistochemical evaluation of tricalcium phosphate (TCP) scaffolds *in vivo*

I Salma[1], M Pilmane[2], J Locs[3], G Salms[1]

[1]*Riga Stradins University, Institute of Stomatology,* [2]*Riga Stradins University, Institute of Anatomy and Anthropology,* [3]*Rudolfs Cimdins Riga Biomaterials innovations and development center of Riga Technical University*

**INTRODUCTION:** Trauma and bone pathologies in maxillofacial region frequently require bone replacement with biomaterials.

Tricalcium phosphate (TCP) ceramic is frequently used for maxillary sinus floor augmentation due to bioactivity and biocompatibility with living body. TCP ceramic is promising due to the particular biodegradation.

The aim of our study was to evaluate bone tissue response to TCP ceramic in animal experiments.

**METHODS:** In current study tricalcium phosphate (TCP) ceramic granules and porous TCP scaffolds were used. Calcium deficient hydroxyapatite (CDHAp) was synthesized by aqueous precipitation technique; porous TCP scaffolds were produced using ammonium hydrogen carbonate provided viscous slurry foaming. Intraosseous implantation of bioceramic granules and porous scaffolds was performed in jaw of 12 rabbits. Bone with biomaterial was obtained after three months. Routine histological method - staining with hematoxilin and eosin was used for obtaining a review picture. To evaluate the scaffold resorbtion and bone regeneration rate morphometric analysis with Image-Pro Plus program was used.Tissues were proceeded for the detection of bone proteins osteopontin (OP) and osteocalcin (OC), proinflammatory cytokine IL-1 and anti-inflammatory cytokine IL-10.

*Fig. 1: Intraosseous implantation of bioceramic granules in rabbit jaw (5 mm trephine).*

**RESULTS:** Results demonstrated pronounced anti-inflammatory cytokines expression, high expression of OC and variable expression of OP. High expression of OC proves unchanged mineralization of newly formed bone. Intraosseous implantation of TCP ceramic scaffolds causes osteogenesis.

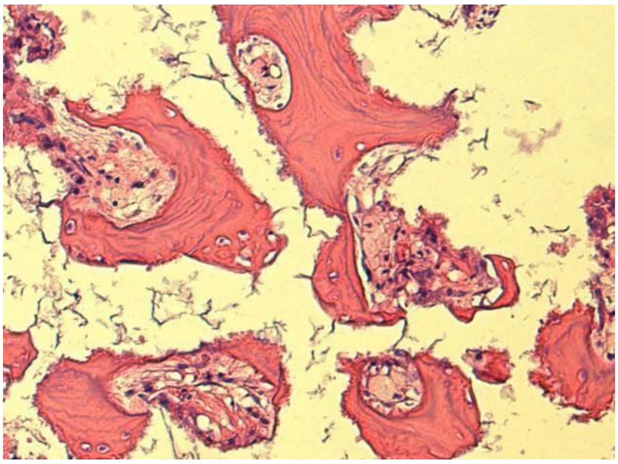

*Fig. 2: Intraosseous implantation of TCP ceramic scaffold causes foci of polyosteogenesis, (h/eo, x100).*

**DISCUSSION & CONCLUSIONS:** From bone ground substance proteins (OC and OP) the most stable is osteocalcin. This proves the practically unchanged mineralization of newly formed bone [1]. Variable appearance and functions of osteopontin gives evidence about this protein as perspective prognostic marker for bone ground substance quality in implantology [2]. The tissue anti-inflammatory cytokine expression dominates over the pro-inflammatory cytokine expression while macroscopical signs of inflammation were not detected.

**ACKNOWLEDGEMENTS:** This work has been supported by the National Research Programme No. 2014.10-4/VPP-3/21 “MultIfunctional Materials and composItes, photonicS and nanotechnology (IMIS$^2$)” Project No. 4 “Nanomaterials and nanotechnologies for medical applications”.

# Design of multifunctional micro-granules based on Sr-substituted hydroxyapatite and poly (vinyl alcohol)

K Salma-Ancane[1], L Stipniece[1], A Vojevodova[1], I Narkevica[1], L Berzina-Cimdina[1]

*[1]Rudolfs Cimdins Riga Biomaterials Innovation and Development Centre, Riga Technical University, Latvia,[2]Institute of General Chemical Engineering, Riga Technical University, Latvia*

**INTRODUCTION:** In recent years, fabrication of porous bioceramic scaffolds, inorganic/organic biocomposites mimicking the composite nature of real bone has attracted research interest in the field of bone regeneration [1, 2]. Investigations on composites based of bioactive calcium phosphate phases and synthetic biodegradable polymers for biomedical applications appear to be an advanced topic in biomaterials research. The aim of this study was to design suitable technology for obtaining multifunctional micro-granules for medical application such as bone filler materials or micro-carriers for drug delivery.

**METHODS:** Sr-substituted HAp/PVA micro-granules were processed by spray drying technique using slurry of *in situ* synthesized Sr-HAp in 5% (w/v) PVA solution. *In situ* synthesis was realized by precipitation method using $Ca^{2+}$, $Sr^{2+}$ (2 mol.% substitution) and $PO_4{}^{3-}$ ions sources as starting reagents with molar ratio of (Ca+Sr/P) = 1.67 in order to obtain spray-dried products containing HAp and PVA at the 50/50, 70/30, 90/10 wt.%. The obtained slurry was spray dried by using a tabletop spray dryer with nozzle of 1.4 mm diameter at a temperature 200°C. To obtained micro-granules based on Sr-substituted HAp bioceramics, the spray-dried powder was thermally treated at 1100°C for 1h. The collected spray–dried and sintered powders were structurally characterized using X-ray diffraction (XRD), Fourier transform infrared spectroscopy (FT-IR), Field emission-scanning microscopy (FE-SEM), differential scanning calorimetry (DSC).

**RESULTS:** FE-SEM studies of obtained spray-dried products before and after thermal treatment confirmed the formation of micro-spheres with diameter in the range 2-10 µm (Fig.1., Fig.2.). Evaluation of physico-chemical characteristics confirmed the formation of nanosized Sr-substituted HAp crystallites with needle-like morphology homogeneously distributed in PVA matrices. However, optimization of number of process parameters of the spray drying is required to fabricate the micro-spheres with homogenous size distribution.

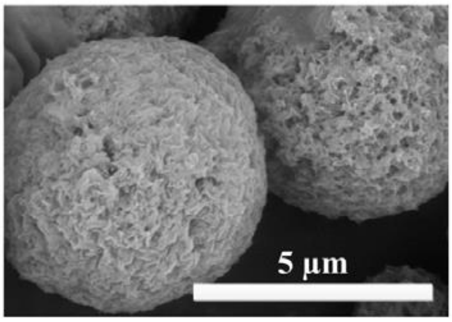

*Fig.1: FE-SEM micrograph of spray-dried microgranules based on Sr-HAp/PVA (70/30 wt.%).*

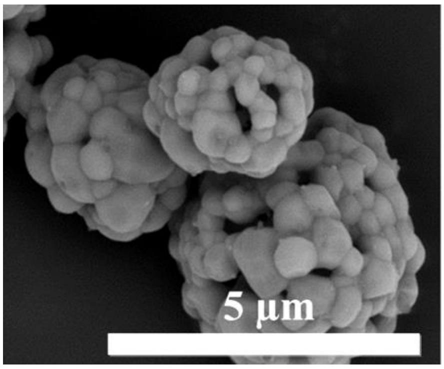

*Fig.2: FE-SEM micrograph of porous microgranules based on Sr-HAp bioceramics sintered at 1100ºC.*

**DISCUSSION & CONCLUSIONS:** This study has provided an alternative technique to fabricate micro-granules with attractive features for multifunctional applications in bone tissue engineering. The obtained microspheres can be used as carriers in drug delivery and bone fillers in tissue engineering.

**ACKNOWLEDGEMENTS:** This work has been supported by European Social Fund within the project “Involvement of new scientist group for synergistic investigation to development of nanostructured composite materials for bone tissue regeneration” No.2013/0007/1DP/1.1.1.2.0/13/APIA/VIAA/024.

# Volumetric analysis of malar augmentation with biphasic calcium phosphate

G Salms[1], S Grybauskas[2], J Locs[3], I Salma[1]

*[1] Riga Stradins University, Institute of Stomatology, [2] Department of Maxillofacial Surgery, Vilnius University Zalgirio Hospital, Lithuania, [3] Rudolfs Cimdins Riga Biomaterials innovations and development center of Riga Technical University*

**INTRODUCTION:** Malar augmentation is often performed as an ancillary procedure simultaneously with orthognathic surgery in order to improve facial appearance. Hydroxyapatite is a well-documented material of choice for facial onlay augmentation [1-3]. Its application in the shape of granules rather than solid shape implants is known to be related with reduced rate of complications. However, the volumetric change of implanted material over time is fairly documented. This study evaluated the volumetric changes of implanted biphasic calcium phosphate in the malar areas from baseline to 4 months, 9-12 months and 18-24 months after surgery by means of cone beam computed tomography (CBCT) surface superimposition.

**METHODS:** CBCT scans of 13 patients who underwent ancillary malar augmentation (25 surgical sites) at the time of bimaxillary orthognathic surgery were the object of this study. Biphasic calcium phosphate (Hap/ β-TCP ratio of 90/10) granules mixed with Avitene Flour microfibrillar collagen had been implanted at the time of surgery. CBCT scans were included from following timepoints: T0 (1 week pre-surgery), T1 (within 1 week post-surgery), T2 (4 months post-surgery), T3 (9-12 months post-surgery) and T4 (18-24 months post-surgery). Semi-automated image segmentation was performed and surface models rendered for each dataset. Manual surface-based superimposition was performed on each of the post-surgical dataset on pre-surgical dataset in Simplant OMS (Materialise, Leuven, Belgium). 3D subtraction of surface models allowed the estimation of volumetric changes over time in Mimics 13.0 (Materialise, Leuven, Belgium).

**RESULTS:** The average decrease of volume of implanted biphasic calcium phosphate during 4 months after surgery was 18.6%. Further volumetric decrease was negligible and contributed to a total volume loss of 21.6% at 18-24 months postoperatively indicating granule compaction as the possible explanation to early volumetric loss. The volume was found to be very stable during the long-term follow-up. The calibration process demonstrated high reproducibility of landmarks yielding superimposition of two identical surface models with an error no greater than 0.4 mm.

**DISCUSSION & CONCLUSIONS:** No similar research on volumetric stability after malar area augmentation could be found in the literature. CBCT superimposition is an informative method for evaluation of volumetric changes of implanted materials. The decrease in volume in our study was calculated with regard to the absolute increase in percentage. The decrease in volume was not unexpected due to the composition and nature of implantable material. The highest rate of volumetric decrease, during T1-T2, phase can be explained by the compaction of the particles, resorbtion of collagen and partial resorbtion of beta-TCP from the granules. The slow rate of volumetric decrease during following periods could be explained by ongoing remodeling of the granules located at the surface.

**ACKNOWLEDGEMENTS:** This work has been supported by the National Research Programme No. 2014.10-4/VPP-3/21 “MultIfunctional Materials and composItes, photonicS and nanotechnology (IMIS$^2$)” Project No. 4 “Nanomaterials and nanotechnologies for medical applications”.

# Development of poly(lactic-*co*-glycolic acid)-based nanoparticles as a drug delivery system for bone regeneration implants

M Schweikle, H Tiainen, H J Haugen

*Department of Biomaterials, Institute of Clinical Dentistry, University of Oslo, Norway*

**INTRODUCTION:** Hard tissue regeneration in in bone defects caused by periodontitis and periimplantitis can be challenging due to critical defect size and high risk of recurrent bacterial infections. Synthetic titanium dioxide ($TiO_2$) scaffolds have shown to feature good osteoconductive capacities paired with high compressive strength, which allows mechanical loading shortly after implantation [1].

However, they are lacking the osteoinductive properties of autologous bone graft material. For that reason they should be combined with poly(lactic-*co*-glycolic acid) (PLGA) nanoparticles as a drug delivery system for doxycycline hyclate (DOX) which in addition it’s antibiotic action has shown to feature bone growth promoting effects when presented in adequate concentrations [2].

**METHODS:** DOX-loaded PLGA nanoparticles were produced by double emulsion water in oil in water technique as previously described [3].

Size and morphology of the fabricated particles were characterized qualitatively and quantitatively by AFM, SEM and DLS. UV-vis and FT-IR were used to characterize and quantify the encapsulated drugs. Several process modifications were investigated to manipulate particle morphology and drug diffusion during particle formation. Furthermore, the developed method was slightly adapted to produce particles loaded with the hydrophobic drug simvastatin (SIM), which has shown to have similar bone growth properties as DOX.

**RESULTS:** The introduced fabrication method was found successful for the production of smooth, spherical nanoparticles within the size range of 200 to 800 nm (see Fig. 1). Particle size and morphology could to some extent be controlled by altering different emulsification parameters.

However, maximal encapsulation efficiency (EE) for hydrophilic DOX was just below 2 %. At the same time hydrophobic SIM could be entrapped at up to 80 % EE. Various process modifications tested to decrease the loss of DOX during the fabrication process did not significantly increase the EE.

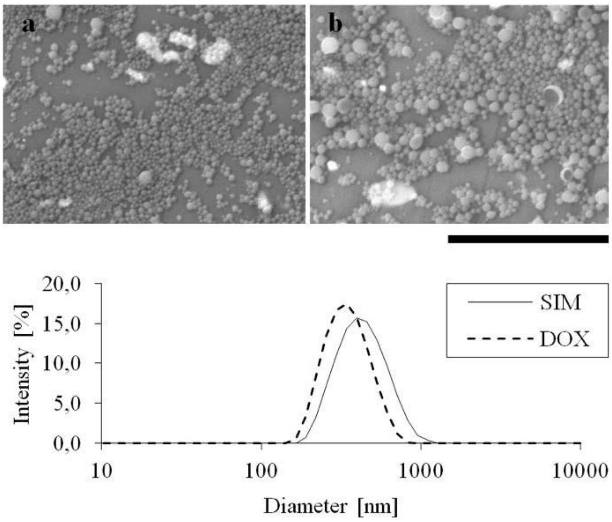

*Fig. 1: SEM-images of (a) DOX- and (b) SIM-loaded PLGA nanoparticles featuring smooth, spherical shape and size distribution measured by DLS. Scale bar 10 µm.*

**DISCUSSION & CONCLUSIONS:** The comparatively high EEs for small hydrophilic molecules in PLGA nanoparticles reported elsewhere [3] could not be reproduced. A huge discrepancy could be observed for the EE of DOX and SIM. These findings suggest that big quantities of hydrophilic DOX diffuse into the outer water phase during particle preparation. Though, none of the various employed process modifications aiming at accelerating polymer precipitation and retarding diffusion kinetics did yield any mentionable effect on the EE.

**ACKNOWLEDGEMENTS:** This study was supported by Research Council of Norway grant NFR 228415.

# Development of multifunctional organic coatings for bioceramics; towards functional cell-engineered bone implants

V Semak, J Sautaux, S Gerber-Lemaire

*Institute of Chemical Sciences and Engineering, EPFL, CH-1015, Lausanne, Switzerland*

**INTRODUCTION:** Tissue engineering of permanent implants is a promising approach for the treatment of large bone defects. While many efforts are currently devoted to the development of porous bioceramics mimicking both the structure and composition of bones, their integration into human tissue remains a challenging issue. In particular, *i*) failure to develop a functional vasculature within the material scaffold and *ii*) fibrotic overgrowth at the implantation site often compromise long term functionality of bone substitute materials. Trans-scaffold migration and in-scaffold survival of human bone-derived cells are mandatory for development of cell engineered permanent implants.

**METHODS:** To achieve organic coating of the bioceramic surface, two structurally different types of organic ligands were designed. The first one, based on discrete molecular approach, consists in the synthesis of well-defined low molecular weight multifunctional ligands. The second strategy, based on a polymeric approach, makes use of water-soluble pHPMA copolymers. Functional composition of both type of coatings is identical and includes the following active subunits: *i*) pyrogallol moieties which were established as robust anchoring groups to the inorganic matrix of bioceramics, *ii*) activated cyclooctynes (DIBO) for biocompatible copper-free [3+2] cycloaddition with azido-modified human osteoblast progenitors and *iii*) specific peptide sequences, e.g. *c*(RGDfK), to promote endothelial cells adhesion. [1-2]

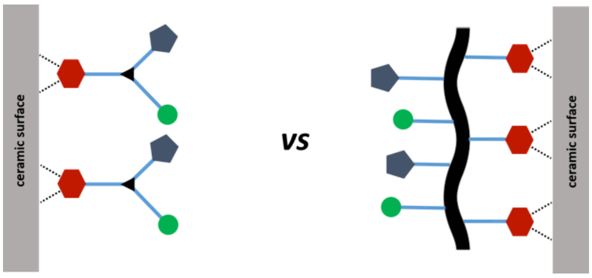

*Fig. 1: Discrete molecule vs. polymer multifunctional ligands; red hexagonal: pyrogallol moiety, green circle: DIBO and blue pentagonal: peptide.*

**RESULTS:** First, the degree of functionalization resulting from both coating strategies was evaluated by XPS analysis of alumina ceramics surface coated with model ligands containing trifluoromethyl moieties for easy quantification of fluorine content. The influence of both types of coatings on the ability of bone progenitor cells to colonize bioceramic scaffolds was then investigated.

**DISCUSSION & CONCLUSIONS:** To ensure long term functionality of bone implants and reduce the occurrence of fibrotic adverse response, a narrow contact between bioceramic surface and surrounding tissue must be achieved. Furthermore, for effective integrin-mediated cell adhesion on surfaces a minimum distance of about 3.5 nm between functional ligands and the surface is required. [3] To fulfil these requirements, organic coatings containing a pyrogallol moiety for binding to the ceramics and a PEG4 linker to guarantee sufficient thickness of the coat were designed. In the polymeric approach additional thickness and coating homogeneity is expected thanks to the pHPMA backbone. [4] Additional benefit consist in ratios variability of chemical bioactive functionalities. While in the discrete molecule approach ratios are dictated by the structure of the scaffold, the use of copolymers allows high ratios variability by simple modulation of the ratios of starting monomers.

In this contribution, chemical synthesis of both types of ligands and ceramic surface coating will be presented.

**ACKNOWLEDGEMENTS:** We thank the Swiss National Science Foundation (Grant Nos. CR23I3-124753 and CR22I2-140866) for financial support.

# Osseointegration of electron beam melted porous Ti6Al4V implants – probing the composition of the bone-implant interface by Raman spectroscopy

FA Shah[1,2], A Snis[3], A Matic[4], P Thomsen[1,2], A Palmquist[1,2]

*[1]Department of Biomaterials, Sahlgrenska Academy at University of Gothenburg, [2]BIOMATCELL VINN Excellence Center of Biomaterials and Cell Therapy, [3]Arcam AB, Mölndal, Sweden, [4]Department of Applied Physics, Chalmers University of Technology, Gothenburg, Sweden*

**INTRODUCTION:** Raman spectroscopy has been used extensively to characterise the organic and inorganic components of bone. Using Raman spectroscopy, we analysed whether bone interfacing implant surfaces having distinctly different geometry and micro-topography could still exhibit compositional differences, despite being considered fully mature histologically.

**METHODS:** Using a standard Arcam Ti6Al4V extra low interstitial (ELI) powder in an Arcam EBM S12 system, (i) Solid, and (ii) Porous implants (5.2 mm diameter, 7 mm length) were manufactured. Cylindrical rods obtained from the build were machined into solid implants. The porous implants had 0.5-1 mm wide struts separated by 500-700 µm. All of the implants were blasted with the Ti6Al4V ELI powder. The implants were placed in the femoral epiphyses of adult sheep and allowed to heal for 26 weeks. Resin-embedded bone-implant blocks were used for Raman spectroscopy. Six positions were analysed in the native bone, and the bone interfacing each implant type (~5–10 µm from the implant surface), three each from the cortical and the trabecular regions. Spectra were collected, three acquisitions of 300 s integration time, at room temperature using a Dilor XY spectrometer, equipped with a 676 nm Ar/Kr laser (~20 mW power, 100x objective, 600 groove/mm$^{-1}$ grating, 300 mm focal length, 530 µm confocal pinhole). Raw spectra were background corrected, the wavenumber axis was adjusted so that the $\nu_1$ PO$_4^{3-}$ peaks corresponded to ~959 cm$^{-1}$, and all spectra were normalised to the $\nu_1$ PO$_4^{3-}$ band intensity.

**RESULTS:** At six months, both implant types showed high amounts of bone-implant contact and bone-area, and no histological differences could be demonstrated[1]. For each group, the spectra recorded from the cortical regions appeared similar to the trabecular regions. The interfacial tissue (both implant types vs. native bone) showed lower carbonate-to-phosphate ($\nu_1$ CO$_3$/$\nu_1$ PO$_4^{3-}$; $\nu_1$ CO$_3^{-}$/$\nu_2$ PO$_4^{3-}$) and carbonate-to-matrix ($\nu_1$ CO$_3$/Amide I) ratios, while mineral crystallinity (1/FWHM $\nu_1$ PO$_4^{3-}$) and the apatite-to-collagen ratios ($\nu_2$ PO$_4^{3-}$/Amide III; $\nu_1$ PO$_4^{3-}$/Amide I) remained similar for all groups. Compared to the native bone, the amino acid (Pro, Hyp, Phe, and Tyr) signals were stronger at the interfacial bone tissue. Phe and Tyr levels decreased in the order: solid implants > porous implants > native bone, however, the Phe/Tyr ratio was similar for all the groups and a correlation was observed between Phe and Tyr peak intensities ($R^2$ = 94%). The $\delta(CH_3)$, $\delta(CH_2)$ deformation band was also stronger at the interfacial tissue. In all cases, the Amide I/Amide III ratio remained similar for the native bone and the interfacial tissue **(Fig. 1)**.

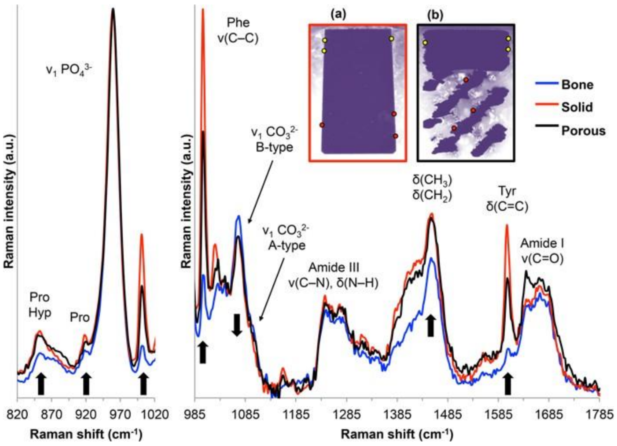

*Fig. 1: Avg. Raman spectra for the native bone, solid (a), and porous (b) implants. Yellow and red dots indicate cortical and trabecular analysis sites.*

**DISCUSSION & CONCLUSIONS:** At six months healing, the interfacial bone was less mature than native bone (lower relative CO$_3^{-}$ content and higher amino acid content). While the implant geometry did not strongly influence the composition of the interfacial tissue, Phe and Tyr levels varied between the two implant types: lower for the porous implants and closer to those detected in the native bone. Despite little or no differences histologically, subtle differences in the composition of bone interfacing different implant surfaces may still exist, and can be detected by Raman spectroscopy.

# Biocomposites on the base of microarc calcium-phosphate coatings and ultrafine grained bioinert metals

Y Sharkeev[1,2], SG Psakhie [1,2]

*[1]ISPMS SB RAS, Tomsk, Russia, [2]TPU, Tomsk, Russia*

**INTRODUCTION:** Implants consisting of bioinert metals (titanium, zirconium, niobium) and their alloys and biocompatible coatings based on calcium phosphates [1] are widely used in modern medical practice.

**METHODS:** The combined method of severe plastic deformation including abs-pressing within a predetermined temperature range and subsequent multiple rolling at room temperature is used to form an ultrafine-grained state with average size of grain-subgrain structure elements 0.1–0.2 μm in the bioinert substrate. This leads to a considerable increase of the physical and mechanical characteristics (microhardness, yield strength, ultimate strength, fatigue strength, and cycle life) by a factor of 1.5–2.5 and more.

The preliminary preparation of the surface, including sandblasting and chemical etching, allowed the required porous surface to be formed and the adhesive strength of calcium phosphate coatings to be increased by the method of microarc oxidation by a factor of 1.5–2.

To bioactivate implants and to strengthen their osteointegration with bone tissue, the calcium phosphate coating containing calcium phosphate phases native to bone tissues were deposited on their surface (fig. 1). The efficient and simple method of microarc oxidation in aqueous solutions of electrolytes was suggested to obtain calcium phosphate coatings with good physical and chemical properties on the implant surface with complicated shape.

The coatings based on calcium phosphates are biocompatible and promote osteointegration with bone tissue. Moreover, the phase composition and crystallinity of coatings are less important factors for bioengineering of the bone tissue in comparison with the coating relief.

The optimal range of roughness of the calcium phosphate coatings, *R*a = 2–3 μm, that promoted osteogenous differentiation of stromal stem cells, was established. The microarc calcium phosphate coating on the surface of the ultrafine-grained substrate reduced corrosion currents in the region of passivation in physiological salt solutions.

Based on the experimental results, models of the physical and mechanical processes regulating the growth of coatings and their dissolution in biological liquids are considered together with the mechanical properties of calcium phosphate coatings.

To describe the deformation and destruction of porous calcium phosphate coatings, multilevel models were suggested based on the method of mobile cellular automats. The coatings were considered as hierarchically organised porous materials. Based on the constructed models, the effective strength and elastic properties of coatings were investigated taking into account the depth distribution of elemental composition of the coating and the salient features of their deformation and destruction upon mechanical loading of various types.

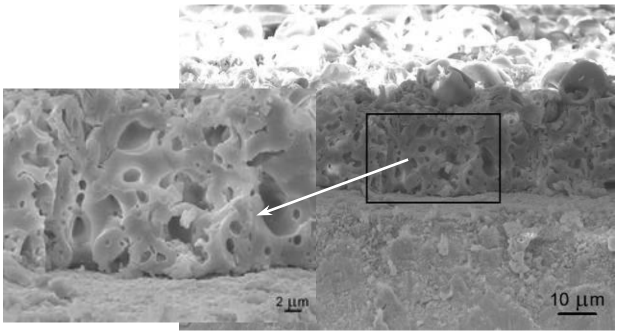

*Fig. 1: SEM cross-section image of microarc calcium-phosphate coating on titanium substrate*

Examples of the biocomposite based on ltrafine-grained titanium and microarc calcium phosphate coatings used in medical practice are presented.

**ACKNOWLEDGEMENTS:** The authors are grateful to their colleagues for participation in this work in all stages, processing, and discussion of the results obtained and preparation of publications. The work was carried out partially under financial support of the Russian Basic Research Program of SB RAS 2013-2016, III.23.2.

# Antibacterial efficiency of biomaterials with biodegradable polymer and antibiotics

I Skadins[1], J Kroica[1], I Salma[2], A Reinis[1], M Sokolova[2], D Rostoka

*[1]Biology and Microbiology Department, Riga Stradins University, Latvia, [2]Biomaterial Innovation and Development Centre, Riga Technical University, Latvia*

**INTRODUCTION:** Despite aseptic and antiseptic techniques, the microorganism's ability to infect and colonize the implanted biomaterial or some other medical device is still serves as a risk factor in the development of nosocomial infections. So all the studies that determine one of the most important properties of biomaterials - the microbial contamination risk become more popular [1]. Local antibiotic therapy have several advantages compared to systemic antibiotic treatment. This advantage can be used in local biomaterial systems to reduce the number of bacterias which bind to implanted biomaterial [2].

**METHODS:** Group A consisted of hydroxyapatite biomaterials with biodegradable polycaprolactone polymer, saturated with ciprofloxacin. Group B consisted of hydroxyapatite biomaterials with biodegradable polylactic acid polymer, saturated with ciprofloxacin. Group C consisted of hydroxyapatite biomaterials saturated with biodegradable polycaprolactone polymer. Group D consisted of hydroxyapatite biomaterials saturated with biodegradable polylactic acid polymer. Group E consisted of hydroxyapatite biomaterials saturated with ciprofloxacin. Antibacterial efficiency of all three group biomaterials were tested using *S. epidermidis* (ATCC 12228) and *Ps. aeruginosa* (ATCC 27853) bacteria reference cultures. The ciprofloxacin saturated hydroxyapatite biomaterials with biodegradable polylactic acid polymer disks were firstly eluted in rabbit blood plasma at 37 $^0$C with 5% $CO_2$ atmosphere and 100% relative humidity for 2h. Studied biomaterials of all groups were incubated at 37$^o$C for 24h 2 ml TSB with investigated bacterial suspension. Suspension consisted of 1 ml TSB and 1ml bacteria suspension with an optic density of 0.5 according to McFarland standard. 2ml TSA bacteria suspension with an optic density of 0.5 according to McFarland standard without biomaterial, which was used as study's control group. After 24h incubation, 0.1 ml suspension was cultured on TSA, in order to test the antibacterial efficiency of studied biomaterials. At the same time the biomaterials of studied groups were transferred to a new TSB and bacterial culture suspension for the next 24 hours. These actions repeated every 24 hours until two days in a row no antibacterial efficiency were observed in the tested biomaterial groups – and TSA colony numbers were equivalent with control group colony numbers on TSA.

**RESULTS:** A much longer antibacterial efficiency was observed on group A and group B biomaterials against both bacterial cultures used in the study when compared to group E biomaterials. The average antibacterial length of group A biomaterials against S.epidermidis was 304,8 h±10.08, whereas the average antibacterial length against Ps. aeruginosa was 280,8h±13,44. The average antibacterial length of group B biomaterials was 187,2h±11,52 against Ps. aeruginosa bacteria culture, whereas the average antibacterial length of group B biomaterials against S. epidermidis culture was 213,6h±8,64. The average antibacterial length of group E biomaterials against S.epidermidis was 72h±9,6, whereas the average antibacterial length against Ps. aeruginosa was 60±12. Antibacterial characteristics were not observed on group C and group D biomaterials against any of the bacterial cultures used in the study.

**DISCUSSION & CONCLUSIONS:** Samples with antibiotics and polymer, ensures the slow secretion of antibiotic substances. Thus ensuring protection from implant related infection for a longer period of time. The polymer is degraded slowly and it also ensures the slow secretion of antibiotic substances. However in situations when samples are saturated with antibiotic substances and they are not covered by polymer, antibiotics secrete rapidly, thus ensuring protection from infection for a shorter period of time and have higher risk to develop implant related infections.

# OPG / RANKL signaling pathway in osteoporotic bone can be targeted by biphasic calcium phosphate bioceramics

S Petronis[1] , M Pilmane[2] , J Locs[3] , A Skagers[4]

*[1] 2nd Riga Hospital, Latvia . [2] Institute of Anatomy and Anthropology, Riga Stradins university, Latvia. [3] Rudolfs Cimdins Riga Center for development and innovation of Biomaterials, Riga Technical university, Latvia. [4] Department of Oral and Maxillofacial Surgery, Riga Stradins university, Latvia*

**INTRODUCTION:** Evaluation of RANK, RANKL and OPG pathway is essential to the understanding processing and regulation of bone formation and resorbtion. RANKL links to the osteoclasts surface receptor RANK and stimulates osteoclastogenesis . OPG secreted by osteoblasts as a decoy receptor for RANKL, prevents RANKL from binding to RANK. The osteoprotective role of OPG is reported from animal studies[1, 2, 3].

**METHODS:** Experimental osteoporosis was induced in 7 female rabbits by ovarioectomy and 1 mg/kg of methylprednisolone daily for 8 weeks [4]. On 4 animals the hole was created in hip bone and filled with a biphasic calcium phosphate bioceramic granules 1 to 1.4 mm of size , containing hydroxyapatite (HAp) and β-tricalcium phosphate (β-TCP) proportion of 90/10 developed in RTU Rudolfs Cimdins Riga Biomaterials innovation and development Centre. The control group had 3 rabbits with the analagous defect of osteoporotic bone without bioceramics implantation. After 3 months animals were euthanased and bone samples collected and prepared to make immunohistochemical analyzis of OPG. Semiquantitative method was used to evaluate results. Few OPG positive cells were marked +, little amount of positive cells were marked +, medium ++ and many +++.

**RESULTS:** The bioactivity of HAp/TCP 90/10 granules showed stable increase in OPG secretion twice as high as in the control group without bioceramic implantation. Results are summarised in tables below.

*Table 1. Summary of results of immunohistochemical analysis of OPG in experimental group of animals with induced osteoporosis 3 months after bioceramics pellet implantation.*

| | Animal No 1 | Animal No 2 | Animal No 3 | Animal No 4 |
|---|---|---|---|---|
| OPG | ++ | ++ | ++ | + |

*Table 2. Summary of results of immunohistochemical analysis of OPG in control group of animals with induced osteoporosis without bioceramics pellet implantation.*

| | Animal No 10 | Animal No 12 | Animal No 15 |
|---|---|---|---|
| OPG | 0/+ | + | + |

**DISCUSSION:** Biphasic calcium phosphate bioceramic granules beside osteoconductive potency in hole of osteoporotic hip bone of rabbits through increased secretion of OPG has positive bioactivity at early stage of bioceramics and bone interaction by decrease of osteoclast activation.

**ACKNOWLEDGEMENT :** This research was supported by Latvia state research programm's project Nr. 4.1.2.

# Degradation behaviour of biodegradable biopolymer and calcium phosphates composites

M Sokolova[1], J Locs[1], A Putnins[1]

[1]*Rudolfs Cimdins Riga Biomaterials Innovations and Development Centre, Riga Technical University, Riga, Latvia*

**INTRODUCTION:** Calcium phosphates (CaP) have excellent biomaterial properties and are widely applied for bone regeneration. A major drawback is the brittle nature of CaP, therefore it has limited use in load bearing areas of skeleton. Biodegradable polymer (e.g. polylactic acid and polycaprolactone) is biocompatible, synthetic polymer with high strength and modulus [1]. It can easily be processed into shapes such as screws, pins and plates for orthopaedic applications, and fabricated into scaffolds for replacement and regeneration of tissues [2]. To capitalize the advantages and overcome drawbacks of CaP, it is combined with biodegradable biopolymer to generate biocomposite material.

**METHODS:** CaP powder was prepared by wet chemical precipitation synthesis method from calcium oxide and ortophosphoric acid solution [3]. Biodegradable polymer and calcium phosphates composites were manufactured using novel liquid/solid suspension technology. Samples with composition 20 wt% PLA / 80 wt% CaP were formed into a 13 mm diameter plates by a pressing method. Fourier-transform infrared spectroscopy (FT-IR) was used to determine the various functional groups in the composite samples. X-ray diffractometry (XRD) was used to analyze phase composition of obtained calcium phosphates and biodegradable polymer composite samples.

Degradation behavior of composite is of crucial importance in tissue engineering, because the degradation rate is essentially linked to cell growth and tissue regeneration. The degradation behaviour was performed according to the ISO 10993-14 “Biological evaluation of medical devices”. The samples for degradation study was prepared as a powder (100CaP and 20PLA/80CaP powder) and as a plate (20PLA/80CaP sample) with total porosity of 20 %. The test was performed in Tris (hydroxymethyl) aminomethane - hydrochloric acid buffer solution (TRIS – HCl) (pH 7.4). Release of the calcium ions was measured using a Ca-ion selective electrode (Mettler Toledo *perfectION$^{TM}$*).

**RESULTS:** Figure 1 shows changes in the concentration of Ca ions in TRIS-HCl as a function of immersion time for 100CaP and 20PLA/80CaP powder and 20PLA/80CaP sample.

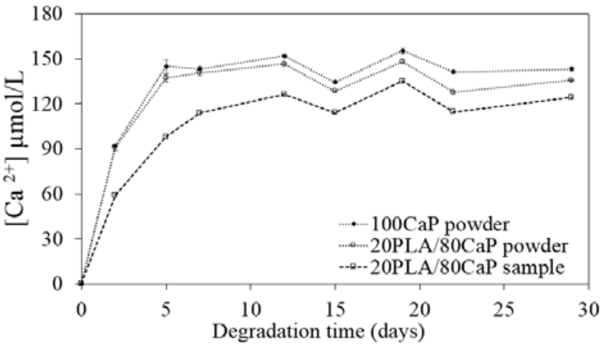

*Fig. 1: Calcium ion release into TRIS-HCl buffer as a function of time.*

**DISCUSSION & CONCLUSIONS:** *In vitro* evaluation of composite showed that the dissolution of the CaP component is not strongly affected by the presence of PLA, at least not at short immersion time. The presence of CaP, on other hand, may enhance the hydrolytic degradation of PLA by ability of improve hydrophilicity. The fact that PLA is a slow degrading polymer, longer immersion times are needed to test the overall degradation kinetics of PLA/CaP composites.

**ACKNOWLEDGEMENTS:** This work has been supported by National Research Programme “Multifunctional Materials and composites, photonics and nanotechnology (IMIS$^2$)” Project No. 4 “Nanomaterials and nanotechnologies for medical applications”.

# Nanostructured RF magnetron sputter deposited hydroxyapatite coating on the surface of permanent and biodegradable alloys

RA Surmenev[1], MA Surmeneva[1], II Selezneva[2], AI Tyurin[3], TS Pirozhkova[3], M Epple[4]

*[1]Tomsk Polytechnic University, Tomsk, Russia, [2]Institute of Theoretical and Experimental Biophysics, Pushchino, Russia, [3]G.R. Derzhavin Tambov State University, Tambov, Russia, [4]University of Duisburg-Essen, Essen, Germany*

**INTRODUCTION:** Surface modification of biomedical materials is one of the most important objectives of research this time. Therefore, different surface modification strategies should be investigated. This study reports on application of radio-frequency (RF) magnetron sputtering to prepare thin CaP-based coatings on the surface of permanent (Ti, NiTi) or biodegradable (Mg-based) metallic substrates.

**METHODS:** Pure hydroxyapatite (HA) and silicon-containing HA coatings with the content of silicon 0.5 and 1.72 mol were deposited via a conventional RF magnetron sputtering set-up operated in high vacuum conditions. Details on the coating deposition regimes can be found elsewhere [1]. Different thickness of the coatings up to 1500 nm was obtained. The physico-chemical and biological properties of the biocomposites were studied via TEM, SEM, EDS, XRD. Wettability, contact angle hysteresis, nanohardness and adhesion strength, corrosion resistance; biological *in vitro* tests were also done. Cross-sections of thin specimens were prepared by FIB to study the microstructure of the coatings by TEM.

**RESULTS:** CaP coating homogeneously covered the entire surface of the substrates. In all cases a single phase coating of HA was prepared. Coating deposition process resulted in a slight increase of the surface roughness and nano-scale grains, generating an amorphous layer at the substrate/coating interface and inducing the growth of a columnar grain structure perpendicular to the substrate surface. A microstructural analysis of the film confirmed that the grain size and crystallinity increased when increasing the deposition time. The potentiodynamic polarization test demonstrated that a 1500-nm thick nanocrystalline HA coating significantly improved the corrosion resistance of the bare AZ31 magnesium alloy in a 3.5 wt.% NaCl solution. In the case NiTi substrates a significant decrease of the Ni release rate compare to the bare substrate was observed [2]. Nanoindentation tests demonstrated that all HA coatings increased surface hardness on both the micro- and nanoscale. The films can significantly enhance the wear resistance of this resorbable alloy. The nanostructured HA-based coatings were not cytotoxic, as proven by *in vitro* assays using primary dental pulp stem cells and mouse fibroblast NCTC clone L929 cells. HA coatings with different thicknesses stimulated cells to attach, proliferate and form mineralized nodules on the surface better than uncoated substrates.

**DISCUSSION & CONCLUSIONS:** The obtained results revealed that RF magnetron sputtering is a versatile technique to prepare nanostructured CaP-based coatings on the surface of biodegradable and permanent implants. The corrosion resistance of the magnesium-based alloys could be effectively improved via RF magnetron sputter deposited nanocrystalline CaP coatings. The experiments revealed that the bias applied during the deposition of HA coating resulted in a decrease of the grain and crystallite size of the film having a crucial role in providing the enhancement of the mechanical properties of the biocomposites.

**ACKNOWLEDGEMENTS:** The authors are thankful to the RFBR (14-08-31027 мол-а, 15-08-08652), the Russian President's Stipend SP-6664.2013.4 and MK-485.2014, NAUKA #11.1359.2014/K.

# pH triggered self-assembly and aggregation of a structurally disordered proline-rich polypeptide

H Tiainen[1], S Geißler[1], R Lund[2], HJ Haugen[1]

*[1]Department of Biomaterials and [2]Department of Chemistry, University of Oslo, Norway*

**INTRODUCTION:** Unfolded, or structurally disordered, proline-rich regions of natural proteins such as collagen, amelogenin, and ameloblastin have recently been found to play an important role in biomineralisation[1]. Short synthetic peptides that mimic the disordered regions of such proteins may therefore be bound onto biomaterial surfaces to stimulate bone formation and regeneration *in vivo*. Since the function and bioactivity of these peptides is likely to be strongly linked to their lack of well-defined three-dimensional structure, it is important to understand the behaviour of such biomolecules when dissolved in aqueous media.

**METHODS:** The structure of two dissolved synthetic proline-rich polypeptides (Table 1) that have previously shown potential in inducing bone mineralisation of both osteoblast-like cells and mesenchymal stem cells[2] were examined.

*Table 1: Amino acid sequence of the two examined proline-rich polypeptides.*

| Peptide | Sequence |
|---|---|
| P2 | PLVPSQPLVPSQPLVPSQPQPPLPP |
| P5 | PLVPSSPLVPCCPLVPCCPSPPLPP |

These polypeptides were dissolved in either TRIS-buffered saline (pH 6-12) or sodium acetate buffer (pH 3-5.5) at 5 mg/ml concentration and their structure was analysed with small-angle X-ray scattering (bioSAXS; BM29 beamline, ESRF, Grenoble). In order to evaluate chain conformation and the size and shape of the peptide aggregates, both model independent analyses (IFT, Guinier) and geometrical body modelling were performed. Circular dichroism spectroscopy (CD) was used to characterise the secondary structures of the polypeptides at three different pH: 5, 7.5, and 9.

**RESULTS:** While P2 maintained its disordered random coil –like structure throughout the tested pH range (pH 3-12), P5 formed aggregates at high pH (pH 8-12) as shown in Fig. 1. Radius of gyration nearly doubled and over tenfold increase in the calculated molecular weight was observed in this pH region, indicating that several polypeptide chains clustered together into nanoparticles whose scattering profile best fitted a triaxial ellipsoidal model. However, no formation of specific secondary structures within these polypeptide aggregates was observed at pH 9.

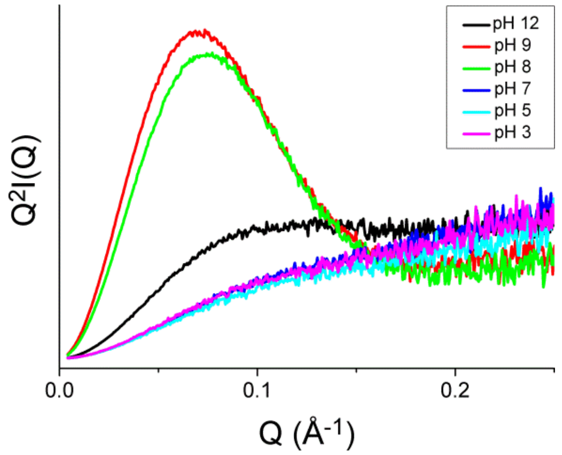

*Fig. 1: Kratky plots reveal the pH dependent self-assembly of P5 to elongated globular structure*

**DISCUSSION & CONCLUSIONS:** The main difference between the two examined proline-rich polypeptides P2 and P5 is the presence of cysteine (C) in the amino acid sequence of P5. Cysteine being the only amino acid that contains a thiol group (-SH), the observed self-assembly and aggregation at high pH may be explained by the formation of disulphide bonds (-S–S-) which link several polypeptide chains together as the thiol groups of the cysteines become deprotonated with increasing pH ($pKa_{thiol}$ = 8.3). Consequently, the disordered polypeptide chains assemble together forming elongated covalently cross-linked clusters that were observed as the characteristic increase in the scatter intensity. Self-assembly and aggregation of the polypeptide chains was not observed within physiological pH range, and it is therefore not expected to influence the bioactivity of the molecule. However, such pH dependent change in peptide characteristic must be taken into account when choosing the appropriate processing conditions for binding the disordered peptides onto biomaterial surfaces.

**ACKNOWLEDGEMENTS:** This study was supported by Research Council of Norway grant NFR 231530 and European Synchrotron Radiation Facility.

# Microstructure development of calcium niobophosphate glass-ceramics with addition of $TiO_2$

J Vecstaudza[1], G Krieke[1], A Stunda-Zujeva[1], L Berzina-Cimdina[1,2]

*[1] Institute of General Chemical Engineering, Riga Technical University, Riga, Latvia. [2] RTU R. Cimdins Riga Biomaterial Innovation and Development Centre, Riga Technical University, Riga, Latvia*

**INTRODUCTION:** Glasses and glass-ceramics containing Ca and P are promising biomaterials because of widely variable composition, structure and therefore properties. $Nb_2O_5$ improves chemical and mechanical properties of phosphate glasses; furthermore calcium niobophosphate glass-ceramics is biocompatible. Unfortunately surface crystallization mechanism is dominant for these glasses and therefore non-uniform microstructure is formed [1-3]. Aim of the work was to investigate and improve microstructure of later glass-ceramics with addition of nucleating agent $TiO_2$. The novelty is the crystal size reduction in controlled manner of bulk calcium niobophosphate glass-ceramics with addition of $TiO_2$ that has never been reported elsewhere.

**METHODS:** At first glasses of $Na_2O$-$CaO$-$P_2O_5$-$Nb_2O_5$ system with 0-10 mol% $TiO_2$, were prepared at 1300 °C by melt quenching and annealing. Bulk glasses were crystallized at 750-900 °C for 1h to obtain glass-ceramics. Glasses were characterized for their chemical composition (SEM-EDS), structure (FT-IR, density and molar volume) and thermal properties (DTA). Microstructure development (SEM) and crystalline phases (XRD) were analysed for glass-ceramics. Both fresh fractures and polished samples were investigated with SEM.

**RESULTS:** Obtained glasses were monolith, transparent to visible light and without cracks. Addition of $TiO_2$ increased density and decreased molar volume of glasses. FT-IR revealed slight shifting of $(PO_3)^{2-}$ and $(PO_4)^{3-}$ bands and intensity increment of coalesced P-O-P and $[TiO_4]$/$[TiO_6]$ bands with increasing amount of $TiO_2$. DTA demonstrated decrement of glass transition temperature and complex crystallization behaviour - shifting and coalescing of thermal effects. Thermal stability of glasses was improved. Glass-ceramics contained several crystalline phases: sodium niobophosphates, calcium phosphates (meta- and pyro-), niobium phosphate, titanium niobium oxide, calcium titanate and unidentified phases as well. Crystallinity of glass-ceramics with $TiO_2$ was comparable to crystallinity of the same sample without $TiO_2$ but obtained at higher crystallization temperatures. Microphotographs showed that addition of $TiO_2$ increased amount of crystalline phases for glasses crystalized at the same temperature (Fig. 1). Uniform, fine-grained and interlocked microstructure was obtained with addition of 5-10 mol% $TiO_2$ for N20, 10 mol% for N25 and 3-10 mol% for N30. Crystallite size of 0.5-5 µm was achieved.

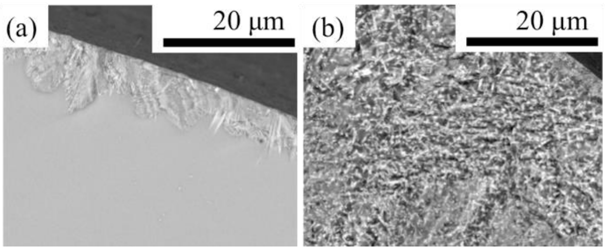

*Fig. 1: N25 glass-ceramics without (a) and with 10 mol% $TiO_2$ (b) obtained at 750 °C.*

**DISCUSSION & CONCLUSIONS:** $TiO_2$ supressed surface crystallization mechanism (Fig. 1.a) of calcium niobophosphate glasses. It can be concluded that $TiO_2$ reduced crystal size and enhanced formation of fine and uniform microstructure in sodium calcium niobophosphate glass-ceramics. $TiO_2$ can be used effectively as microstructure controlling agent in the given glass system. Interesting mechanical properties are expected from developed glass compositions.

**ACKNOWLEDGEMENTS:** This work has been supported by the European Social Fund within the project «Support for the implementation of doctoral studies at Riga Technical University».

# Biocompatibility comprehension: semantic and biomedical approach

J Vetra

*Department of Morphology, Riga Stradins University, Latvia*

**INTRODUCTION:** Biomaterials classification, titles of testing methods should be coherently connected with biomedical basic principles and concepts. Our study indicated necessity to introduce among different terms, such as Biocompatibility, Bioactivity, Inductivity, Conductivity**,** Integrativity etc. another one – Reactogenecity.

**METHODS:** There are different objects for implantation - biomaterials, implants, devices, scaffolds. All of them made using biomaterials. In general, there are two terms in which a biomaterial is described or classified into representing the tissues interactions/responses:

- Bioinert , including - biostable
- Bioactive, including - bioresorbable

Objects-tissues interaction we can characterize by Biocompatibility, Bioactivity, Inductivity, Conductivity**,** and Integrativity. Why do we need to introduce Reactogenecity?

**RESULTS:** Our analysis of different biomaterials studies, including our own results, as well as different sources with definitions , completed with creation of new definition of reactogenecity. Reactogenicity – inherent property of a biomaterial to induce a local reaction.

We concluded, that it was important for clarification of term bioactivity. If a material has been designed to induce specific local biological activity, it is bioactive with specificē reactogenicity.

Specific Reactogenicity – Bioactivity, OsteoInductivity, OsteoConductivity, OsteoIntegrativity

Implantation of biomaterials (implants) to cause growth factors and cytokines expression, to activate enzymes and to influence apoptosis.

Non-specific reactogenicity (influence on inflammation and its after-effects) :

Inflamation – connective tissue (incl. bone tissue) reaction. 1st phase – alteratio, 2nd phase-proliferatio.

Reactogenicity is a combination of non-specific and Specific reactogenicity!

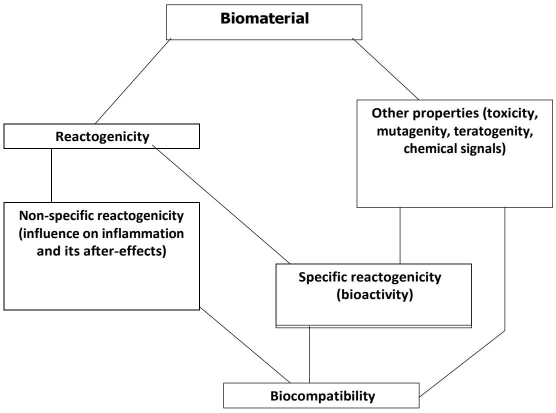

*Fig. 1: Biomaterial – organism interaction properties independence scheme*

**DISCUSSION & CONCLUSIONS:** Biocompatibility mainly characterise implants and devices (local, systemic, biomechanical, biochemical etc. interactions).

Reactogenicity incl. Bioactivity mainly characterize biomaterials.

Tissue response to implantation of biomaterials (reactogenicity) consists of non-specific and specific properties, which together with toxicity, mutagenity, teratogenity and chemical signaling results in biocompatibility.

# Antibacterial debridement strategy for infected permanent dental implants

D Wiedmer[1], H Tiainen[2], H Haugen[2]

*[1]Corticalis AS, Norway [2]Department of Biomaterials, University of Oslo, Norway*

**INTRODUCTION:** Currently used methods for peri-implantitis treatment often fail the requirement to efficiently remove the bacteria caused biofilm, but at the same time, retain the original implant surface. A new strategy combines mechanical and chemical debridement to overcome this challenge. The chemical treatment is based on the potential bactericidal effect of reactive oxygen species (ROS) generated by $H_2O_2$ activated $TiO_2$ nanoparticles and is investigated in the following study.

**METHODS:** The generation of ROS by $H_2O_2$ activated $TiO_2$ surfaces was evaluated by the degradation of the cationic, organic dye methylene blue (MB). A dye solution containing 3% $H_2O_2$, a concentration used in clinical practice [1], was compared to a solution in which $TiO_2$ nanoparticles were added. Dimethyl sulfoxide (DMSO), an efficient radical scavenger, was added to verify the presence of ROS. Ultraviolet-visible spectroscopy (UV-vis) was used to examine degradation of MB. All experiments were made in darkness. A time scale of the measurement is shown in *Figure 1*.

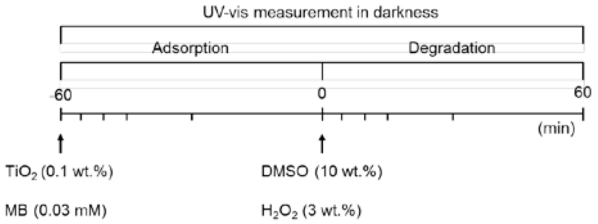

*Fig. 1: Schematic diagram of the experimental procedure for UV-vis measurements.*

**RESULTS:** The results in *Figure 2* display the normalised degradation within 60 min. $TiO_2 + H_2O_2$ showed a significantly stronger degradation of MB compared to $H_2O_2$ alone. The addition of DMSO significantly suppressed the degradation capacity of $TiO_2 + H_2O_2$. Minor adsorption was detected for the tested $TiO_2$ nanoparticles (data not shown).

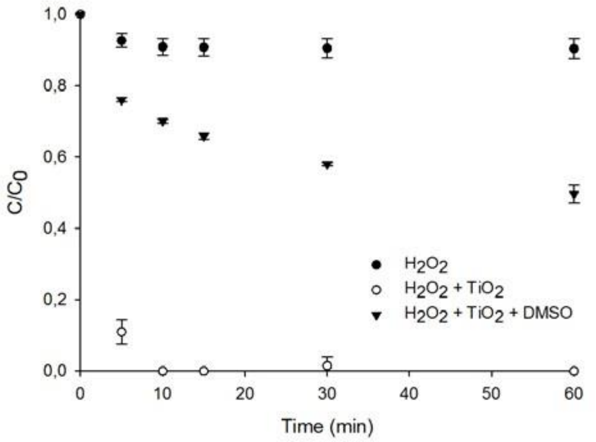

*Fig. 2: MB degradation for different experimental conditions. Data are presented as mean ± SD. Statistically significant differences were found between all groups for all time points ($p < 0.001$, $n=3$).*

**DISCUSSION & CONCLUSIONS:** A combination of $TiO_2$ nanoparticles and low concentration $H_2O_2$ can efficiently decompose MB. Reduced degradation in the presence of DMSO indicates the generation of oxygen species. ROS generation on $TiO_2$ surfaces activated by high concentration $H_2O_2$ had been shown earlier [2,3]. The use of low concentration $H_2O_2$ enables the possibility to use this mixture as a chemical debridement for peri-implantitis. In a next step, an electron paramagnetic resonance (EPR) study will be conducted to identify the species of the generated ROS. Furthermore, an *in vitro* bacteria study is planned to both verify the bactericidal effect and compare it with other debridement strategies.

**ACKNOWLEDGEMENTS:** This study was supported by EUREKA Eurostars E!8320 NuGel.

# Atomic layer deposition technology for biomaterial surface modification

## An application in anticoagulation

LC Wang[1], HC Lin[1], MJ Chen[1], YY Han[2,3], CC Wu[4,5], KC Yang[6]

[1]Department of Materials Science and Engineering, National Taiwan University, Taiwan [2]Department of Traumatology, National Taiwan University Hospital, Taiwan, [3]Department of Surgery, National Taiwan University Hospital, Taiwan, [4]Department of Orthopedics Surgery, National Taiwan University Hospital, Taiwan, [5]Department of Orthopedics, En Chu Kong Hospital, Taiwan, [6]School of Dental Technology, Taipei Medical University, Taiwan

**INTRODUCTION:** Extracorporeal membrane oxygenation (ECMO) is used to treat patients with severe cardiovascular disease and respiratory disorder [1]. However, concerns including cardiac thrombosis and pulmonary haemorrhage are remaining [2]. Anticoagulation regimen, such as heparin, is routinely used to prevent aforementioned problems, though it may cause thromboembolism or life-threatening bleeding [3]. Atomic layer deposition (ALD), a technique which was widely used in semiconductor industry, can deposit high quality nanoscale films with a uniform thickness. Thus, ALD technology is used for surface modification of cannula in this study.

**METHODS:** Medical grade poly(vinyl chloride) (PVC, raw materials of cannula for ECMO) were used as substrates and ultrasonically cleaned with deionized water before study. $Al(CH_3)_3$ was reacted with water vapor to form a thin $Al_2O_3$ film on PVC substrates using a low-temperature ALD technique. Prepared $Al_2O_3$-coated PVA samples were characterized, and the hemocompatibility tests were conducted.

**RESULTS:** The thickness of deposited $Al_2O_3$ film was about 20 nm. The surface morphology and water contact angle of untreated and $Al_2O_3$-coated PVC samples were shown in *Fig. 1 and Fig. 2*.

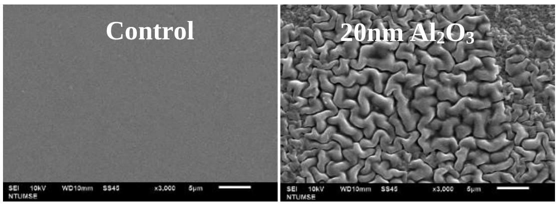

*Fig. 1: Surface morphology of untreated and $Al_2O_3$-coated PVC substrates.*

Protein adsorption tests showed more albumin and fibrinogen adsorbed on the surface of $Al_2O_3$-treated substrate than that of PVC. The treated substrates also showed less blood cells adhesions (*Fig. 3*).

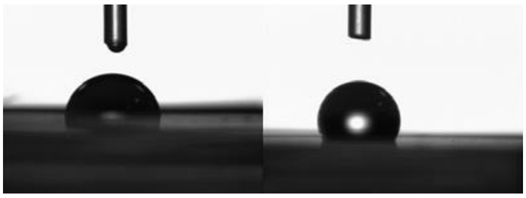

*Fig. 2: Wettability of untreated and $Al_2O_3$-coated PVC samples.*

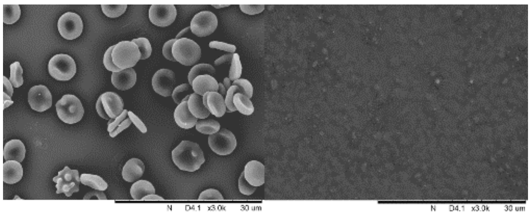

*Fig. 3: Blood cells adhesions on untreated and treated substrates.*

**DISCUSSION & CONCLUSIONS:** A highly uniform thin $Al_2O_3$ layer was successfully grown on the PVC substrates. This surface modification approach makes PVC more hydrophobic, and improves protein absorption on the substrates. Albumin films also prevent blood cells adhesion and platelet activation. Analysis of soluble activation markers showed ALD-treated substrates prevent coagulation cascade, which may decrease the formation of thrombosis. This *in vitro* study reveals surface modification using ALD technology can improve the hemocompatibility of PVC and can also be applied to modify other biomaterials.

**ACKNOWLEDGEMENTS:** This study was supported by Ministry of Science and Technology under grant number 101-2325-B-002-013 and 103-2218-E-002-028.

# Formation of pancreatic beta-cell spheroids using micropatterned substrates

KC Yang [1], G Yanai[1], Y Shirouzu[1], S Sumi[1]

*[1]Department of Organ Reconstruction, Institute for Frontier Medical Sciences, Kyoto University, Kyoto, Japan*

**INTRODUCTION:** For islets, the integrity and hierarchical structure influence β-cells physiology dramatically [1]. It is known that cell-cell interactions are critical to insulin secreting [2]. Moreover, the size of cell spheres influences biological behaviors of cells [3]. Thus, formation of uniform cell spheres with controllable size shall benefit cell therapy for diabetes [4].

**METHODS:** Murine pancreatic β-cells (MIN-6) were cultured on micropatterned substrates at different cell density. The size, number, proliferation, survival, activity and apoptosis were demonstrated. Insulin gene expressions and insulin secretion were analyzed. Cell spheroids were further transplanted into diabetic C57BL/6 mice to evaluate the *in vivo* performance. Animals were humanely sacrificed at predetermined intervals for histologic examinations.

**RESULTS:** Beta-cells aggregated as cell spheroids on micropatterned substrates. Cell density determined the size of cell spheroids as well as survival rates. Cells did not proliferation after spheroid formation. Apoptosis is noticed in irregular and large cell aggregates.

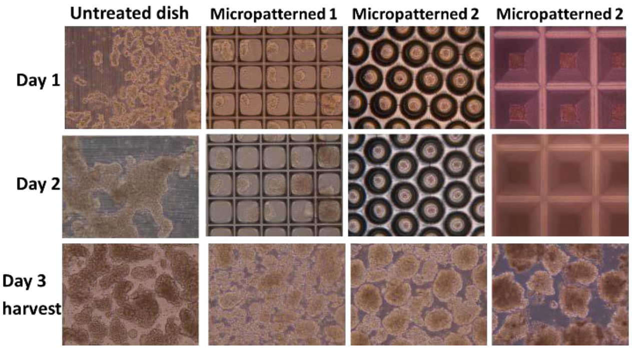

*Fig. 1: MIN-6 cell spheroids formed on different substrates.*

Compared with monolayer cells, cell spheroids had a higher insulin stimulation-index. The mRNA expressions of insulin related genes of cell spheroids were up-regulated. Western blot analysis revealed that cell spheroids had higher connexin 36 protein productions. Conversely, E-cadherin and MafA were down-regulated. Animals that received both monolayers and cell spheroids had decreased blood glucose levels and regained body weight. Histologic studies showed monolayers and cell spheroids were positive to insulin staining. Interestingly, the area under curve for the intraperitoneal glucose tolerance test (IPGTT) and serum insulin levels showed cell spheroids had superior *in vivo* performance.

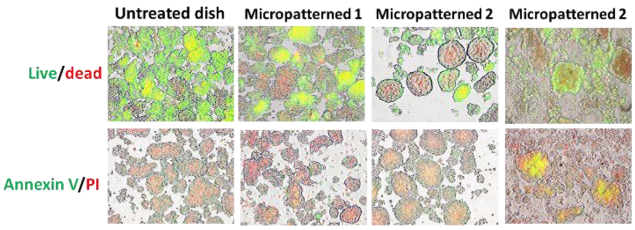

*Fig. 2: Survival and apoptosis of β-cell spheroids.*

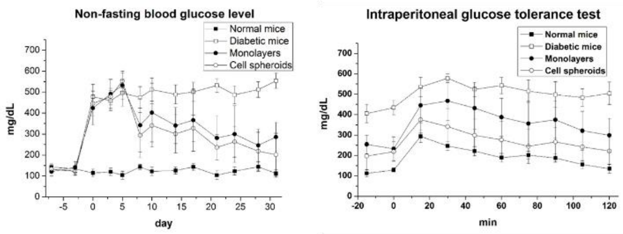

*Fig. 3: Blood glucose levels and IPGTT of diabetic animals received monolayers and cell spheroids transplantation.*

**DISCUSSION & CONCLUSIONS:** This study reveals that micropatterned substrate promotes β-cells aggregating. Formation of cell spheroid regulates insulin gene expression to improve insulin secretion. The *in vivo* performances of β-cell were also enhanced. Therefore, the isolated islets or insulin-producing cells can be cultured on micropatterned dishes to improve/maintain integrity prior to transplantation.

**ACKNOWLEDGEMENTS:** KC Yang is supported by Japan Society for the Promotion of Science under the grant number P12099.

# Preparation of Sr and F co-substituted hydroxyapatite *via* wet precipitation method

V Zalite[1], J Locs[1]

[1]*Rudolfs Cimdins Riga Biomaterials Innovations and Development Centre, Riga Technical University, Riga, Latvia*

**INTRODUCTION:** Various chemically and structurally modified calcium phosphates (CaP) are used in medicine and have a great interest among scientists representing different research areas. In recent years, CaP systems have been investigated for enhancement of tooth enamel remineralization [1]. Strontium (Sr) and fluorine (F) co-substituted hydroxyapatite (SrFHAp) could be a good candidate for tooth enamel remineralization due to HAp structural similarity to mineral part of enamel, a long known anti-caries effect of fluorine [2] and a potential of strontium as dentin desensitising agent [3]. Therefore it is challenging to obtain partly co-substituted HAp with desired amount of fluorine and strontium in the apatite structure.

**METHODS:** SrFHAp powder was prepared by a wet precipitation method. All chemical reagents ($Ca(NO_3)_2•4H_2O$, $Sr(NO_3)_2$, $NH_4F$ and $(NH_4)_2HPO_4$) were provided by Sigma-Aldrich, reagent grade. $NH_4F$ and $(NH_4)_2HPO_4$ were dissolved in the deionized water to prepare 0.03 M solution. Obtained solution was added into the 0.05 M solution containing $Ca(NO_3)_2•4H_2O$ and $Sr(NO_3)_2$ as $Ca^{2+}$ and $Sr^{2+}$ ion source. The chosen amounts of reagents were selected to prepare solution with (Ca, Sr)/P molar ration of 1.67. Synthesis was carried out at the ambient temperature under continuous stirring. During precipitation reaction, $NH_4OH$ (26 wt%) was used to adjust pH of suspension between 9-9.5 till the end pH remains in the range from 9.4 to 9.5. Obtained precipitates were left overnight, afterwards centrifugated and washed threefold with deionized water, followed by drying at 105°C. Fourier transform infrared spectrometry (FT-IR) and X-ray diffraction (XRD) were applied for chemical and phase analyses of SrFHAp. The morphology of the powder cristallites was observed using a field emission scanning electron microscope (FE-SEM).

**RESULTS:** X-ray diffraction pattern (see, Fig.1) of the as-synthesized SrFHAp powder showed maximum at 25.8° $2\theta$ and a set of broader peaks around the HAp characteristic regions from 31 to 34.5° $2\theta$, from 38.4° to 40.9° $2\theta$ and from 46.8° to 53.5° $2\theta$. The nature of XRD pattern indicated SrFHAp powder with low crystallinity.

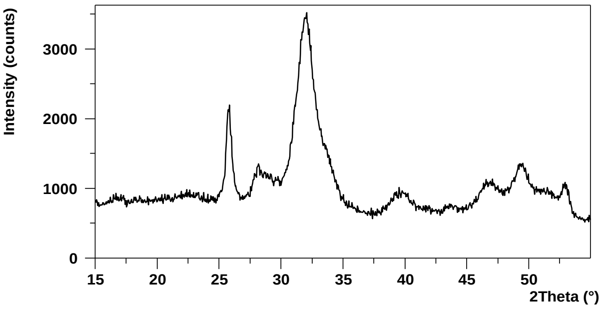

*Fig.1: X-ray diffraction pattern of as-synthesized SrFHAp.*

FT-IR spectrum was similar to pure as-synthesized HAp spectrum, indicating physically attracted $H_2O$ presence with broad absorbance bands between 3650-3200 $cm^{-1}$ and 1890-1600 $cm^{-1}$. The characteristic bands of $[PO_4]$ group were located at 1200-920, 600 and 570 $cm^{-1}$, but existence of $[HPO_4]$ group was confirmed with peak around 880 $cm^{-1}$. FE-SEM analyse revealed nanosized, rode-like morphology of obtained SrFHAp crystallites.

**DISCUSSION & CONCLUSIONS:** The results of current study indicate, that obtained SrFHAp powder chemically and structurally is very similar to pure as-synthesized HAp. Further investigation will be devoted to the assessment of actual amount of Sr and F, incorporated into HAp structure, and optimization of technological parameters of selected synthesis method to manipulate with Sr and F substitution level.

1

**ACKNOWLEDGEMENTS:** This work has been supported by the National Research Programme “Multifunctional materials and composites, photonics and nanotechnology (IMIS$^2$)” Project No. 4 “Nanomaterials and nanotechnologies for medical applications”.

# Tailoring the degradation of hydroxyapatite/poly (vinyl alcohol) composites

L Stipniece[1], K Salma-Ancane[1], V Rjabovs[2], L Berzina-Cimdina[1]

*[1] Institute of General Chemical Engineering, Riga Technical University, Latvia, [2] Institute of Technology of Organic Chemistry, Riga Technical University, Latvia*

**INTRODUCTION:** The overall goal of this work is to develop HAp/PVA composites for medical application. PVA has been exploited for use in drug delivery due to its high hydrophilicity, ease of processing, mechanical and thermal stability, and its non-toxic and biodegradable nature [1]. Depending on the processing parameters, PVA may dissolve instantly upon contact with aqueous mediums. Thus, there has been limited use of PVA composites in biomedical applications [1,2]. However, those shortcomings could be eliminated by modification of the composites through various post-treatments to alter the physicochemical properties, thereby producing a structure with poorer solubility characteristics, which is suitable for biomedical devices [2,3]. Moreover, PVA can be chemically modified to provide various functionalities [3].

**METHODS:** PVA was modified with carboxylic acid residues that can further be modified with organic biologically active compounds. PVA modification reaction was carried out in N,N-dimethylformamide at elevated temperature and the product was precipitated from ethyl acetate. The composites were obtained using two different preparation techniques: (a) aqueous solutions of the pure or modified PVA (M-PVA) and as-synthesized HAp suspension were mixed; (b) HAp was synthesized in the presence of aqueous solutions of the PVA or M-PVA. In both cases, HAp were synthesized from $Ca(OH)_2$ and $H_3PO_4$ through wet chemical precipitation. In order to obtain moldable composites, the suspensions were spray dried at temperature under boiling point of PVA and the physico-chemical characteristics of the products such as morphology, chemical and phase compositions *etc*. were studied. Isostatically pressed (at 700 kN) composites were subjected to the thermal (at 60 °C) crosslinking treatment. The composites were characterized by their water uptake ratio and mass loss profiled as a function of degradation time. The possibilities of chemical and physical interactions of HAp and the polymers were evaluated using FT-IR.

**RESULTS:** Apatite was identified to be the main mineral phase in the composites (Fig. 1).

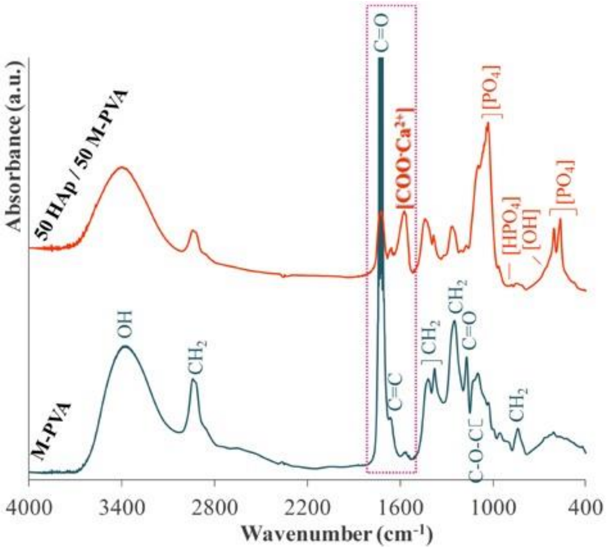

*Fig.1: FT-IR spectra of the M-PVA and the HAp/M-PVA composite indicating the presence of carboxylic acid residues and formation of inorganic-organic bonds in the composites*

Results confirmed that intermolecular crosslinking of the PVA and the M-PVA was obtained at elevated temperatures**.** Thus, the water resistance of the composites was improved.

**DISCUSSION & CONCLUSIONS:** This study has provided an alternative technique to produce moldable materials with attractive features for applications in bone tissue engineering. The optimal conditions for the post-treatment of HAp/PVA or HAp/M-PVA composites such as heat-treatment period were screened out.

**ACKNOWLEDGEMENTS:** This work has been supported by European Social Fund within the project “Involvement of new scientist group for synergistic investigation to development of nanostructured composite materials for bone tissue regeneration” No.2013/0007/1DP/1.1.1.2.0/13/APIA/VIAA/024.